JAERI 1297

JAERI 1297

SPEEDI : A Computer Code System for the Real-Time Prediction of Radiation Dose to the Public due to an Accidental Release

October 1985

日 本 原 子 力 研 究 所

Japan Atomic Energy Research Institute

JAERIレポートは，日本原子力研究所が研究成果編集委員会の審査を経て不定期に公刊している研究報告書です。

入手の問合わせは，日本原子力研究所技術情報部情報資料課（〒319-11茨城県那珂郡東海村）あて，お申しこしください。なお，このほかに財団法人原子力弘済会資料センター（〒319-11 茨城県那珂郡東海村日本原子力研究所内）で複写による実費頒布をおこなっております。

JAERI reports are reviewed by the Board of Editors and issued irregularly.

Inquiries about availability of the reports should be addressed to Information Division Department of Technical Information, Japan Atomic Energy Research Institute, Tokai-mura, Naka-gun, Ibaraki-ken 319-11, Japan.

編集兼発行　日本原子力研究所
印　　刷　いばらき印刷㈱

A LIST OF ERRATA

Page/line		
p.i 21-22	calculation in the system is	=> calculations in the system are
p.3 26	was	=> were
p.7 3	small	=> small-scale
p.12 Fig.2.7	ENERGY SITE	=> POWER PLANT
p.13 12	National Land Agency	=> Land Agency
p.16 29	has start	=> has started
p.17 1	omposition	=> composition
p.17 20	WEADUS2,	=> WEADUS2
p.17 23	are	=> is
p.21 3	Figure	=> Figures
p.34 13	is	=> are
p.36 17	are	=> is
p.45 7	measurement	=> measurements
p.50 11	data identify	=> data to identify
p.50 20	trajectory	=> trajectories
p.51 8	rawin sonde	=> rawin-sonde
p.52 35	between TRA2 and TRA3, but	=> the same as TRA3, and
p.53 Fig.3.13	UTSUNUMIYA	=> UTSUNOMIYA
p.69 5	requirement	=> requirements
p.69 21	surface dose	=> dose
p.70 19	are	=> is
p.71 5	LWR	=> PWR
p.72 15	valued	=> values
p.74 45	outlook	=> outlooks

SPEEDI : A Computer Code System for the Real-Time Prediction of Radiation Dose to the Public due to an Accidental Release

Kazuhiko IMAI, Masamichi CHINO, Hirohiko ISHIKAWA,
Michiaki KAI, Kiyoshi ASAI+, Toshimitsu HOMMA,
Akihide HIDAKA, Yasuhiro NAKAMURA+,
Toshinori IIJIMA and Shigeru MORIUCHI

Department of Environmental Safety Research,
Tokai Research Establishment,
Japan Atomic Energy Research Institute
Tokai-mura, Naka-gun, Ibaraki-ken

Received February 12, 1985

Abstract

SPEEDI, a computer code system for prediction of environmental doses from radioactive materials accidentally released from a nuclear plant has been developed to assist the organizations responsible for an emergency planning. For realistic simulation, have been developed a model which statistically predicts the basic wind data and then calculates the three-dimensional mass consistent wind field by interpolating these predicted data, and a model for calculation of the diffusion of released materials using a combined model of random-walk and PICK methods. Therefore, SPEEDI gives more realistic prediction of radioactivity distribution and doses using the sophisticated models, and makes it possible to consider the effect of complicated topography on the transport and diffusion of effluents. These calculation in the system is carried out in conversational mode with a computer so that we may use the system with ease in an emergency. SPEEDI has also versatile files, which make it easy to control the complicated flows of calculation. In order to attain a short computation time, a large-scale computer with performance of 25 MIPS and a vector processor of maximum 250 MFLOPS are used for calculation of the models so that quick responses have been made. Simplified models are also prepared for calculation in a minicomputer widely used by local governments and research institutes, although the precision of calculation as same with the above models can not be expected to obtain.

The present report outlines the structure and functions of SPEEDI, methods for prediction of the wind field and the models for calculation of the concentration of released materials in air and on the ground, and the doses to the public. Some of the diffusion models have been compared with the field experiments which had been carried out as a part of the SPEEDI development program. The report also discusses the reliability of the diffusion models on the basis of the compared results, and shows that they can reasonably simulate the diffusion in the internal boundary layer which commonly occurs near the coastal region.

Keywords: Computer, Code, Nuclear Plant, Emergency, Accident, Prediction, Release, Diffusion, Plume, Puff, Wind Field, Concentration, Dose, SPEEDI, ARAC, Environment

---

+ Computing Center, Tokai, JAERI

SPEEDI：事故放出に伴う公衆被曝線量の実時間予測計算コードシステム

日本原子力研究所東海研究所環境安全研究部

今井　和彦・茅野　政道・石川　裕彦
甲斐　倫明・浅井　　清[+]・本間　俊充
日高　昭秀・中村　康弘[+]・飯嶋　敏哲
森内　　茂

1985年2月12日受理

要　　旨

原子力施設の事故の際に環境中に放出される放射性物質からの被曝線量を予測計算して，緊急時の防災対策に役立てるための情報を提供する計算コードシステムSPEEDIを開発した．SPEEDIでは，統計を用いた風の時間的予測を行ない，質量保存則を満たす3次元風速場を変分解析により求め，複雑地形上での移流拡散をランダムウォーク法とPICK法の混合モデルによって計算し，より現実的な被曝線量の推定が行なわれる．またコードシステムとして，従来から使われてきたパフモデルおよびガウスプルームモデルの簡易計算コードも参考計算用に組込まれている．本報告では，各計算モデルのほかSPEEDIの構成および機能について述べた．さらに，拡散モデルの野外実験と風洞実験との比較について述べ，計算モデルの性能，その他システムとしての実用性について入力データおよび運用方法などの点から論じた．

＋ 計算センター

CONTENTS

目　　次

1. Introduction

The importance of emergency preparedness has been well recognized since the beginning of nuclear energy development in Japan. Program of environmental emergency monitoring was prepared to some extent both in national level and local governmental level.

For instance, the prefectural government of Ibaraki-ken where the early reactors were operated, had discussed the environmental emergency planning with the national government and other bodies having nuclear facilities, and the result was tested by an exercise carried out at Tokai-mura in 1971. There were an inactive period of the discussion on emergency preparedness while the discussion was strengthened on follow-up of the requirement for the reduction of release amount of radioactive gaseous waste at the normal operation of light-water-cooled reactors.

The discussion of emergency preparedness started again in Japan but it was not active before Three Mile Island Unit 2 (TMI-2) reactor accident in 1979. After TMI-2 reactor accident, discussions and inspections were made to learn the lessons and were concluded as the recommendations including needs for research and development.

The Japan Nuclear Safety Commission revised the National Research Program of Environmental Radiation Protection in 1980. This five-year program 1981-1985 includes the emergency related researches as "safety assurance at an extraordinary release of radioactive materials". Then JAERI made the detailed research program and set a committee to check and review the program and the performance.

The development of a computer code system for the real-time prediction of environmental radioactive contamination and radiation dose to the public due to an accidental release from a nuclear site is one of the most important items. JAERI sent a mission to survey the development of such systems in other countries and in 1981 started the development of a code system in cooperation with the Meteorological Research Institute (MRI). In order to support the development and supply data for verification of the effectiveness of computational models and the system, series of atmospheric diffusion experiments and wind tunnel experiments were planned by JAERI and MRI, respectively.

In the United States, Lawrence Livermore National Laboratory is operating ARAC (Atmospheric Release Advisory Capability) project sponsored by the Department of Energy (DOE) and the Department of Defense (DOD)[1]. The ARAC project was initiated in 1972 and has evolved from a research and development phase to an operational phase. It has responded to approximately 60 situations, including exercises. Savannah River Laboratory has a similar system named WIND (Weather Information and Display). The computational models in both systems have been verified by field experiments.

The European countries such as Italy and Sweden have their programs to develop real-time prediction systems.

At the start of the development of the computational models of our system, we followed MATHEW for wind field calculation and ADPIC for concentration calculation of ARAC system. This report describes the code system SPEEDI (System for Prediction of Environmental Emergency Dose Information), the results of verification of models and future plans. The fundamental structure of SPEEDI was designed and the first version was completed at the end of FY 1981, i.e. March of 1982, then it was revised into the second version in FY 1982, and the third version which could be used for practical application has been completed

at the end of FY 1983.

Design concepts are described in Chapter 2. The objective of the development is the practical use of the system. In order to reach the goal fast, the system was designed as a modular system convenient for the development itself. Basic utility softwares such as conversational control, data file handling and graphic display are common in the system. Computational models are incorporated in the system as independent modules and each of them can be operated either as a module in a whole system or as a stand-alone module. Their addition or deletion is also done easily without modification of the whole system.

The models calculating wind field and concentration distribution have been verified with experiments as described in Chapter 3. Necessary environmental data such as terrain height, road and lakes, etc. are provided for eleven areas which include fourteen nuclear power stations. In addition to these data, the system has the nuclear data for the approximation of source term in order to cope with the case where no sufficient data on source terms are available.

The practical realization of the SPEEDI system, including data transmission, terminal minicomputers and local meteorological data acquisition systems is being planned in the Science and Technology Agency (STA) of Japan and will be expected in use within two or three years. Further research items will be incorporated into next revision of the national research program which is to cover the coming five years.

The authors who wrote each section of this paper are shown as follows.

Kazuhiko Imai	1.
Kiyoshi Asai	2.1.1, 2.1.3 and 2.3
Masamichi Chino	2.1.2, 3.1.3, 3.2.1 and 4.2
Hirohiko Ishikawa	2.2.2, 3.1.1, 3.1.2, 3.2.2, 4.1.1 and Appendix
Michiaki Kai	2.2.1, 2.2.3, 3.1.3 and 4.1.2
Toshimitsu Homma	3.3.2
Akihide Hidaka	3.3.1
Toshinori Iijima	5.
Shigeru Moriuchi	5.

2. Design and Function of SPEEDI

2.1 Design

2.1.1 Design Concepts

In the period of 1960-1975 the dominant method of systematization of nuclear codes is the sequential connections of already existing nuclear codes by adjusting the contents and formats of their input/output files.

A code system made by this method requires much manpower and computer time in modifications, deletions and additions of codes in the system. The method of recent years adopts a procedure which is commonly used in construction of buildings.[2] According to the procedure, one at first constructs utility softwares such as graphics, file handling programs, data files, user interfaces and a control program which are common to all codes in the system. Then computational codes for physical models are set in the code system as modules. When the code system is designed so that its components, i.e., a code or library are easily changeable, the system and the component are called a modular code system and a module, respectively.

SPEEDI has been constructed by this method. The conversational control program, data files and file handling programs and graphic programs are basic utilities common to all computational codes in SPEEDI. The merits of this method are that firstly using the system the user can use every single code or all relevant codes to some subject, and secondly it is very easy to add, delete or modify codes in the system. The demerit of the method is that it requires much manpower and cost in construction of basic utilities. To avoid the demerit, SPEEDI makes use of existing softwares and data such as DATAPOOL[3] for file handling, ARGUS[4] for graphics and the numerical mesh data on topography provided by the Land Agency of Japan.[5] In addition to the adoption of the method mentioned above, the following features of the system are pursued in the design and construction of SPEEDI.

(1) Coexistence of research and practice use

When the design and construction of SPEEDI was started, the computational codes for physical models of JAERI to be included in the system were yet in their research and development phase.

Owing to the efforts of researchers of the Geophysical and Environmental Sciences Division at Lawrence Livermore National Laboratory, we can follow physical models and computational codes for three-dimensional wind field and concentration calculations.[6),7] Even if starting from the same models, however, the codes will differ gradually from original ones in the process of model validation and code verification mainly by adopting the results of experiments.

This shows that although the ultimate goal of the development is to construct a useful code system for practice, we must also maintain the system for research use, and that the codes in the system will be improved frequently. For this reason SPEEDI must allow easy additions, deletions and modifications of codes by researchers. The changes must be done independently of other computational codes or functions of the system. In the practical use of the system, however, codes and functions in the system must be fixed and may not be changed so often. For the coexistence of these two conflicting uses, SPEEDI is designed to be controlled in conversational mode and each computational code is linked up with it very loosely. The method of the linkage is described in Section 2.1.3. The number of parameters

of each conversational command is reduced to a minimum. The system is designed to ask no further questions unless the user requests them.

(2) Realization of modular code system

In a development stage of the system, some computational codes are added and some are deleted from the system because of continuous improvements and assessments. The addition and deletion must not cause modifications of the system scheme, i.e., the system should be a modular code system.

For the modularization, the control method of the conversational control program must be independent of any specific code and the formats of input and/or output files of all codes must be the same. To achieve the modular control method, the input of every computational code should be divided into two parts, i.e., the one which depends on the input through a control table of the conversational control program, and the other which depends on data files of the system or the outputs of other codes. The control method of the former input will be described in Section 2.1.3. As for the latter input, such a file structure as the DATAPOOL must be adopted to unify the format of the observed wind data and results of computational codes.

(3) Partial use of system

In research use, users will calculate only wind field, concentration, or dose according to their interest. In the system every calculation should be done independently of others.

(4) Common data files

It is most important to equip unified data files with SPEEDI because every computation or display is based on common environmental and physical data. SPEEDI has five types of common data files which are automatically invoked before the execution of calculation. More detailed descriptions of the files are given in the Section 2.1.3.

(5) Unification of file format

Every data set which is used in the calculation of wind field, concentration, dose or drawing of maps will also be used in other calculations. For this reason it is best to fix standard formats which are common to all relating calculations.

(6) Easy control of system

It is desirable to operate the system without user's manuals. For this purpose the system should have instructive functions. SPEEDI has two such functions. One is the HELP command and its text. Using this command the user can learn the syntax of an arbitrary command and physical meanings of its parameters. The other is a method of input and system control by menus. Usually a menu corresponds to a mode or a kind of calculation and it indicates the operand and default values of parameters. By changing the values and assigning next menu the user can input and control the system easily.

(7) Real-time processing

In case of an emergency SPEEDI must reflect on the calculation such real-time data as the release information and observed meteorological data which are varying with time. All computational codes must use the same input data. Any computational code or graphic routine of SPEEDI receives automatically the newest input data from a table of the conversational control program. The observed meteorological data are assumed to be given directly from an online network to the SPEEDI data file, though the user can display or modify the data before their use.

(8) Graphic output

It will be difficult and very time-consuming tasks to interpret the three-dimensional numerical output of wind field, concentration or dose calculation. The code system should provide the user with functions which produce graphic outputs of computational results over

a specified underlying map. The unified file format makes it easy for the graphic routine to draw the output from any computational code in the system.

(9) Automatic provision of initial data

The default data which are necessary for the interpretation of unspecified parameters of commands and the execution of computational codes should be automatically provided by the system to save time and prevent human errors. The longitude, latitude, and height of a stack, for example, should be loaded automatically by only specifying the site and facility names.

(10) Automatic logging

In an emergency the interlaced input information and sequences of computation may sometimes cause confusions in use of results among users. In that case the user of the system will be forced to trace back exactly the interaction between the user and the system. For this purpose the system should retain the records of input commands with their operand parameters, and also the system messages returned to the commands. These records should be displayed at any instance by using a command.

(11) Utilization of existing softwares

It is now a well-known fact that the construction of a code system requires much man-power and that the cost of the construction is mostly consumed in making basic software packages such as graphics, file handling programs, etc. Considering those points, two existing software packages are utilized in construction of SPEEDI. One is a general purpose graphic package ARGUS and the other is a three-structured file handling package DATAPOOL. Both softwares are developed at JAERI and widely used in several application fields.

(12) Systematization for practical application

As is stated in Chapter 1, the SPEEDI system is expected to cover all areas in which Japanese nuclear power plants are located. A network as shown in **Fig. 2.1** is an example of operational scheme when the development of SPEEDI has been accomplished. The meteorological data and monitoring data of the areas are gathered by minicomputers of local governments and sent routinely by telephone lines to a small-scale front-end computer of the SPEEDI system.

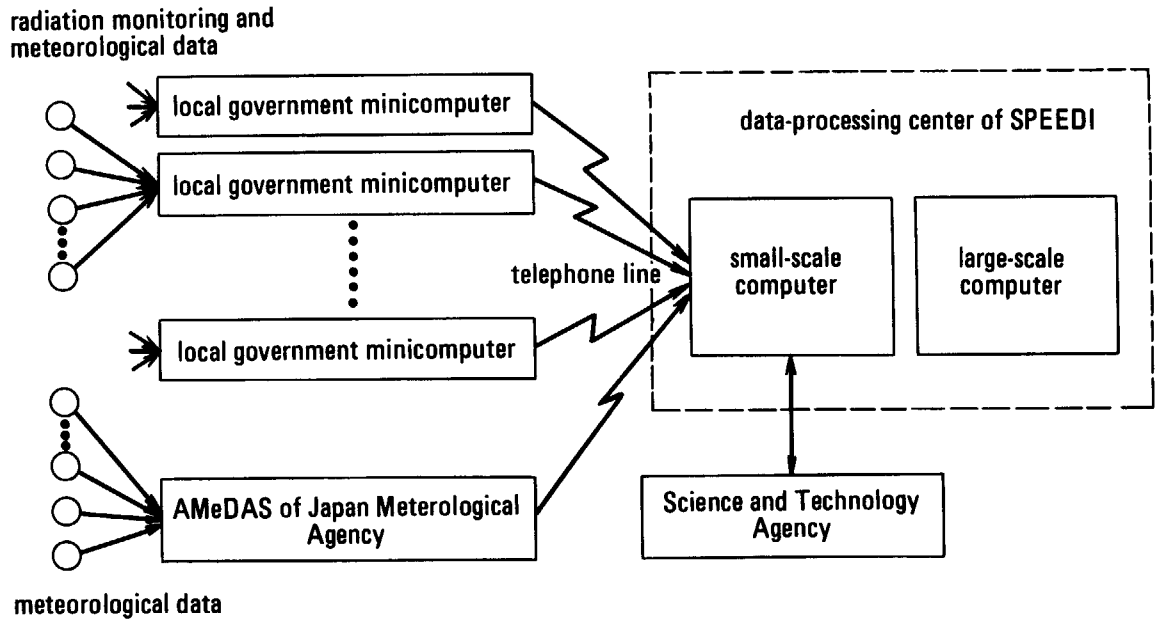

Fig. 2.1 Configuration of SPEEDI network.

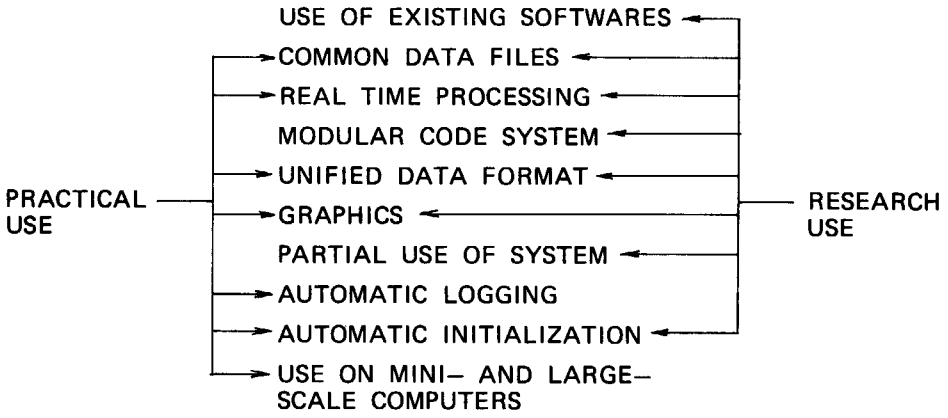

Fig. 2.2 Two sided design concepts.

Table 2.1 Code and utility program in the SPEEDI code system

Category	Name	Explanation	CPU time (s)	Memory (kB)	I/O times	Source statements
Command Control	EMER	Command control and decay calculation		1800		8208
Datapool	DISPDP	Display control information of datapool				250
	DISPW	Display and update weather datapool				980
Graphics	GWIND	Display weather and wind field data	7	1452	2592	5186
	GCONC	Display concentration data	12	1688	4971	6932
	GDOSE	Display dose data	4	1300	1391	5020
	GBACK	Display regional data	2	1140	802	3036
	PLAN	Display areas by countermeasures	4	1210	1613	4020
Other	SITEMDP	Determine site location automatically				83
Wind Field	WIND04	3 dim. calc. by variational method	72	3028	4633	1591
Concen-tration	PRWDA	Concentration by particle dispersion	151	2636	4542	3660
	LSPUFF	Quick calculation by puff model	4	768	777	1923
Dose	CIDE	Dose calculation by grid-cell model	6	1228	2630	1816
	GSDOSE	Quick calc. by Gaussian plume model	7	828	3901	3602
Datapool Construc-tion	RGONDP	Construct regional datapool (file)	8	536	7996	6258
	WCREAT	Create weather DP by batch mode	16	1000	5083	505
	WEADUS	Create weather DP by TSS mode		768		2967
Datapool Access	DPAC	Interface between physical models and datapool files				4662
Graphic Package	ARGUS	General purpose graphic package		3508		39715
Datapool System	DPLIB	Datapool program library		476		21419
	DPTSS	Interactive display of datapool		768		15962
	PREPROC	Preprocessor for datapool user program		376		9368
Basic Graphic Library	GGS	Basic graphic library		587		10455
	PDS	Library for DSCAN graphic terminal		283		3322
	PTS	Library for TEKTRONIX graphic terminal		165		4551
	PNL	Interface for Japanese language line printer		65		2700

Note. 1) Memory of EMER contains file handling and graphic routines in execution time
2) CPU time, memory size and I/O times are measured by FACOM M-380 large-scale computer (25 MIPS, or 9 MFLOPS).

Owing to the design concept, the user can use the system for both practice and research. The items relating to the two uses can be categorized as **Fig. 2.2**.

When an abnormal value is found in the monitoring data, the small computer calls a large-scale computer and asks to predict the situation by sending the meteorological data. The large-scale computer can perform both simple and detailed calculations by using its high speed capability.

It is, however, desirable for the local governments to be able to calculate the same computational codes by using their minicomputers regardless their computation time because it may happen to lose the connection between the computers by some accidents, and because it will improve the robustness of the system by distributing a part of its functions to many computers.

Taking into account the considerations mentioned above, we have taken care that any component of the system does not require redundant memory size and computation time as shown in **Table 2.1**.

2.1.2 Computational Codes in the System

In this section, computational codes in the SPEEDI system are described. The requests for models used in an emergency are firstly that models are practical ones which require the relatively small input and little computation time for the real-time response, and secondly that models have an ability to realistically predict the behavior of radioactive materials released in complex and coastal region.

From a practical point of view, a Gaussian plume model has been currently used because of little computation time and simpleness of the model. The recent advance of computer techniques, however, has made more accurate models applicable to practical predictions. **Figure 2.3** shows the computational models which are recently developed to accurately simu-

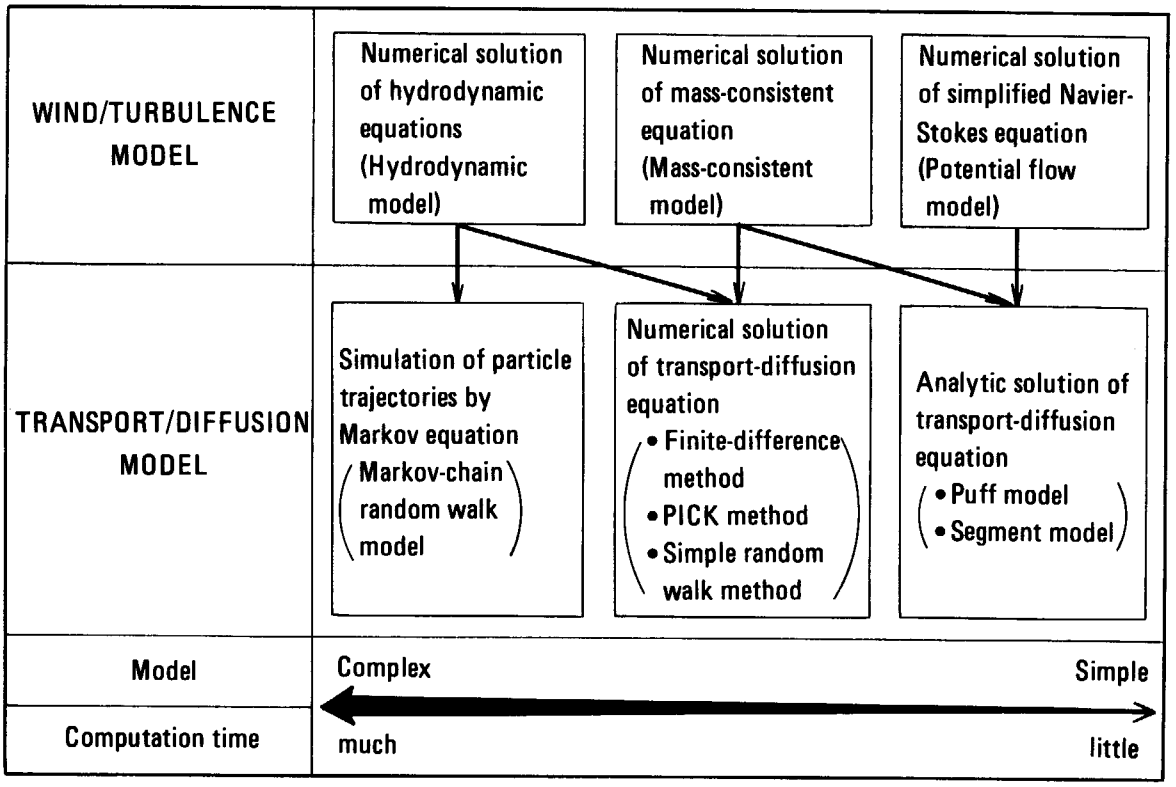

Fig. 2.3 The computational models which are recently developed for accurate simulations of the behavior of pollutants.

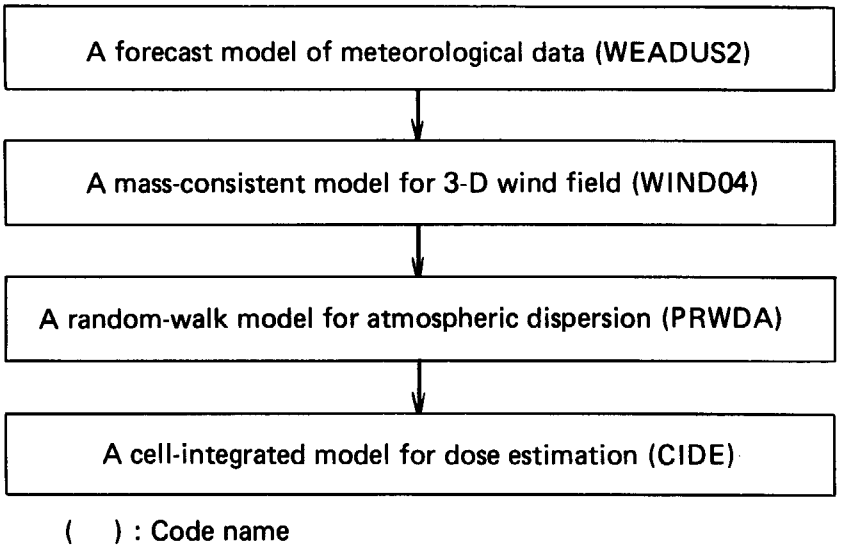

Fig. 2.4 Connection of main codes in SPEEDI.

late the behavior of pollutants. In general, it is difficult to improve the accuracy of models with reduction of computation time. Consequently, intermediate models must be selected for relatively accurate and urgent simulations. For the more accurate simulations, the combination of a three-dimensional hydrodynamic model and a Markov-chain model may be the most suitable one. However it requires much computation time. On the other hand, the Gaussian plume model that is the most suitable to the urgent computation has not adequate ability to simulate the airborne concentration in such complex terrains as the surroundings of Japanese nuclear power plants. Therefore, as the main codes in SPEEDI, we selected the combination of a mass-consistent wind field model and a dispersion model which solves a transport-diffusion equation numerically. The first model calculates three-dimensional wind fields and the second calculates the transport and diffusion of pollutants. The connection of main codes in SPEEDI is shown in **Fig. 2.4**.

The first step of the prediction is to forecast the meteorological condition automatically whenever the observed data are input. To forecast meteorological data, the WEADUS2 code has been developed. Based on a statistical analysis of observed data, this code forecasts the wind speeds and wind directions at the measuring points. The advantage of the model used in this code is to require the considerably less computation time than the three-dimensional hydrodynamic model. The disadvantages are that it cannot predict the variation of turbulence and the rapid change by a front and so on. The method of statistical analysis was developed by the Meteorological Research Institute (MRI), the Meteorological Agency of Japan. The output data file generated by WEADUS2 has both observed data and forecasted data.

For main calculations considering the effect of coastal region and complex terrain, three codes are prepared, i.e., the WIND04 code to calculate wind fields, the PRWDA code to simulate the diffusion of airborne and the CIDE code to evaluate the dose.*

The WIND04 code uses a three-dimensional mass-consistent model to calculate wind fields that is influenced by terrain. The approach of this model is a diagnostic wind field analysis and its accuracy depends on the quality and quantity of observed wind data. It cannot estimate the atmospheric turbulent motion.

---

* The dose is used with the meaning of dose equivalent (rem) or exposure (roentgen) without notice in this paper.

Table 2.2 Summary of the codes in the SPEEDI system

Purpose	Code name	Model	Output variables
Forecast of meteor. data	WEADUS2	Statistical-analysis model	Forecasted U, V at the measuring points
Wind field	WIND04	3-D mass-consistent model	U, V and W in (x,y,z,t)
Concentration	PRWDA	Random-walk model for the gradient-transfer theory	Concentration in (x,y,z,t) and in (x,y,t)
Dose	CIDE	Cell-integrated dose model	External gamma-dose and internal dose in (x,y,t)
Reference calculation	GSDOSE	Gaussian plume model	External gamma-dose and thyroid dose in (x,y,t)
	LSPUFF	Puff-plume model	External gamma-dose and thyroid dose in (x,y,t)

By using wind fields generated by WIND04, the PRWDA code, which employs a random-walk method to simulate a gradient-transfer process numerically, predicts the spatial and temporal airborne concentration and the surface concentration. The reason why this model is adopted with the SPEEDI system is that finite-difference methods including a PICK method are unsuitable for the estimation of a point release.

The CIDE code has been developed to estimate the external gamma-dose from a radioactive cloud and the internal dose due to inhalation. It is a main characteristic that the CIDE code does not employ a submersion model but a cell-integrated dose model to calculate the external gamma-dose from a randomly distributed radioactive clould.

Besides these main codes, two codes that employ simple models are prepared for reference calculations of the main codes, i.e., the GSDOSE code using the Gaussian plume model and the LSPUFF code using a puff-plume model.

Although a three-dimensional hydrodynamic model is not available in this stage, the research is being continued by MRI. In future, this model may be included in the SPEEDI system, when it can predict the meteorological condition within a reasonable computation time.

A summary of the codes in the SPEEDI system is shown in **Table 2.2**, and detail computational procedures and verifications will be described in Chapter 3.

2.1.3 System Control and Utility Programs

(1) Method of system control

The computational flow of our SPEEDI code system is shown in **Fig. 2.5**.

The software of the system consists of five parts, i.e., i) a control program of conversational mode, ii) datapool for topography, lakes, roads, railroads, and administrative boundaries, iii) datapool for calculated results, iv) a package for graphical output, and v) computational codes for physical models.

The control program for conversational mode is the nucleus of SPEEDI. The control program receives and stores real-time data, executes computations with physical models, displays and outputs the calculated results. The control of SPEEDI is done by inputting commands through a timesharing terminal.

The major commands of SPEEDI are listed in **Table 2.3**. SITE, TIME and REL commands are used for input of data such as the site location, time of release, rate of release, etc. WIND, CONC and DOSE commands are used to initiate calculation of wind field, concentration and

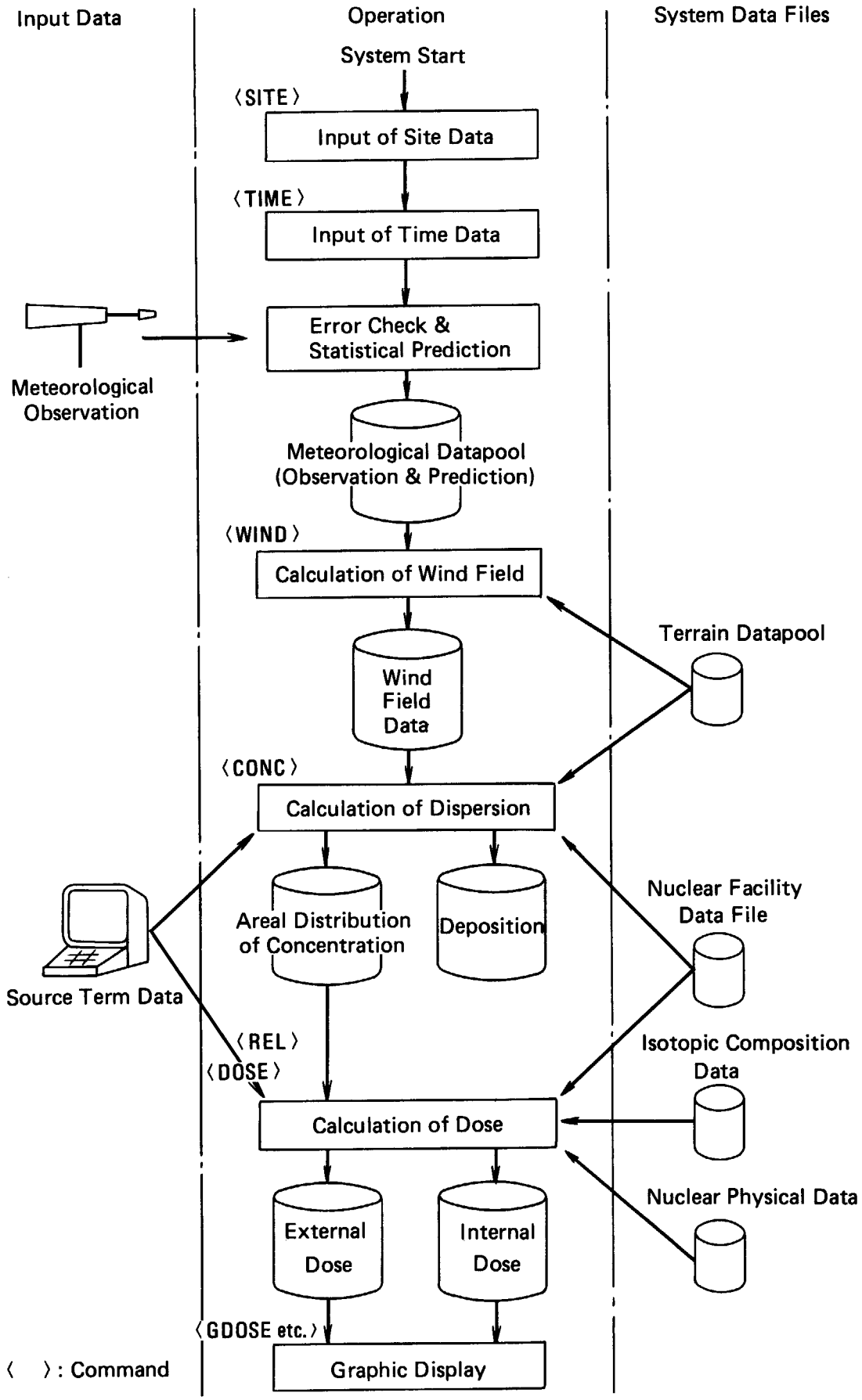

Fig. 2.5 Computational flow of SPEEDI.

dose, respectively. GWIND, GCONC and GDOSE commands are used for graphic output of the calculated results of the wind field, concentration and dose, respectively. The user can input and display additional information such as the time of display, name of region, underlying map, etc. by specifying additional information in the operand fields of these commands.

The input data in the command operands are retained in a table in the control program and they reflect the most recent values during the execution until other new input data are given to SPEEDI.

Any input sequence of commands to the system is allowed and we can, for example, execute repeatedly only wind field calculations or display contents of some calculated results.

The system is designed to be initiated with a minimum amount of external input data. For this purpose the system contains standard data which are specific to sites or physical models and the data are used automatically unless new values are inputted explicitly. For example we can use SITE command only by specifying site and facility names because such data as the location, stack height, terrain height of the facility are automatically provided in the system. The system has all data of the fourteen sites where nuclear power reactors of Japan are now operating. Every command has those types of default values and this provision makes it easy to use the system in conversational mode.

Table 2.3 Summary of major commands

Command Name	Explanation
EMER	Initiate or restart the code system
SITE	Set informations of an accident site
REL	Set informations of radioactive release
DISPW	Display observed meteorological data of the site
SETW	Set meteorological data of a meteorological station to fill a lack of data of the station
WIND	Calculate the wind field of a specified region
CONC	Calculate the concentration of a specified region The region is included in the one specified by WIND
DOSE	Calculate the dose of the region specified by CONC
GWIND, GCONC GDOSE	Display results over specified maps
PLAN	Display dose and conc. isopleths over maps with regulation values for emergency planning
SUB	Submit a computational module to the computer as a batch processing job
RUN	Process a computational module as a TSS job
GO	Same as the above
DPARAM	Display control parameters of SITE, REL, WIND, CONC, DOSE, GRAPH, PLAN mode, or files
SET	Set control parameters of modes
CLOG	Display the past conversational records logged in a logging file
HELP	Help users by displaying informations on commands
SAVE	Save the control informations for restart
END	End the session of the code system

When a 'Q' is added to each command, the system automatically questions the user about input parameters.

(2) Input and system control by menus

Although the method of conversational input to SPEEDI is rather simple as will be shown in Section 2.2.1, a further improvement has been made for a quicker input and easier use of the system. A menu input system by Japanese characters or by English alphabet has been introduced. An example of the menu in Japanese characters is given in **Fig. 2.6** and an example of English one is given in **Fig. 2.7**. The character strings after the colons are default values and when they are changed, the changed values are assumed as inputs. When operating

```
..... サイト情報 ..... (08/28 16:03)
原子力サイトデータを入力

  入力タイプ==> _ (下のAまたはBを選択して下さい)

A) 原子力サイトをサイト名で入力して下さい
  (1) サイト名=_____
  (2) 施 設 名=_____
  (3) 放 出 高=_____(M)          (数値又は*)
                                 (*;スタック高度が自動設定される)
   *  燃 焼 度:_____(MWD/MTU)

B) 放出点を緯度・経度で直接入力する時は以下に入力して下さい
  (1) 緯    度=____度 ____分____秒
  (2) 経    度=____度 ____分____秒
  (3) 標    高=_____(M)
  (4) 放 出 高=_____(M)
   *  燃 焼 度:_____(MWD/MTU)

PF1:時刻設定画面    PF3:キャンセル    PF4:前画面表示
PF2:現画面                            PF5:前画面表示解除
コマンド名==> _____(設定, CRにより対象画面表示;未設定時はコマンド画面)
```

Fig. 2.6 An example of Japanese menu.

```
---------- S I T E ---------- (08/28 16:17)
INPUT NUCLEAR SITE DATA

  INPUT TYPE ==> ___ (SELECT A OR B)

A) INPUT SITE NAME OF NUCLEAR ENERGY SITE
   (1) SITE NAME      = _____
   (2) FACILITY NAME  = _____
   (3) RELEASE HEIGHT = _____ (M)      (NUMBER OR *)
                                       (*: STACK HEIGHT IS USED)
    *  BURNUP         : _____ (MWD/MTU)

B) INPUT RELEASE POINT DIRECTLY
   (1) LATITUDE           = ____ °____' ____"
   (2) LONGITUDE          = ____ °____' ____"
   (3) SITE TERRAIN HEIGHT = _____ (M)
   (4) RELEASE HEIGHT     = _____ (M)

    *  BURNUP             : _____ (MWD/MTU)

PF1 : TIME MENU      PF3 : CANCEL      PF4 : PREVIOUS MENU
PF2 : PRESENT MENU                     PF5 : PUT BACK PRESENT MENU
COMMAND NAME ==> _____ (SET AND 'CR', DISPLAY OBJECT MENU, ELSE GENERAL MENU)
```

Fig. 2.7 An example of English menu.

the system the user can change the mode of input from this type to the old one described in the Section 2.2.1 and vice versa.

(3) System data files

The invariable data needed to use SPEEDI are locations of power plants, its surrounding topography, isotopic composition of noble gas and iodine in the reactor core and physical constants of anticipated nuclides. These data are stored in the datapool files of SPEEDI and are automatically used by computational models or are displayed by using commands.

1) Regional data

SPEEDI has two types of topographical data files, i.e., one is local, twenty-five kilometer distance from the site and the other is regional, a hundred kilometer distance from the site. The data of the local and the regional files are made for the fourteen operating reactors of nuclear power plants in Japan by using the numerical mesh data of the National Land Agency of Japan. The data consist of terrains, coast lines, administrative boundaries, location names, roads, railroads, and lakes. The terrain of local files is divided into 1 km X 1 km mesh horizontally and 25 m mesh vertically. The terrain of regional files is divided into 4 km X 4 km mesh horizontally and 25 m mesh vertically. The average terrain height in a mesh is assumed as the height in the mesh. These terrain heights are used for detail calculations of wind field and concentration. Although the minimum size of the mesh of the numerical mesh data of the Land Agency of Japan is 250 m X 250 m, we are using the above mentioned wider mesh because of limitations from computer memory and computation time. The other data are used to draw underlying maps when the user wants to make outputs of concentration.

The local or regional data files are provided for every site and by specifying a site name in the SITE command and by specifying the LOCAL or REGIONAL parameter in the WIND, CONC or DOSE command, the corresponding terrain data file are automatically loaded for the execution of computational codes.

SPEEDI has also a utility program which produces the local or regional data file for any location in Japan within ten minutes from the numerical mesh data prepared by the Land Agency of Japan.

2) Site data

The site data file contains longitudes, latitudes, terrain heights, stack heights and types of all power reactors. By specifying a site name and a facility name in the operand of a SITE command, these data are loaded from the file into a table in the conversational control program.

3) Isotopic composition data

The isotopic composition data file contains isotopic fraction of krypton, xenon and iodine in the fuel depending on types of reactors and their burnup. The data are used to anticipate the isotopic composition in the initial stage of an accident.

4) Physical constant data

The physical constant data file contains decay constants, average photon energies, effective photon energies, each photon energy emitted from noble gases, seven isotopes of iodine, thirty-four isotopes of fission nuclides such as cesium and strontium, etc. The data are referred to by dose calculation codes for the estimation of external dose.

(4) Input data to SPEEDI system

There are two kinds of real-time input data to the SPEEDI system. One is the information on release of radioactive materials and the other is the meteorological data.

1) Meteorological data

From a viewpoint of online data acquisition, it is supposed that only data of AMeDAS[8] and/or those supplied by the local governments around the site are available to the system.

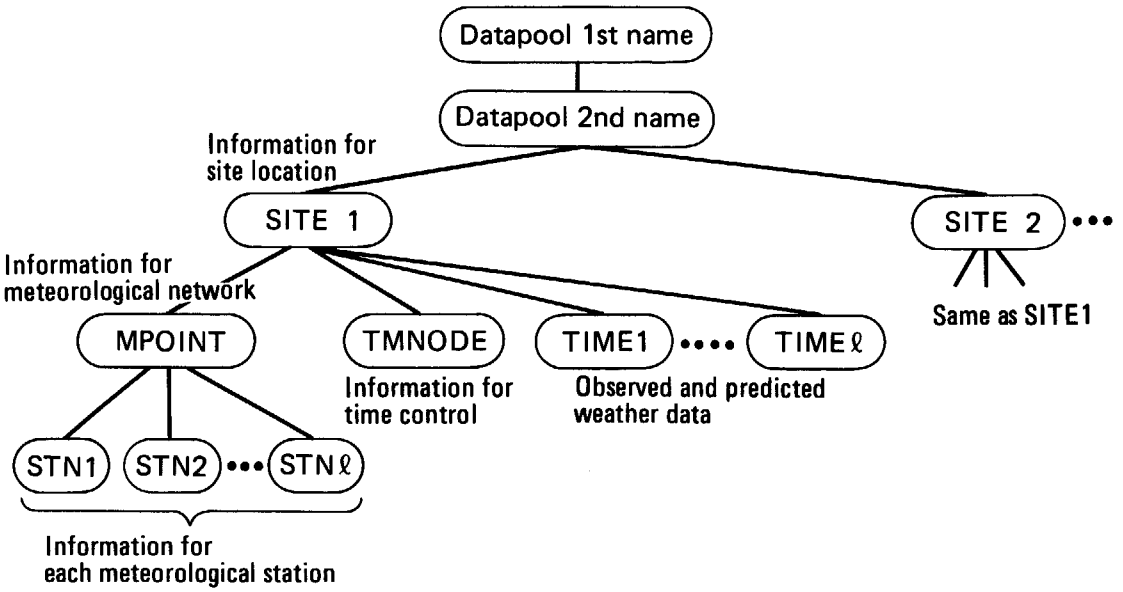

Fig. 2.8 Tree structured meteorological file.

Thus the number of observation stations will be limited within ten to twenty in twenty square kilometers around each site. As for the vertical distribution of wind directions and speeds we can only expect data obtained by instruments attached to an observation tower in the site. Considering this situation on meteorological data, the meteorological data file of SPEEDI is designed to record wind directions, speeds, rain falls and atmospheric stabilities with the corresponding locations of measuring stations and heights of instruments. As shown in **Fig. 2.8**, the meteorological data are stored in a tree-structured file and they are separated in two parts, i.e., one for the invariable and the other for the variable part. The variable part is designed to store and quickly retrieve any time series data of all observation or measuring stations.

2) Information on released radioactive materials

The information on release of radioactive materials is the most important parameter for the calculation of dose. Although it is needed for SPEEDI to know the time-dependent rates of released nuclides, it is difficult to fix the type of input in one way because the real-time information available to the user of the system may be different by accidents.

Thus SPEEDI provides following three types of input by assuming data from the stack monitor.

(a) Release rates of total noble gas and iodine, or the rate of a nuclide of noble gas and the rate of an isotope of iodine.

(b) Value in mR/h measured by an ionization chamber type monitor.

(c) The release rate of another fission nuclide.

When the input of type (a) or (b) is specified, assuming releases of isotopes of krypton, xenon and iodine, using data of measured time of the release, reactor shutdown time and a rate of isotopic composition in the fuel, SPEEDI calculates remaining quantities of the noble gas and iodine at an arbitrary time. The information on the calculated quantities is given to the computational codes of dose calculation through the control table of SPEEDI. The procedure for this calculation is described in (5) in detail. The isotopic composition in the fuel determined by burnup is pre-calculated and tabulated in a data file of SPEEDI.

(5) Linkage of computational codes and system

The computational codes of SPEEDI are loosely coupled with the code system in two ways, i.e., one is through in-core control tables and the other is file handling software

DATAPOOL. The feature of the DATAPOOL is described elsewhere.[3] Input/output statements of every computational code are replaced by statements of subroutine calls which activate the functions of the DATAPOOL software. The files created by using the DATAPOOL are called datapool files, or datapools shortly.

In the following we will describe another way of coupling the codes with the system, i.e., the in-core control tables.

SPEEDI has two kinds of in-core control tables. The in-core control table of the first kind ICT1 is loaded on the main memory by inputting EMER command for system initiation. A part of ICT1 is shown in **Table 2.4**. In **Table 2.4** the character string S01C means as follows: S indicates that the site name to be assigned in a SITE command mode, 01 is the identification number of the "site name" among parameters of the SITE command, and C indicates that the value of the parameter must be a character string. Also the character I or R of W03I or W15R means that the value must be an integer or a real number, respectively. The contents of the ICT1 of SPEEDI is listed in Appendix 3.

The first character R, C, D, G, or P for the parameter specification means that the parameter should be specified in the corresponding command, i.e., in REL for release, CONC for concentration, DOSE for dose, GRAPH for graphic display, or PLAN for emergency planning calculation. A close investigation of the list will reveal the capability of the present SPEEDI code system. The in-core control table ICT1 may be made by using usual text-editing functions of the timesharing system. It is saved as a member in a file of partitioned organization and is loaded in the memory of the system when the user has specified the member and the file name in the operand of an EMER command. Thus the user can change ICT1 easily. The ICT1 shown in Appendix 3 is the default currently used in SPEEDI.

The in-core control table of the second kind ICT2 must be prepared for each computational code in the system. It contains a list of input parameters which is also contained in ICT1. Usually a code needs a key information which controls the calculation. The key information which controls the calculation. The key information is read before the execution by the code using the namelist feature of FORTRAN in the code.

Table 2.4 A part of ICT1

```
J9298.WIND04.LOAD
J3359.SYSNAMV3.DATA(WIND04)

  WIND04
  MAPTP¥          W02 C
  IMAX            W12 I
  JMAX            W13 I
  KMAX            W14 I
  DX              W15 R
  DY              W16 R
  DZ              W17 R
  IISTAB          W07 C
  ZO              W11 R
  ISTRD¥          W03 I
  ISTRT¥          W04 I
  ITINT¥          W05 I
  IOPEN¥          W18 I
  NAMES¥          S01 C
  NOSIT¥          S03 C
  F¥MAP           F11 C
  F¥WET           F12 C
  F¥WIN           F13 C
```

Table 2.5 ICT1 for WIND04

```
& PARM1  PR=.01, PR2=.001, OM=1.88,
         LIMIT1=300, IBC=0,
         A1=0.20, A2=1.00,
         IMAX=51, JMAX=51, KMAX=21,
         DX=1000.0, DY=1000.0, DZ=25.0,
         IISTAB='D       ',
         Z0=0.1, NSTMAX=40, REF=25.,
         NMODL¥=2,IOPEN¥=0,
         X00=-30., Y00=-15.,
         IFLGUP=2&END
```

If some of the predefined default values in the namelist are different from those of the ICT1, the predefined values must be replaced by values of the ICT1, because ICT1 contains the newest ones. Sensing that new values are inputted, the conversational control program of SPEEDI replaces the values. In this replacement procedure, several routines are invoked for conversions of physical dimensions and units of the values if necessary. ICT2 of the WIND04 code is shown in **Table 2.5**. This ICT2 has been registered in the system and retained in the conversational control program when the system is in execution.

WIND04 code that is invoked by the command WIND reads its key information in namelist No.1, e.g., a list in **Table 2.5**. Before the invocation, the conversational control program reads the namelist No.1 and compares the contents with ICT1's. If values of some parameters in the namelist No.1 are found to be changed, they are renewed using the corresponding values of the ICT1. Then, the new namelist No.1 is written into the input file of WIND04 as namelist No.2.

After the first read of the namelist No.1, WIND04 reads next the namelist No.2 and the renewed values replace the old ones in WIND04. WIND04 also reads the observed meteorological information from the weather datapool file and writes the calculated wind field into a datapool file of wind field via subroutine interfaces.

These ICT2 table and the subroutine interfaces for datapool files are only the link of WIND04 and the code system. Thus a computational code is connected with the system very loosely. Every computational code is not resident in the computer memory when the system is intiated, but the code is loaded and linked dynamically when the code name is specified in the operand of a command. This technique helps the system to save the computer memory needed for codes.

2.2 Procedure of Usage

2.2.1 Computational flow of SPEEDI

The SPEEDI code system is designed to operate in conversational mode. The computational flow of SPEEDI is shown in **Fig. 2.5**. The user can order sequential calculations of wind field, concentration of radioactive materials and dose by each corresponding command.

At the first onset, after the SPEEDI code system has start, several input parameters such as the location of a nuclear accident site are required. SPEEDI has data on fourteen nuclear reactor sites in Japan, such as longitude, latitude and stack height. These characteristic data on the sites are available by specifying only a nuclear site and facility in the operand of SITE command. After the SITE command, parameters on the time when a reactor shutdown occurs and radioactive materials begin to be released into the atmosphere, etc. are required in the operand of TIME command.

On these bases, sequential calculations of wind field and nuclide concentration are carried out. The topographical data to be used in these calculations are automatically assigned by means of the SITE command which is inputted as mentioned above.

The execution of dose calculation follows the input of source terms; nuclide names and their release rates are expected to be received as usual from a nuclear site in the system. For the cases where availability of the source information is limited, SPEEDI has a program to estimate the isotopic composition of noble gas and iodine as a function of reactor type, i.e., BWR or PWR, and of burnup data depending on the operational history of a reactor. This function is used for giving data required for dose calculation during early periods after an accident occurs. The atmospheric dispersion of nuclides is normally calculated on the assumption of continuous unit release without decay. The result is calibrated by using the

calculated isotopic omposition, taking into account the radioactive decay, inside SPEEDI and the available release rate, e.g. total amount of noble gas including ^{133}Xe and ^{85}Kr etc., outside SPEEDI. Photon energy and decay constants of 56 nuclides available for dose calculation are stored in the nuclear data file of SPEEDI. The results of such calculations as wind field, concentration and dose are then stored in datapool files of SPEEDI and displayed on a graphic display terminal together with some map elements, which are contained in the topographical data file. The user can select several kinds of map elements such as administrative boundaries, coastlines, road/railroad, contours of terrain height and locations of towns.

All the data files used in SPEEDI are summarized in **Table 2.6.**

2.2.2 Weather Data Acquisition

The function of collecting and editing meteorological data is necessary in the use of the SPEEDI system. During the development stage of SPEEDI, two computer softwares are made and used for creating and editing the weather datapool. The first one is called WCREAT, which creates the weather datapool using the AMeDAS data and the observation by local government stored in the magnetic tape. The weather datapools created by WCREAT have been used for the system check and the verification studies of the wind field and diffusion models. WCREAT has only the function of creating a new weather datapool. The other one is called WEADUS (Weather Datapool Update System), which creates a new datapool and updates the existing datapool. By the use of WEADUS, an operator can input the temporal weather data into the existing weather datapool. The revised version of WEADUS, WEADUS2, has functions of data check and predicting the wind field up to 6 hours ahead. WEADUS and WEADUS2 are described in Appendix 1. The statistical method for the data check and the wind prediction are explained in Section 3.1. In the operational stage of SPEEDI, the meteorological data should be collected and edited automatically. The outline of automated system for the data acquisition is being designed now.

The above system of weather data acquisition exists independently of the following command system. Though the weather data acquisition including prediction is considered to be a subsystem at present, therefore, the user will not need to operate this subsystem when the meteorological data are collected and edited automatically.

2.2.3 Commands and their Usage

Through the above calculational flow, the usage of the commands of SPEEDI will be explained briefly in an orderly manner. The following assumption of an accidental release from a nuclear plant is made as an exemplification. At 12:00 am. on August 20th in 1981, a shutdown of JPDR (Japan Power Demonstrating Reactor) in JAERI could occur and three hours immediately after the shutdown noble and iodine nuclides, consisting of 15 and 7

Table 2.6 Summary of data files in SPEDDI

Computed data files*)	System data files**)
Wind field data	Nuclear site characteristic data
Concentration data	Meteorological observation data
Dose data	Topographical data
	Isotopic composition data
	Nuclide physical data

*) Files for calculated results.

**) Files prepared in advance by SPEEDI.

nuclides, would be released at the rate of 1000 Ci/hour* and 1 Ci/hour, respectively. The plume would be released at the height of 10 m and the burnup would be assumed to be 10000 MWd/t.

i) Through the SITE command the accident site and facility etc. are specified in the operand in the following format.

SITE[Q]	{ site name, facility name, { * / release height } / , longitude, latitude, terrain height, release height } [, burnup]

It should be noted that the user must choose one item of the two in the brace. When items in the bracket is not specified, a default value is automatically used by SPEEDI. By means of the addition of Q just after the command, SPEEDI issues prompt messages to the user so that he can operate SPEEDI without taking care of the input format. In the case of the accident assumed here, the following input should be made.

```
SITE    TOKAI,    JPDR,    10.,    10000.
```

ii) By using the TIME command, shutdown and release starting time, etc. are inputted.

TIME[Q]	release starting time (YYMMDD) , release starting time (HHMMSS) , shutdown time (YYMMDD) , shutdown time (HHMMSS) , prediction starting time (YYMMDD) , prediction starting time (HHMMSS) , predicted period (HHMMSS) , damping interval (HHMMSS)

The input for the accident is shown as follows.

```
TIME    810820,  150000,  810820,  150000, +
        810820,  150000,  20000,   10000
```

iii) On the basis of above condition, wind field calculation among sequential ones leading to doses starts through the WIND command. Atmospheric stability, computational codes and domain which can be selected between the two, local scale in 50 km X 50 km or regional scale in 200 km X 200 km, etc. are required to calculate the wind field.

---

* As the units of activity, dose equivalent and exposure we use not the SI unit but Curie (Ci), rem and roentgen (R) which are in common use from the viewpoint of practice.
1 Ci = 3.7×10^{10} Bq, 1 rem = 10 mSv, 1 R = 2.58×10^{-4} C/kg.

WIND[Q]	model name ,{LOCAL / REGIONAL} [, prediction starting time (YYMMDD) , prediction starting time (HHMMSS) [, predicted period (HHMMSS) [, damping interval (HHMMSS)]]] [, WEF = meteorological data file name] [, WIF = wind field data file name] [, STAB = {A / B / C / D / E / F / G}]

After the WIND command, the execution command SUB is used for starting computation. When the SUB command is specified, SPEEDI issues values of its table of the conversational control program, so that the user can confirm the values of parameters to be used in the corresponding calculation. By checking the display the user can correct erroneous input before the calculation. The input of the accident is shown as follows.

```
WIND    WIND04,    LOCAL,    STAB = D
```

On the basis of these data, using the observed wind data as shown in **Fig. 2.9**, the calculation is carried out and the results of the wind field is shown in **Figs. 2.10** and **2.11**. **Figure 2.10** represents a horizontal section at the height of 100 m above sea level.

iv) The CONC command for calculating nuclide concentration is used in the following input format.

CONC[Q]	model name ,{LOCAL / REGIONAL} [, prediction starting time (YYMMDD) , prediction starting time (HHMMSS) [, predicted period [, damping interval]]] [, RELT = release continuing period] [, N1 = release nuclide 1 (group)] [, N2 = release nuclide 2 (group)] [, N3 = release nuclide 3] [, R1 = total release of nuclide 1] [, R2 = total release of nuclide 2] [, R3 = release of nuclide 3] [, WIF = wind field data file name] [, INCF = instant concentration data file name] [, SFCF = surface concentration data file name]

The input for the assumed accident is

```
CONC    PRWDA,   LOCAL
```

With respect to this calculation the concentration is calculated on the assumption of continuous unit release without decay of radioactivity. If a more detailed information on source terms such as the temporal variation of the release were available, e.g., at several hours after the accident, the concentration would be calculated in a refined way by means of inputs of accurate information on duration of the release, etc.

The calculated results of the concentration are exemplified in **Figs. 2.12** and **2.13**, which represent hourly average concentration of noble gas near the ground and surface concentration of ^{131}I, respectively.

v) As a next command, release information for source terms, such as time at which release rate is measured or estimated, etc. is employed in the following format.

```
REL[Q]
        , mode number of release information
        , determined time of release rate ( YYMMDD )
        , determined time of release rate ( HHMMSS )
      [ , nuclide name 1
        , release rate 1
      [ , nuclide name 2
        , release rate 2
      [ , nuclide name 3
        , release rate 3 ] ] ]
```

Mode number of release information indicates an available type of that, e.g., either total release rate of noble gas or release rate of a particular nuclide, which will be described in detail in Chapter 4. The input of the assumed accident is

```
REL  1, 810820, 150000, NOBLE, 1000., IODINE, 1.
```

vi) As a final sequential calculation through the DOSE command dose calculation is performed using the concentration data file created by the preceding calculational flow.

```
DOSE[Q]
        model name
      , { LOCAL    }
        { REGIONAL }
      [ , prediction starting time ( YYMMDD )
        , prediction starting time ( HHMMSS )
      [ , predicted period
      [ , damping interval ] ] ]
      [ , INCF  = instant concentration file name ]
      [ , GMF   = exposure rate data file name    ]
      [ , CUMF  = external dose data file name    ]
      [ , THYF  = thyroid dose data file name     ]
      [ , INHF  = internal dose data fiel name    ]
```

The input of the assumed accident is

```
DOSE    CIDE,  LOCAL,  PRWDA
```

Figure 2.14 and **2.15** show the examples of display obtained in this dose calculation; the former indicates the distribution of external gamma-dose from the radioactive cloud and the latter the thyroidal dose distribution.

The several displays of the results in the preceding calculations are obtained through the graph commands made by adding G in front of the corresponding commands, e.g., GWIND, GCONC, or GDOSE. The input format of GDOSE command is shown as an example of the graph commands in the following.

GDOSE[Q]	figure name , model name [, associated parameters]

In **Table 2.7**, printing and graphic outputs of SPEEDI are summarized.

2.3 Computer System Used for Calculation

2.3.1 Computer System and SPEEDI

The SPEEDI code system has been developed by using the computer system installed at JAERI Computing Center. The hardware configuration of our computer system is shown in **Fig. 2.16**. Three large-scale computers are being operated on loosely-coupled-multi-processor (LCMP) mode.

The global processor, i.e., system B is dedicated for timesharing use and accepts the commands from a timesharing terminal for SPEEDI.

The computational codes for simple and quick calculation can be executed on the system B in timesharing mode. The user can obtain the calculated results in thirty seconds. The codes for complex and detail calculation are executed on the system A or C. In operation of scalar mode on the system A or C, the user can obtain the calculated results of the wind field, concentration or dose in three minutes. In vector mode operation on the system A, the time is reduced within one minute.

Table 2.7 Printing and graphic outputs of SPEEDI

	Calculation (unit)	Display
Wind data		Wind arrow
Wind field	Wind vector at each mesh (m/s)	Wind arrow (Horizontal section) (Cross section)
Concentration	Hourly average (Ci/m^3) Surface concentration (Ci/m^2)	Horizontal isopleth Cross isopleth Temporal variation
Dose	Exposure rate ($\mu R/hr$) External gamma-dose (mrem) Internal dose (mrem)	Isopleth Temporal variation

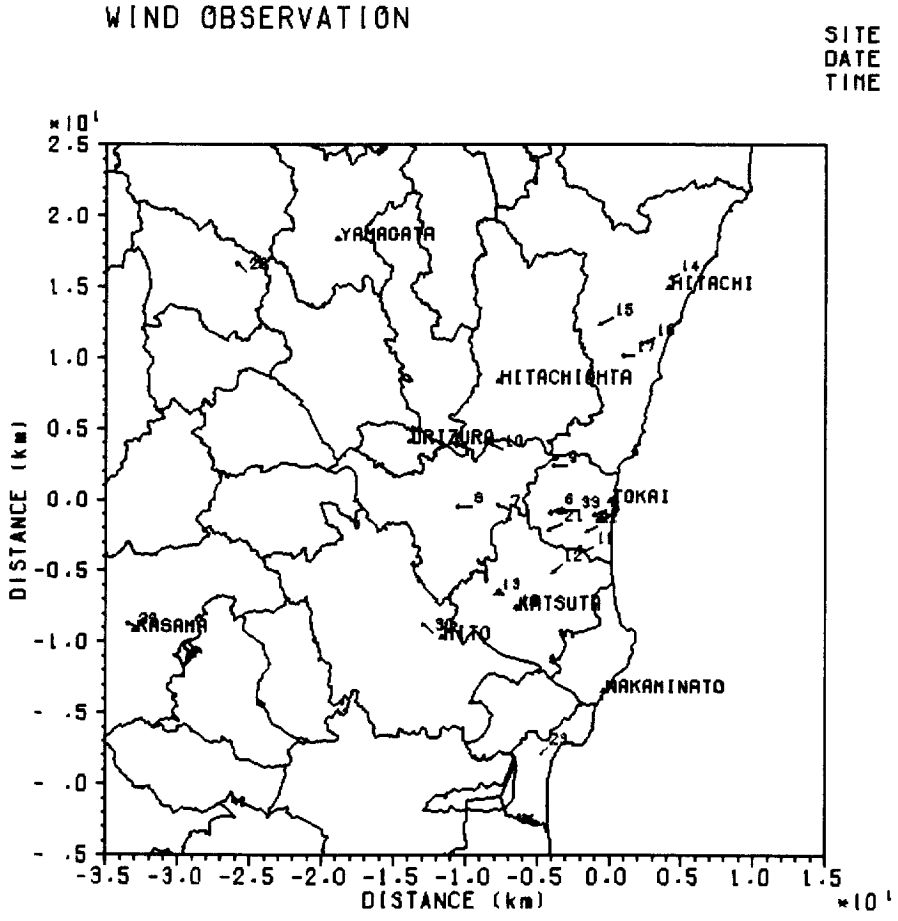

Fig. 2.9 Graphic output of observed wind data.
(original hard copy of the color graphics of SPEEDI)

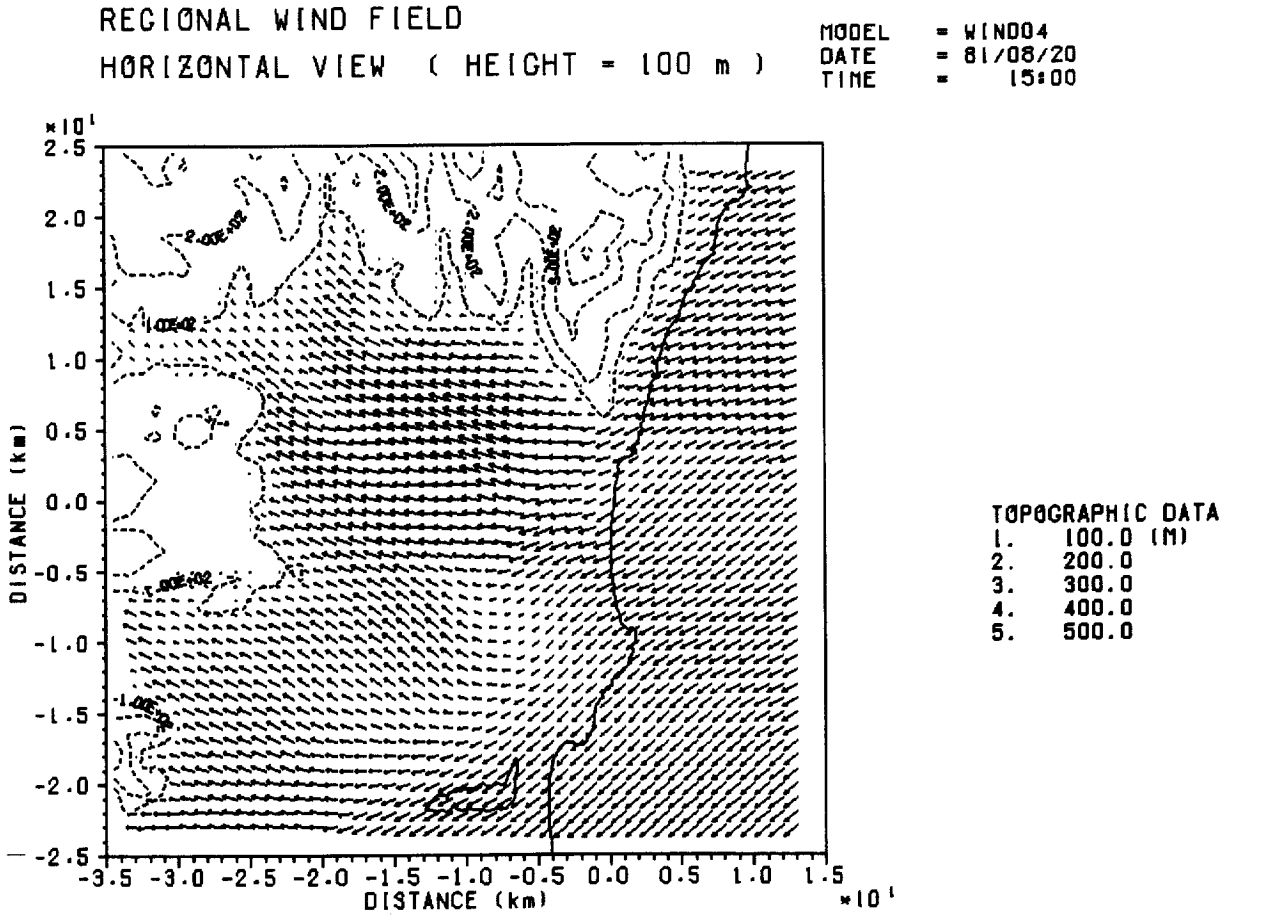

Fig. 2.10 Graphic output of calculated wind field, horizontal view. (original hard copy of the color graphics of SPEEDI)

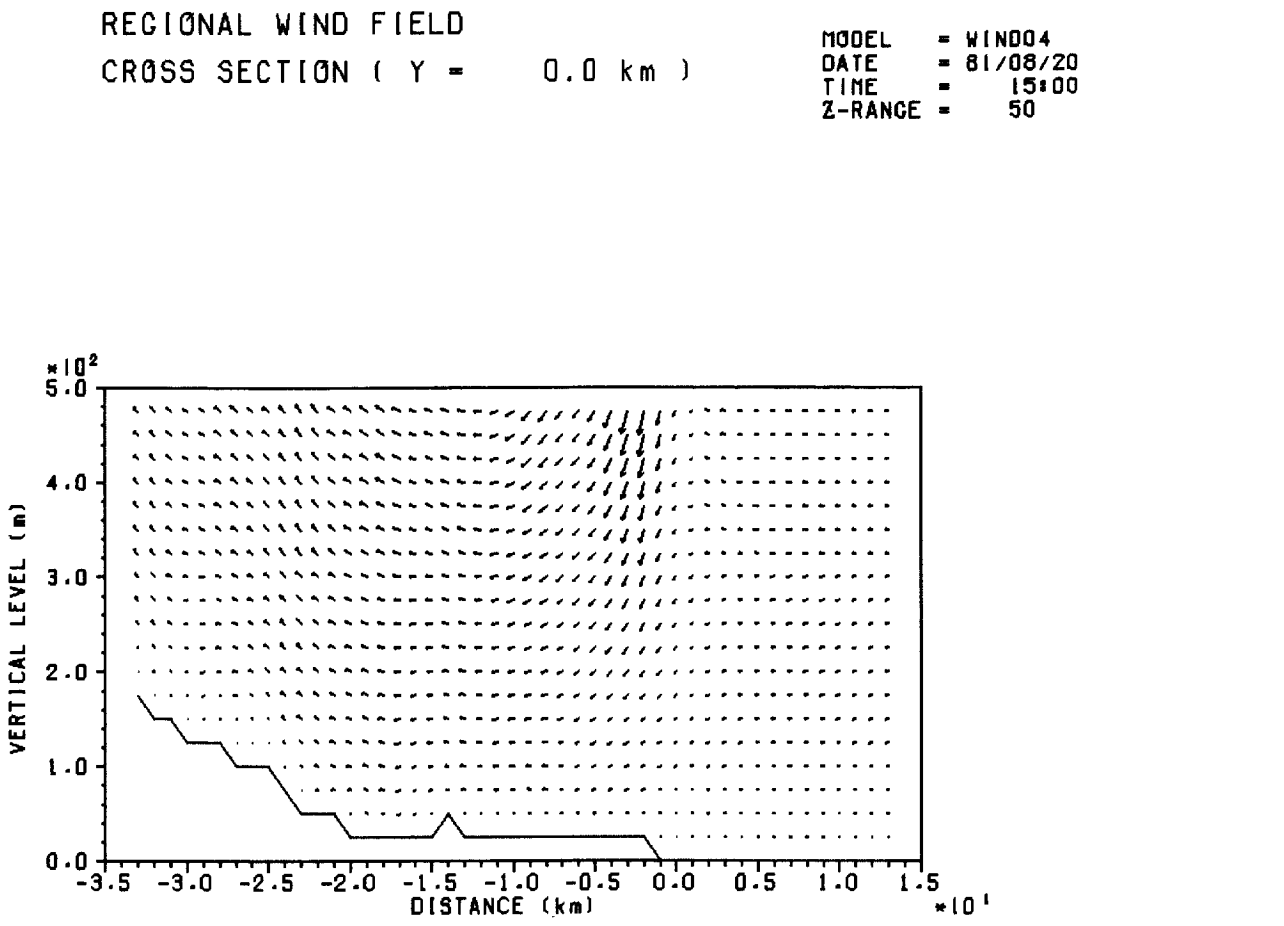

Fig. 2.11 Graphic output of calculated wind field, cross sectional view. (original hard copy of the color graphics of SPEEDI)

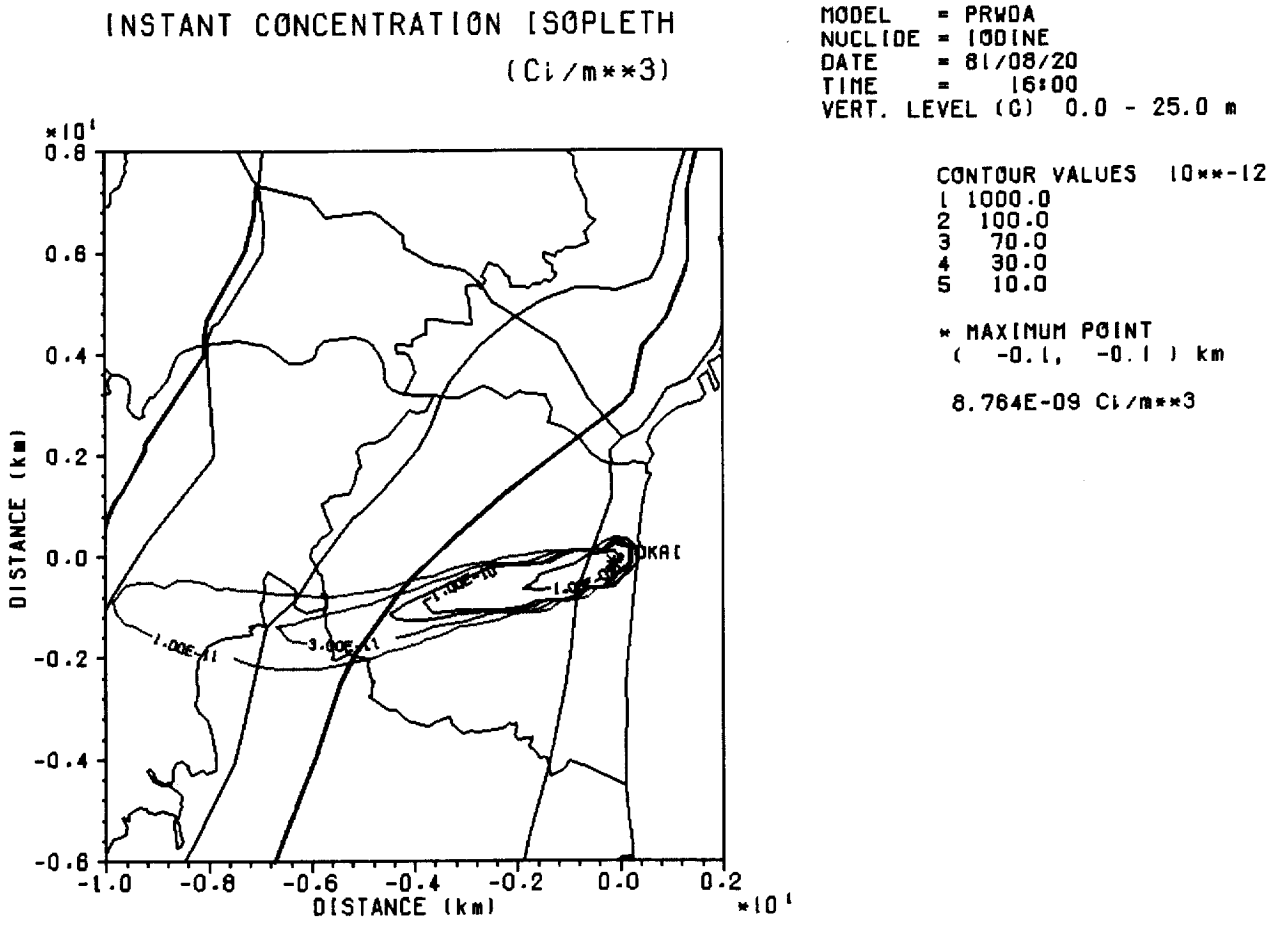

Fig. 2.12 Graphic output of concentration distribution at the ground level. (original hard copy of the color graphics of SPEEDI)

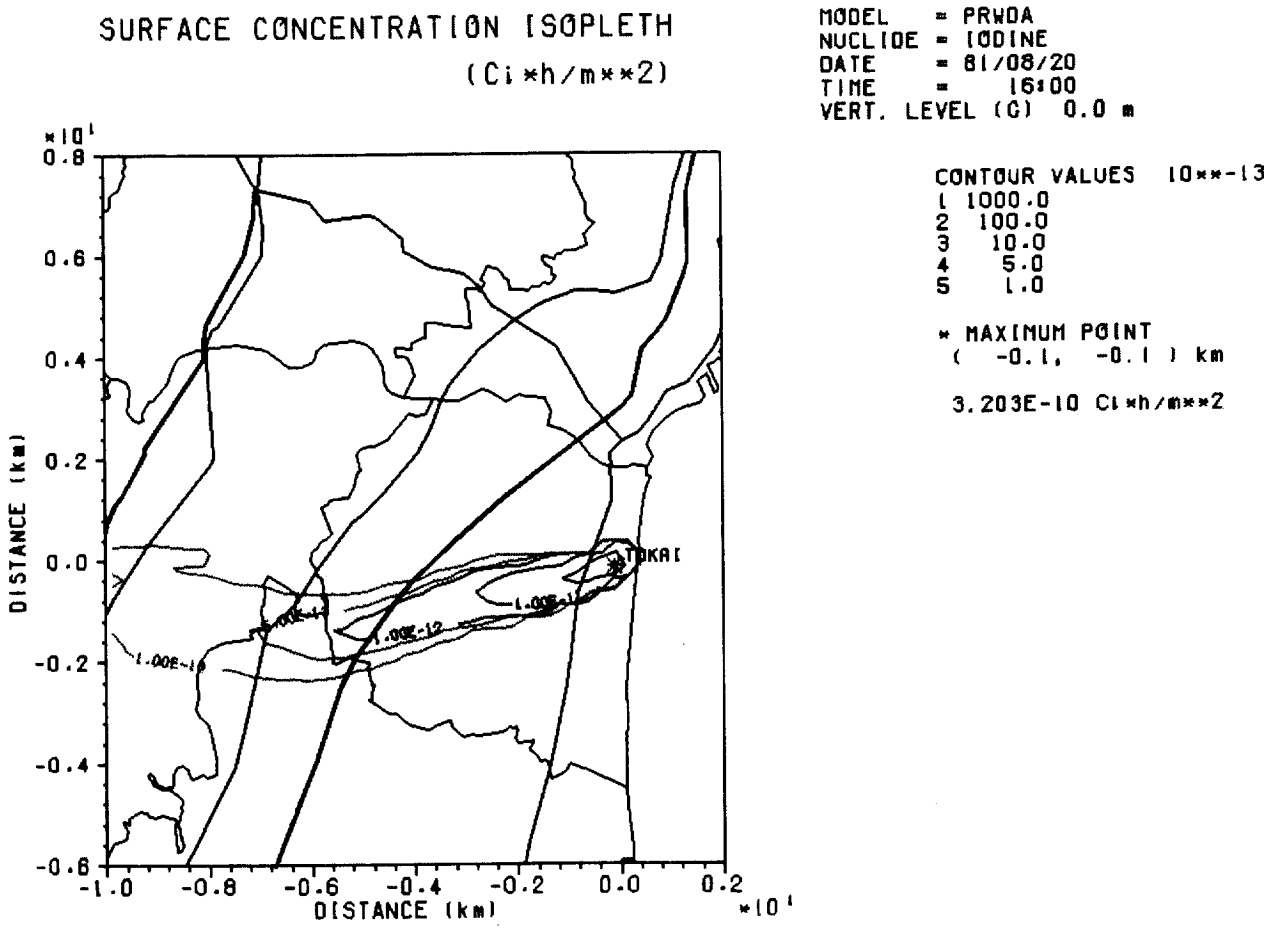

Fig. 2.13 Graphic output of distribution of iodine deposited on the ground. (original hard copy of the color graphics of SPEEDI)

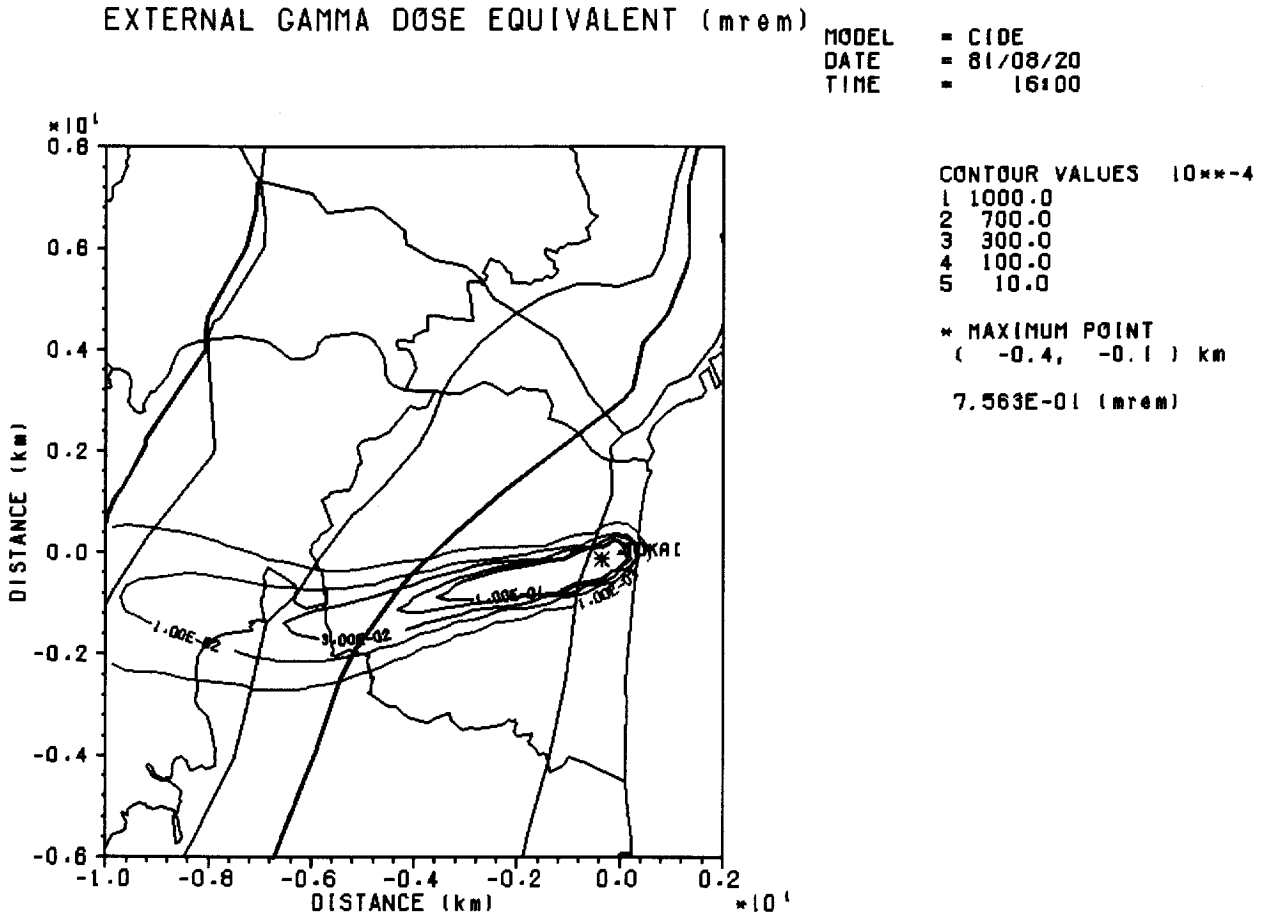

Fig. 2.14 Graphic output of external gamma-dose-equivalent distribution. (original hard copy of the color graphics of SPEEDI)

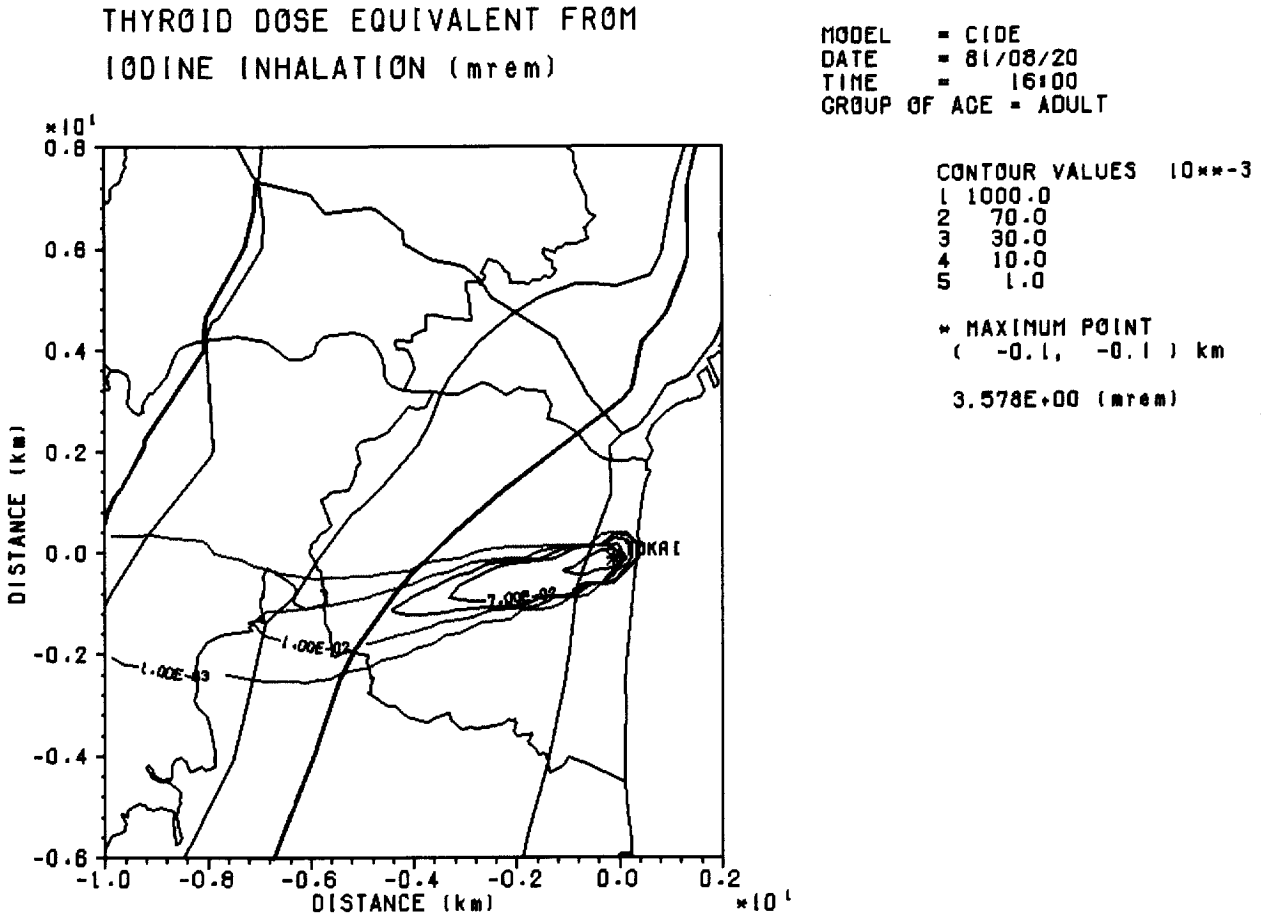

Fig. 2.15 Graphic output of thyroid dose-equivalent distribution. (original hard copy of the color graphics of SPEEDI)

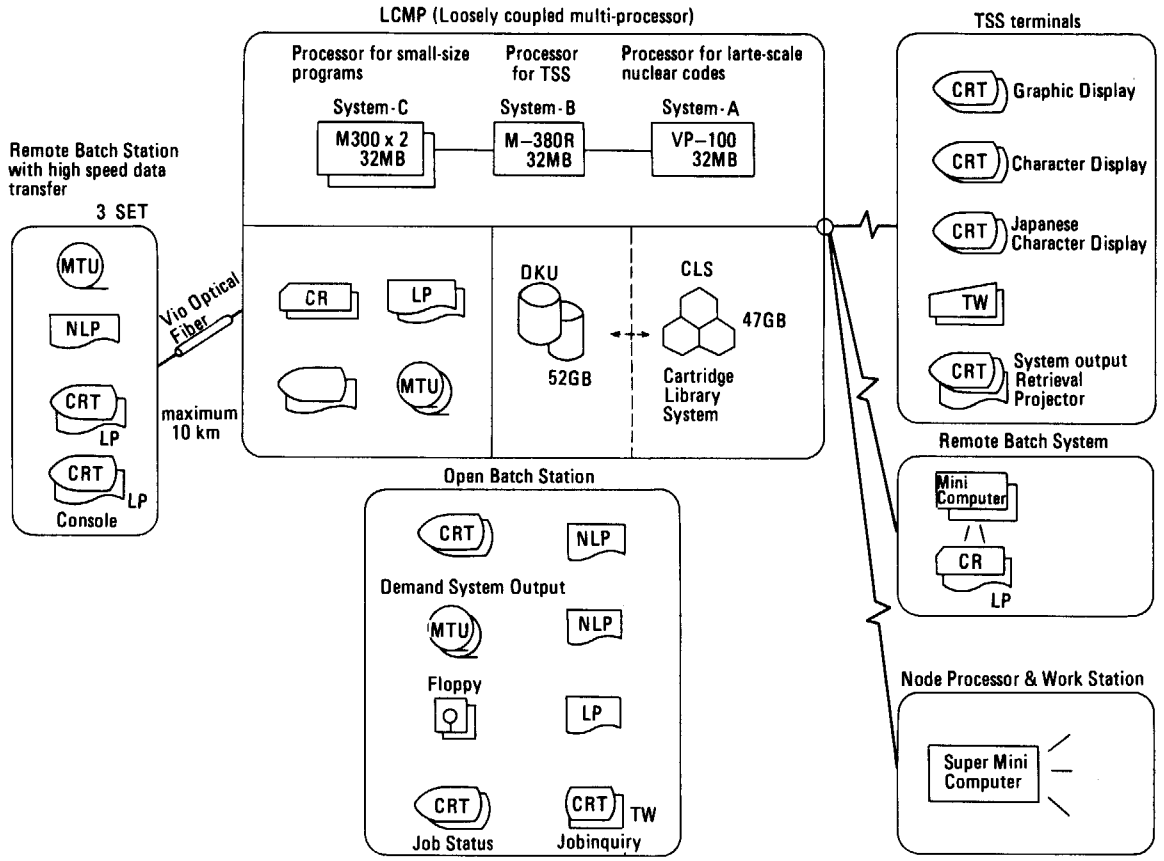

Fig. 2.16 Computer system at JAERI.

As for the timesharing terminal for SPEEDI, we are using a Japan-made rester-scan type color graphics terminal with 4000 X 4000 resolution. It is connected with the system B, i.e., the computer dedicated for timesharing use, using a 9600 bits/second communication line.

2.3.2 High Speed Computation by Vector Processor

In the present SPEEDI code system, codes for detailed calculation such as WIND04 and PRWDA require rather lengthy computation time. For example WIND04 and PRWDA require two and three minutes of execution time respectively on FACOM M-380 computer with performance of 25 MIPS (Million Instructions Per Second) or 9 MFLOPS (Million Floating Operations Per Second). It is desirable to reduce the computation times for quick responses in case of an emergency. Thus the codes WIND04 for wind field, PRWDA for concentration and CIDE for dose calculation have been rewritten in the forms suitable to vector processing and tested on a vector processor. The results are shown in **Table 2.8**. As is shown in the Table the codes attained good performances and the performances will be more improved by refine-

Table 2.8 Computation speed ratio to FACOM M-380 computer due to vectorization of WIND04, PRWDA and CIDE code

Code	Speed ratio	Computer
WIND04	9	FACOM VP-100
PRWDA	4	FACOM VP-100
CIDE	6	FACOM VP-100

ments of vectorization in the near future.

2.3.3 Portability of SPEEDI with Minicomputers

In addition to the implementation of SPEEDI on the large-scale computers, it was one of our development goals to construct a portable code system with minicomputers. As is shown in Section 2.1, the system is rather complex one, so that it will be difficult to implement it on a minicomputer of small memory size and different architecture from our large-scale computers. For this reason, we have selected a minicomputer (FACOM S-3300) which has the same architecture, very similar functions as our large-scale computers. In the process of implementation, slight modifications on the softwares of the SPEEDI system were done to adjust it to the minicomputer. The modifications are as follows:

(1) Datapool files of direct access method (DAM) organization have been changed to ones of virtual storage access method (VSAM) organization.
(2) Name strings of files of maximum forty-four characters have been truncated to twenty-six characters.
(3) Timesharing commands in catalogued procedures and the conversational control program have been converted to those of the minicomputer.
(4) Job control procedures written in the job control languages of our large-scale computers have been converted to those of the minicomputer.

After these modifications the code system SPEEDI has been successfully implemented on the minicomputer and it has produced the same calculated results.

3 Physical Models

3.1 Main Models

3.1.1 Statistical Prediction Model

The methods for weather prediction are categorized into the dynamical methods and the statistical ones. The dynamical methods are widely used in the short term weather prediction of synoptic and global scale, and they achieve considerable success. However, it is not easy to apply the dynamical methods to the weather prediction of local scale. The main difficulty arises from the shortage of the data for the initial and the boundary conditions. The local wind circulation is complicated and dependent on the places, so that it requires dense observation of meteorological data to define the initial state and the boundary conditions. Though several researchers have proposed the dynamical models for the local-scale weather prediction, they are still in research level and they cannot be used routinely.

The statistical prediction method is commonly used in the long term weather prediction. The method is modified and applied to the regional wind flow by Sakagami[9] as described below. The method consists of two stages, the first stage is a pre-analysis of the wind by the statistical factor analysis and the second is the prediction in the routine operation. In the pre-analysis, eigenvectors which describe the statistical features of the temporal variation of wind vectors are composed using the wind data for a long term, usually one year or two. By the use of these eigenvectors, a set of observed wind data at time t, expressed by a vector form, $W(t)$, is expanded as

$$\boldsymbol{W}(t)=\sum_{k=1}^{2N} A_k \cdot \boldsymbol{P}_k, \qquad (3.1.1\text{-}1)$$

where P_k is the k-th eigenfunction, A_k is its amplitude and N is the number of meteorological stations. The reason why the dimensions of $\boldsymbol{W}$ and $\boldsymbol{P}$ are $2N$ is that a wind vector at each station is a two dimensional vector. A_k is obtained by

$$A_k(t)=\boldsymbol{W}(t)\cdot\boldsymbol{P}_k, \qquad (3.1.1\text{-}2)$$

because $\boldsymbol{P}_k$s are orthogonal with each other. If the summation of Eq. 3.1.1 is done for all eigenfunctions (k = 1, $2N$), Eq. 3.1.1 is exactly valid. However the summation is sometimes done for the components of major contribution. The advantage of the transformation of Eq. 3.1.1-1 into Eq. 3.1.1-2 is that one may follow the temporal variation of each A_k instead of that of $\boldsymbol{W}$. The temporal variation of A_k is more systematic than that of each component of $\boldsymbol{W}$, because each eigenfunction $\boldsymbol{P}_k$ expresses a statistical feature common to many stations. Although A_k shows systematic variation with time, the change is still large so that the temporal extrapolation is difficult. In order to get the time series which changes moderately, a further transformation is carried out. The time series of A_k is rearranged to vectors as

$$\boldsymbol{A}_k(t) \quad =(A(\ t\ ), A(t+1), A(t+2), A(t+3), A(t+4), A(t+5))$$

$$\boldsymbol{A}_k(t+1)=(A(t+6), A(t+1), A(t+2), A(t+3), A(t+4), A(t+5))$$

$$\boldsymbol{A}_k(t+2)=(A(t+6), A(t+7), A(t+2), A(t+3), A(t+4), A(t+5))$$

$$\boldsymbol{A}_k(t+3)=(A(t+6), A(t+7), A(t+8), A(t+3), A(t+4), A(t+5))$$

$$\boldsymbol{A}_k(t+4)=(A(t+6), A(t+7), A(t+8), A(t+3), A(t+4), A(t+5))$$

$$\boldsymbol{A}_k(t+5)=(A(t+6),\ A(t+7),\ A(t+8),\ A(t+3),\ A(t+10),\ A(t+5))$$

$$\boldsymbol{A}_k(t+6)=(A(t+6),\ A(t+7),\ A(t+8),\ A(t+3),\ A(t+10),\ A(t+11))$$

. . . . . .

. . . . . .

. . . . . .

. . . . . .

The eigenfunctions for the variation of A are also obtained in the pre-analysis and a set of A is expanded as

$$\boldsymbol{A}(t)=\sum_l B_l(t)\cdot\boldsymbol{H}_l \qquad (3.1.1\text{-}3)$$

where $\boldsymbol{H}_l$ is the eigenfunction, and the subscript k is omitted. The coefficient B_l is obtained by

$$B_l(t)=\boldsymbol{A}_l\cdot\boldsymbol{H}_l \qquad (3.1.1\text{-}4)$$

The B_l changes so moderately with time that the extrapolation is not difficult. The future values of B_l are predicted by the extrapolation and the $\boldsymbol{A}$ is obtained by Eq. 3.1.1-3. The predicted values of wind are also computed by Eq. 3.1.1-1. The general flow of a routine prediction is summarized in **Fig. 3.1**. The arrows show the data flow.

In the SPEEDI system, the statistical wind prediction model mentioned above is combined with WEADUS2, Weather Data Update System. Then the predicted values of wind can be used in the same manner as observed ones for the computation of wind field.

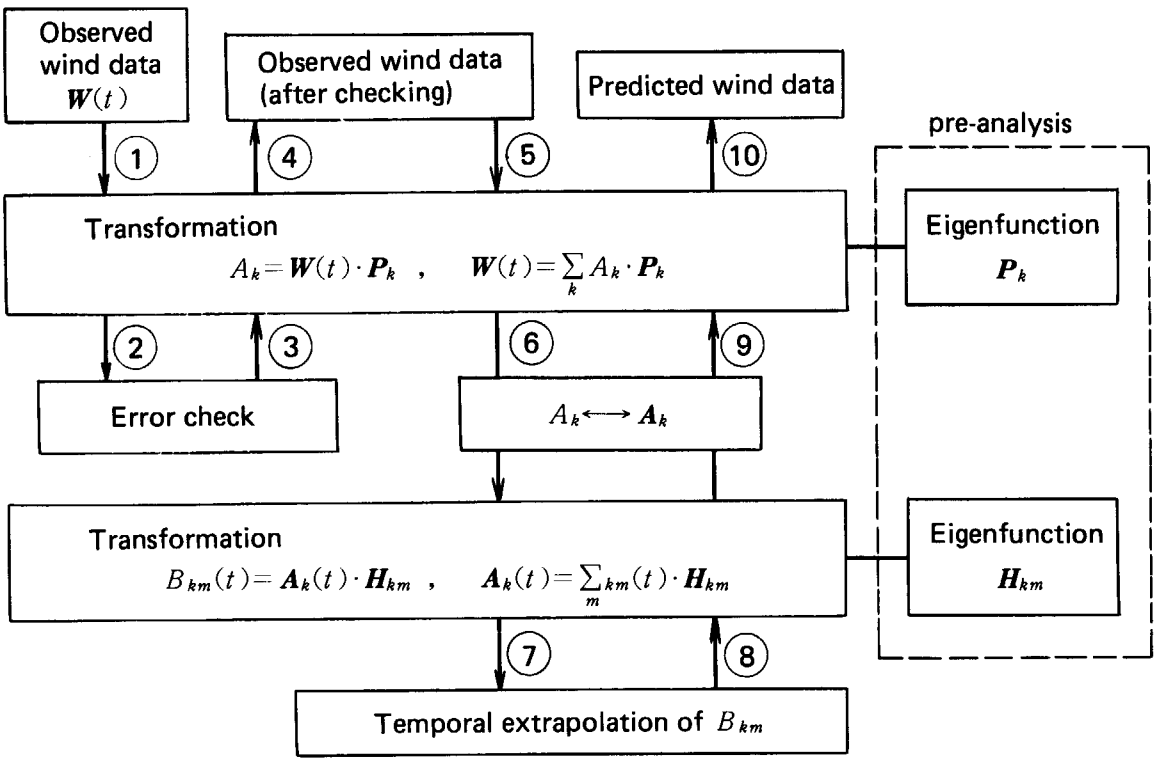

Fig. 3.1 Overview of the statistical prediction method. The arrows show the data flow.

3.1.2 Wind Field Model

(1) Description of the model

WIND04[10] is a computer code that calculates three dimensional mass-consistent wind field using data of wind and atmospheric stability. It is important that the wind field in which materials are transported should satisfy the mass conservation law, because the erroneous convergence or divergence in the wind field may result in the convergence or divergence of the materials which causes unrealistically high or low concentrations. If the divergence of the wind field is 2.78×10^{-6} (s^{-1}), the total mass in a unit cell changes by 1% during an hour's integration. When a regional wind field is interpolated by weighting observed data with inverse square of the distances, its evaluated divergence included is nearly 10^{-4} (s^{-1}). Suppose that the difference of the interpolated wind is 1 m/s between the neighboring grid points and the mesh width is 1 km, the magnitude of divergence is 10^{-3}. Then the error of divergence must be reduced by the order of three.

As the consequence of the imposition of mass conservation, WIND04 reflects the effect of topography on the wind field. Over the complex terrain the structure of the wind field is rather complicated even in the neutrally stratified condition. A part of the airflow goes over the mountain and the other part goes around it. When the atmosphere is stably stratified, the major flow goes around the mountain. On the other hand, when the atmosphere is unstable the major flow may go over it. A valley may cause a channeling effect for the wind. It is difficult to monitor such various kind of airflow by a network of anemometers. Furthermore, the vertical component of the wind, which is essentially important in the flow over complex terrain, is not directly measured by an ordinary observation. Then a certain model is needed to deduce the three dimensional wind field from limited number of wind data. The computer code, WIND04, computes the airflow around topographic obstacles by the iterative computation for reduction of the divergence and convergence at the surface of topography.

This type of the computer code is originally developed by Sherman[6] and is used in the

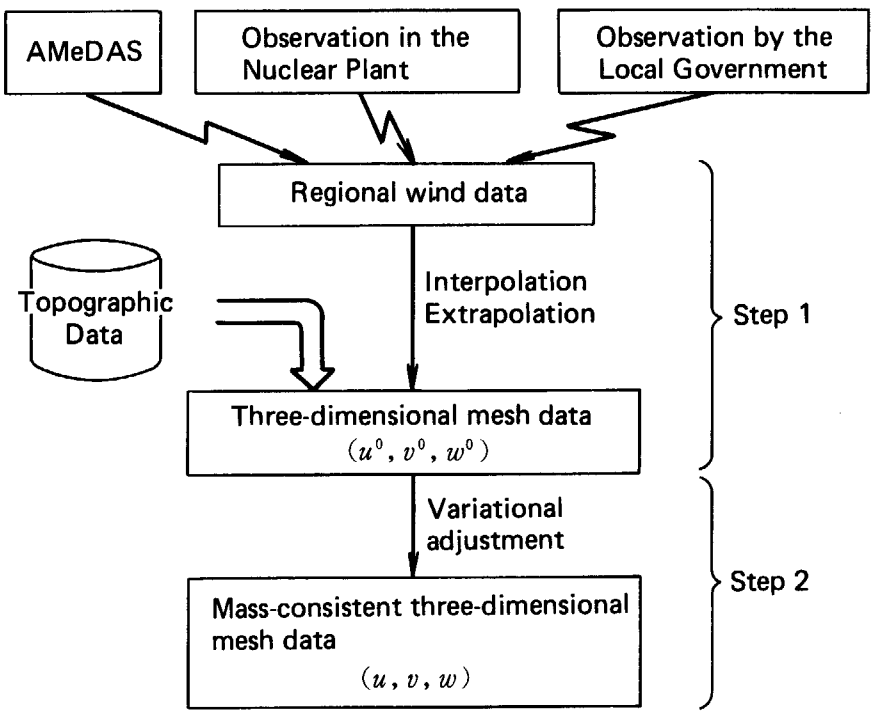

Fig. 3.2 Overall concept of the method for the calculation of three-dimensional mass-consistent wind field.

ARAC system.[1] The general concept of the calculational flow is expressed in the **Fig. 3.2.** In the first step of the calculation, an initial guess of the wind vector at each grid is computed using the observed or predicted wind data produced by WEADUS2. The surface wind is interpolated by

$$(u,v)_{i,j}=\frac{\sum_{n=1}^{N}(u,v)_n/r_{n,ij}^2}{\sum_{n=1}^{N}(1/r_{n,ij}^2)}, \tag{3.1.2-1}$$

where $(u,v)_{i,j}$ is the horizontal components of the wind at the (i,j)-th grid, $(u,v)_n$ is the observed wind components at the n-th meteorological station, and $r_{n,ij}$ is the distance between the n-th station and the (i,j)-th grid. The wind vectors in the upper layers are interpolated and/or extrapolated as follows. The interpolated surface wind $(u,v)_{i,j}$ is extrapolated up to 200 m above the ground by the power law expressed as

$$u(z)=u_{\mathrm{obs}}\left(\frac{z}{z_{\mathrm{obs}}}\right)^p. \tag{3.1.2-2}$$

Above this layer, the observed upper wind data is used. If the upper wind data (u_1,v_1) and (u_2,v_2) is obtained at the height of z_1 and z_2, the wind data between these two levels is interpolated by

$$u=a\log z+b, \tag{3.1.2-3}$$

$$v=c\log z+d. \tag{3.1.2-4}$$

The coefficients $a.b, c$ and d are determined so that the interpolated values coincide with the observed values at z_1 and z_2. Above the highest level of wind observation, the wind is assumed to be constant. When upper wind data are not available, the power law, Eq. 3.1.2-2 is extended to higher levels.

In the second step, the initial guess is adjusted so that the wind field satisfied the equation of mass conservation,

$$\frac{\partial u}{\partial x}+\frac{\partial v}{\partial y}+\frac{\partial w}{\partial z}=0, \tag{3.1.2-5}$$

with possibly small adjustment. The wind field (u, v, w) should satisfy Eq. 3.1.2-5 and the total of the adjustment,

$$\int_V[\alpha_1^2(u-u^0)^2+\alpha_1^2(v-v^0)^2+\alpha_2^2(w-w^0)^2]\,dV \tag{3.1.2-6}$$

should be kept as small as possible. According to the variational method, such wind field is obtained as a set of functions which minimizes a functional

$$E=\int_V\left[\alpha_1^2(u-u^0)^2+\alpha_1^2(v-v^0)^2+\alpha_2^2(w-w^0)^2+\lambda\cdot\left[\frac{\partial u}{\partial x}+\frac{\partial v}{\partial y}+\frac{\partial w}{\partial z}\right]\right]dV, \tag{3.1.2-7}$$

where u^0, v^0, w^0 are the interpolated wind components, α_1 and α_2 are weighting coefficients which prescribe the ratio of horizontal adjustment to vertical adjustment and λ is a Lagrangian multiplier. In this case, this Lagrangian multiplier plays the role of velocity potential of the adjustment. The condition giving a stationary value of E yields four Eular-Lagrange equations,

$$u=u^0+\frac{1}{2\alpha_1^2}\cdot\frac{\partial\lambda}{\partial x} \tag{3.1.2-8}$$

$$v=v^0+\frac{1}{2\alpha_1^2}\cdot\frac{\partial\lambda}{\partial y} \tag{3.1.2-9}$$

$$w=w^0+\frac{1}{2\alpha_2^2}\cdot\frac{\partial\lambda}{\partial z} \tag{3.1.2-10}$$

and

$$\frac{\partial u}{\partial x}+\frac{\partial v}{\partial y}+\frac{\partial w}{\partial z}=0, \tag{3.1.2-11}$$

with three boundary conditions,

$$\lambda\delta(u)\cdot n_x=0,\ \lambda\delta(v)\cdot n_y=0,\ \lambda\delta(w)\cdot n_z=0, \tag{3.1.2-12}$$

where $\delta(u)$, $\delta(v)$ and $\delta(w)$ are the first variations of variables, and n_x, n_y and n_z are direction cosines of a unit vector vertical to the boundary surface for computation area. Rearranging the Eqs. 3.1.2-8 to 3.1.2-11, a Poisson's equation for λ,

$$\frac{\partial^2\lambda}{\partial x^2}+\frac{\partial^2\lambda}{\partial y^2}+\frac{\alpha_1^2}{\alpha_2^2}\cdot\frac{\partial^2\lambda}{\partial z^2}=-2\,\alpha_1^2\cdot\left[\frac{\partial u^0}{\partial x}+\frac{\partial v^0}{\partial y}+\frac{\partial w^0}{\partial z}\right] \tag{3.1.2-13}$$

is derived. The right-hand side expresses the divergence of the interpolated wind field. The problem is reduced to solve Eq. 3.1.2-13 with the boundary conditions 3.1.2-12. Once λ is obtained, the adjusted wind components are computed by Eqs. 3.1.2-8 to 3.1.2-10.

For the numerical computation, Eqs. 3.1.2-8 to 3.1.2-13 are transformed to finite difference equations. The staggered scheme is employed in order to avoid the computational error and to increase the resolution of the topography. Eq. 3.1.2-13 is solved iteratively by SOR (successive over-relaxation) method.

(2) Efficiency of variational adjustment

The divergence involved in the adjusted wind field is computed at each grid point for various stages of iterative calculation. The result is listed in **Table 3.1**. In the left-hand column the degree of the precision of the solution is described by the relative change of λ. The values written in the top line express the order of magnitude of the divergence, and the figures in the Table are numbers of cells which contain the divergence listed at the top line. It is clearly seen that the erroneous divergence contained in the interpolated wind field is reduced by the order of four, even if a rather rough convergence criterion is adopted for λ.

(3) Discussions

WIND04 is not a hydrodynamic model that is currently under study. It is basically a code that uses one of the interpolation methods, so that the quality and the quantity of input data directly affect results. So long as the each wind observation represents the wind of the wide region around the station well, the results of WIND04 are of much confidence.

Table 3.1 Divergence of adjusted wind field

Criteria used in the iteration for λ	Order of magnitude of divergence calculated at each cell															
	10^{-6}	10^{-7}	10^{-8}	10^{-9}	10^{-10}	10^{-11}	10^{-12}	10^{-13}	10^{-14}	10^{-15}	10^{-16}	10^{-17}	10^{-18}	10^{-19}	10^{-20}	
10^{-2}	71	2599	891	47	2	0	0	0	0	0	0	0	0	0	0	
10^{-3}	29	2587	929	61	3	1	0	0	0	0	0	0	0	0	0	
10^{-4}	0	1740	1681	182	7	0	0	0	0	0	0	0	0	0	0	
10^{-5}	0	1729	1679	184	16	2	0	0	0	0	0	0	0	0	0	
10^{-6}	0	1737	1723	143	7	0	0	0	0	0	0	0	0	0	0	
10^{-7}	0	0	326	1999	1189	86	10	0	0	0	0	0	0	0	0	*
10^{-8}	0	0	0	1464	1875	270	1	0	0	0	0	0	0	0	0	*
10^{-9}	0	0	0	418	2027	1143	22	0	0	0	0	0	0	0	0	*
10^{-10}	0	0	0	428	517	1998	662	5	0	0	0	0	0	0	0	*
10^{-12}	0	0	0	428	518	63	251	2216	134	0	0	0	0	0	0	*
10^{-14}	0	0	0	428	518	63	0	0	1234	1336	31	0	0	0	0	*
10^{-16}	0	0	0	428	518	63	0	0	0	979	1355	251	11	3	2	*

* Calculated in double precission

Under some conditions, however, the distribution of the wind is so complicated that the network of wind observation is insufficient to describe it. Such a condition may occur, for instance, in winter midnight when the ground surface is cooled and the local drainage flow dominates. In such a case, the results of WIND04 may contain a large error. The function of WIND04 is only to adjust the interpolated wind field, so that it cannot predict the dynamical effects such as the wakes at the lee side of a mountain if they are not included in the observation.

The appropriate values of the parameter α_1 and α_2 are somewhat uncertain. As mentioned before, the ratio α_1/α_2 prescribes the fraction of the horizontal and vertical adjustment. When the ratio is low, the horizontal adjustment dominates and the airflow goes around the topographical obstacles, while the ratio is high, it goes over the obstacles. The atmospheric stability may concern with the value of the ratio. When the stability is unstable, the vertical component of the wind is fairly large and the ratio should be high. On the other hand, when the atmosphere is stably stratified, the horizontal adjustment is relatively large and the value of the ratio should become lower. The value may also be affected by the complexity of the terrain. The ratio has not yet been determined in high confidence. An appropriate value between 0.01 and 0.2 are temporally used at present, which seems to assure the reasonable results. Determination of the value is now planned by the use of results of wind tunnel experiments and those of wind observation over the complex terrain. Hydrodynamic models will offer many suggestions for the values of α_1 and α_2.

A typical computation time for the running of WIND04 was 90 seconds for the calculation of $51 \times 51 \times 21$ meshes on FACOM M-380 computer. The vectorized version of WIND04 has completed the same calculation in less than ten seconds by a vector computer FACOM VP-100.

3.1.3 Transport and Diffusion Model

(1) Random-walk method to solve a transport-diffusion equation

Numerical solutions of the transport-diffusion equation based on the assumption of gradient-transfer theory(K-theory) and the continuity equation have long been used to simulate the spatial and temporal concentration in complex terrain. The ADPIC[7] code in ARAC, which employs a PICK[11] method to solve the equation, is a famous one as the code successfully applied to accidental releases.

Although finite-difference methods and the PICK method are currently used to solve the equation, these methods are mainly applicable to the volume source whose spatial scale is at least two times the grid interval used in the model. Due to this major limitation in predicting the concentration from a point source such as a release from a stack, the PRWDA[12] code employs the random-walk method of particles based on K-theory. The advantages are firstly that, the enough large scale of cloud to determine the concentration gradient, which the PICK method also needs, is not necessary because the random-walk method moves each particle independently. Secondly, the procedure is simple, and thirdly, the fictitious Eulerian numerical diffusion from which simple finite-difference methods suffer is eliminated by using Lagrangian marker particles.

Several random-walk methods have been proposed and are categorized into two types;
(a) those[11], using a simple random-walk displacement based on K-theory, and
(b) those[14,15], which use Markov process taking into account the turbulence spectrum.

Although the simulations of the atmospheric diffusion with a combination of turbulent closure theory and Markov process theory have been performed recently for the research purpose[16], these models require a considerable amount of computation time. Therefore,

the method of type (a) is used in the PRWDA code. The defect of the simple random-walk methods is that the unrealistic flux is generated which is not proportional to the concentration gradient but to the concentration when the methods fail to account for the inhomogeneous turbulence varying with height. To avoid this problem, PRWDA employs the PICK method for vertical diffusion after the evolution of cloud exceeds two times as wide as the vertical grid cell.

In order to simulate motions of a particle, a sequence of turbulent fluctuation steps, Δx_i, Δy_i and Δz_i at time intervals of Δt_i, will be necessary. The particle location at the sequential time step is determined from

$$x_{i+1}=x_i+u_i\Delta t_i+\Delta x_i,$$

$$y_{i+1}=y_i+v_i\Delta t_i+\Delta y_i,$$

$$z_{i+1}=z_i+w_i\Delta t_i+\Delta z_i, \tag{3.1.3-1}$$

where u_i, v_i and w_i are components of mean velocity which are calculated by the interpolation of three-dimensional wind field generated by WIND04. The turbulent fluctuation steps for the (x)- and (y)- components by the random-walk method are represented by random numbers which are generated following a probability density function. This function's standard deviation $\sigma_j((j=x, y, z))$ is expressed by

$$\sigma_j=\sqrt{2K_j\Delta t_i}, \tag{3.1.3-2}$$

where K_j is an eddy diffusivity coefficient. For the convenience, the PRWDA code uses an uniform probability function, so the generation of Δx_i, for example, can be expressed by

$$\Delta x_i=[R]_{-l}^{+l}, \tag{3.1.3-3}$$

where $[R]_{-l}^{+l}$ indicates a random number distributed uniformly in the range from $(-l)$ to $(+l)$. The variable (l) is selected so that Eq. 3.1.3-2 should be satisfied

$$l=\sqrt{6K_j\Delta t_i}. \tag{3.1.3-4}$$

In the PICK method applied to the (z)-direction diffusion, Δz_i is expressed by

$$\Delta z_i=w_i'\Delta t_i, \tag{3.1.3-5}$$

where w_i' is the turbulent velocity defined by

$$w_i'=(K_z/\chi)(\partial\chi/\partial z), \tag{3.1.3-6}$$

and χ means the concentration.

By using these equations, we rewrite Eq. 3.1.3-1 as follows;

$$x_{i+1}=x_i+u_i\Delta t_i+[R]_{-l}^{+l},$$

$$y_{i+1}=y_i+w_i\Delta t_i+[R]_{-l}^{+l},$$

$$z_{i+1}=z_i+w_i\Delta t_i+w_i'\Delta t_i. \tag{3.1.3-7}$$

However, the random-walk method is also used in the (z)-direction before the cloud expands.

Variables of K_j and Δt_i are selected as follows. From a practical point of view, K_j is calculated from the atmospheric stability category which is routinely observed in a nuclear power plant. The eddy diffusivity coefficient K_j is defined by

$$K_j=\frac{1}{2}\frac{d\sigma_j^2}{dt}, \tag{3.1.3-8}$$

where σ_j is a standard deviation of plume. From a practical point of view, σ_j is given as functions of the downwind distance and the stability category which is obtained in routine

observation. The formulae of $\sigma_y(=\sigma_x)$ and σ_z in this code are derived from Pasquill-Gifford (P-G) chart[17], so Eq. 3.1.3-8 is rewritten as Follows;

$$K_j = \frac{1}{2}\frac{dr}{dt}\frac{d\sigma_j^2}{dr} = u\sigma_j\frac{d\sigma_j}{dr} \quad . \tag{3.1.3-9}$$

Although the surface roughness and the sampling time vary according to the accidents, no correction to the formulae of P-G chart is given. The P-G σ_z is derived from the experiments using a ground source. Consequently, it is a problem to apply it to the elevated source in case that the turbulent condition at the release height is different from the observed stability category. In this code, three horizontal layers that piled vertically can be modeled. These are, for example, equivalent to the fully mixed layer, the neutral layer and the stable layer above mixed layer in the daytime. Upper two layer's turbulent conditions are assigned from the observation of temperature lapse rate or fluctuation of wind direction. In the later discussions, we call this assumption a multi-layer model. When efficient vertical data about the turbulence cannot be obtained, the neutral condition is assumed for the second layer. Although the main aim of this model is the simulation of the dispersion in the existence of capping inversion and so on, this is also effective for the simulation of fumigation by an

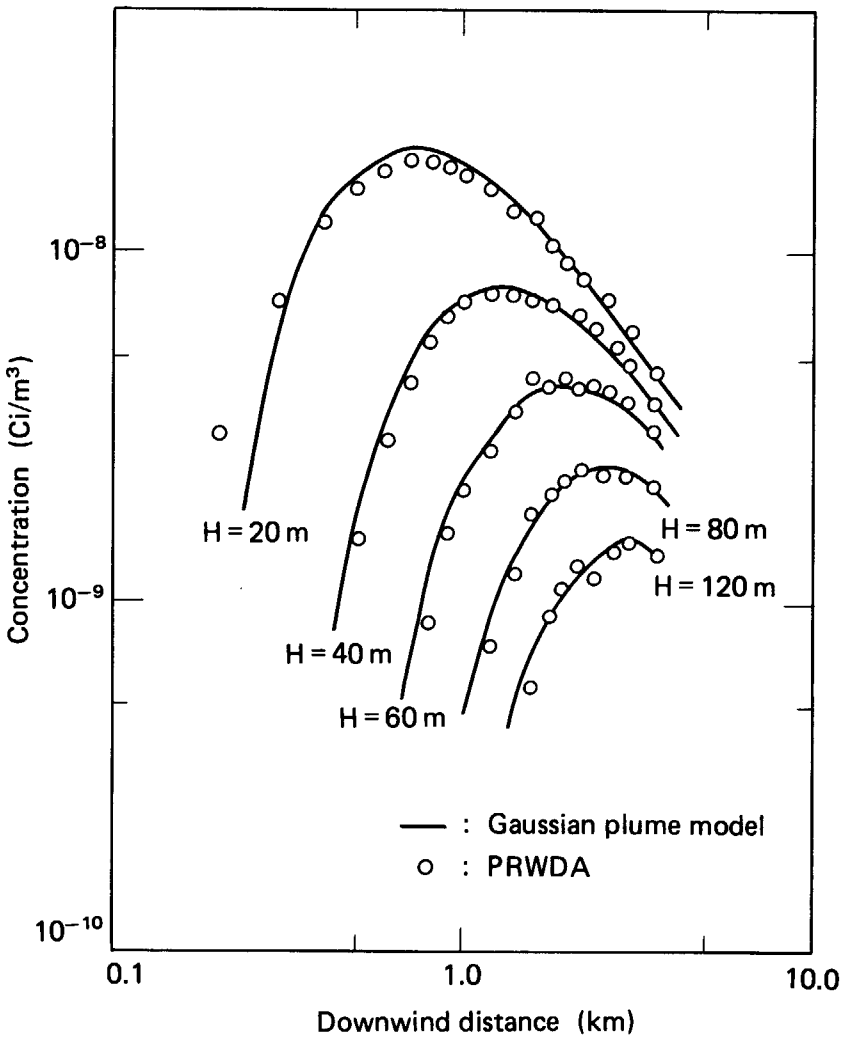

Fig. 3.3 Comparison of downwind concentration at the ground level between a Gaussian plume model and PRWDA.
The calculational conditions are that atmospheric stability is D, wind speed is 1 m/s and release height H is variable.

internal boundary layer, as will be discussed later.

Another variable, Δt_i, is restricted so that no particle moves more than one cell within one time step.

The verification of model in homogeneous airflow is performed. **Figure 3.3** shows the comparison of downwind concentration at the ground level between the Gaussian plume model and the present model. The calculational conditions are that atmospheric stability is D, wind speed is 1 m/s and release height H is variable. The good agreement of the results between models shows that the PRWDA code can simulate the gradient-transfer process correctly in the simple airflow.

The outputs of the PRWDA code are the airborne concentration (Ci/m^3) and the surface concentration (Ci/m^2) which are averaged in the predicted time. As shown in **Fig. 3.4**, the concentration presented as a cell average is calculated by the volume (or area) apportionment of a particle's activity between cells. In the figure, the overlap of a shaded area with the Eulerian grid cell determines the activity apportionment. This shaded area shows the cell in which the activity of a particle is spread uniformly. The volume(or area) averaging procedure is an effective way to reduce the statistical fluctuation caused by the sparse distribution of particles. The Eulerian cell size for recording the concentration distribution is defined automatically according to the grid cell size of topographic data. In addition, the user can change the size, if necessary.

Besides these outputs, data of particle positions are outputted when the prediction is ended. Those are utilized as the initial condition of airborne effluent at the start of the next sequential prediction, when the simulation are carried out intermittently in a real-time response.

(2) Short discussion

The PRWDA code still has several problems, though the first stage of code development has finished. The P-G standard deviation for calculation of the eddy diffusivity coefficient K_j is originally obtained under the condition in a rather smooth surface and a sampling time

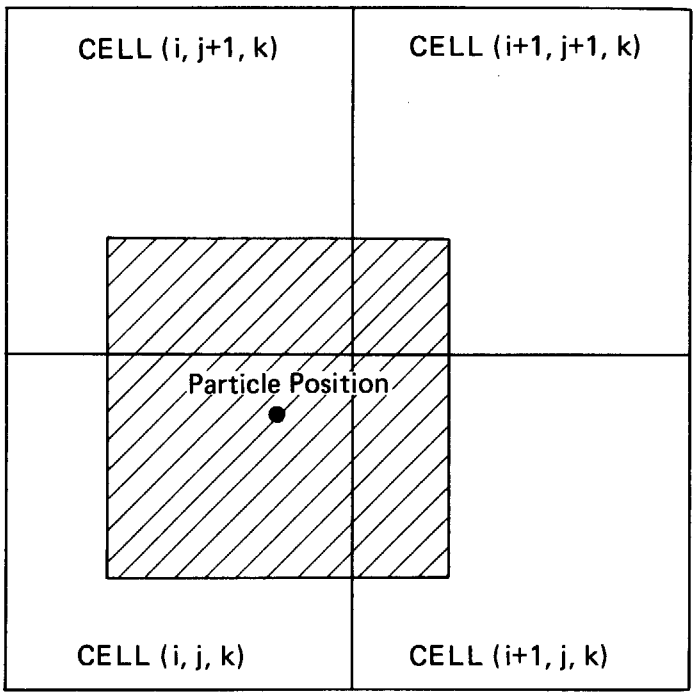

Fig. 3.4 Area weighting interpolation for calculating cell concentration.

of three to ten minutes. However in the PRWDA code, we apply K_j derived from P-G σ_j to the calculation for different conditions, because diffusivities computed by this method can be obtained easily from the routine measurements of meteorological conditions. In future, K_j will be derived from a numerical simulation such as a second-order closure model or from the precise observation of turbulence.

For the realistic estimation of deposition, a surface depletion model is employed to the dry deposition. However the washout coefficient and the deposition velocity of nuclides have big uncertainty according to the ground condition and the chemical form of nuclides, etc. Therefore, the reliability of the results of deposition may be valid only in the relative distribution pattern.

The method to present the concentration by averaged value in the cell always has more or less the defect of underestimation of the concentration near the release point. The degree of underestimation depends on the volume of grid cell, the turbulent condition and the down-wind distance.

3.1.4 Dose Model

(1) Cell-integrated dose model

A computer code using a cell-integrated dose model has been developed mainly for calculation of the external dose from an arbitrarily distributed radioactive cloud. We refer to this code as CIDE (Cell Integral Dose Evaluation)[18], which includes calculation of the internal dose due to inhalation. The available codes at present for dose evaluation only deal with the exposure to a Gaussian plume in which the concentration can be described in an analytical expression.[19,20] Therefore, the dose calculation from an arbitrarily distributed plume is needed for estimation of the radiological consequence due to the dispersion corresponding to wind field in complex terrain.

In the cell-integrated dose model, nuclides in a cell, into which a calculation space is divided, are assumed to be uniformly distributed in every part of the cell by the mean concentration. The three-dimensional integration over the cell is carried out as a constant concentration by a point kernel method. Therefore, doses attributable to each cell having unit concentration of nuclides can be evaluated independently of concentration distribution of a ratioactive cloud, and those are tabulated in order to reduce running time of computation. This is the characteristics of the cell-integrated dose model developed for SPEEDI.

The dose evaluated by the cell-integrated dose model is obtained by summing the attributable cell doses, that is :

$$D_c(x_i, y_j, 0) = \sum_{l}^{L}\sum_{m}^{M}\sum_{n}^{N} \chi(l, m, n) \cdot AD(i-l, j-m, n) , \qquad (3.1.4\text{-}1)$$

where

$D_c(x_i, y_j, 0)$ = exposure rate at the point $(x_i, y_j, 0)$ of the cell $(i, j, 1)$,

$\chi(l, m, n)$ = nuclide concentration of the (l, m, n),

$AD(i-l, j-m, n)$ = attributable dose to the point $(x_i, y_j, 0)$ from the cell(l, m, n) having unit concentration,

L , M, and N = numbers of each cell of x, y and z-coordinates.

The attributable cell dose is :

$$AD(i\ \ l, j\ \ m, n) = \int_{(i-l-1/2)DX}^{(i-l+1/2)DX} \int_{(j-m-1/2)DY}^{(j-m+1/2)DY} \int_{(n-1)DZ}^{nDZ} \frac{K \cdot \mu_{en} \cdot E \cdot \exp(-\mu r)}{4\pi r^2} \cdot B(E, r)\, dx\, dy\, dz$$

(3.1.4-2)

where

DX, DY and DZ = cell sizes of x, y and z-coordinates,
K = conversion factor into exposure rate,
μ_{en} = linear energy absorption coefficient in air,
μ = linear attenuation coefficient in air,
E = initial energy of photon,
r = distance from an infinitesimal element in the radioactive cloud to the point $(x_i, y_j, 0)$,
$B(E, r)$ = dose buildup factor.

When the concentration of plume is a Gaussian distribution, the results of CIDE code are compared with those of GAMPUL[21] which is a code developed for the accurate calculation of dose from the Gaussian distribution by numerical integration in three dimensions. **Figures 3.5** and **3.6** show the result of comparison of distribution to the downwind axis and that of distribution to the crosswind axis, respectively. The results of CIDE code may become accurate with decreasing cell size. It appears that the cell size of x and y-coordinates less than 250 m would permit us to practically use CIDE code. The cell size of 1000 m could, however, be selected for the purpose of calculating the doses at the points of 10 km apart from a release point. The results of further comparisons have been obtained in the reference (18) using different conditions of atmospheric stabilities and release heights.

(2) Thyroid dose from iodine

It is important to estimate thyroid doses due to inhalation of iodine that concentrates in thyroids weighing 20 g in adults. For deciding whether any remedy actions should be taken into account, therefore, we must estimate the doses to thyroids as accurate as possible considering age-dependence.

The thyroid dose is obtained by the equation :

$$D(Sv)=51.2\times\frac{q\cdot f_1\cdot T_{\mathrm{eff}}}{0.639}\times\frac{\varepsilon}{m}\times\frac{1}{3.7\times10^6}, \qquad (3.1.4\text{-}3)$$

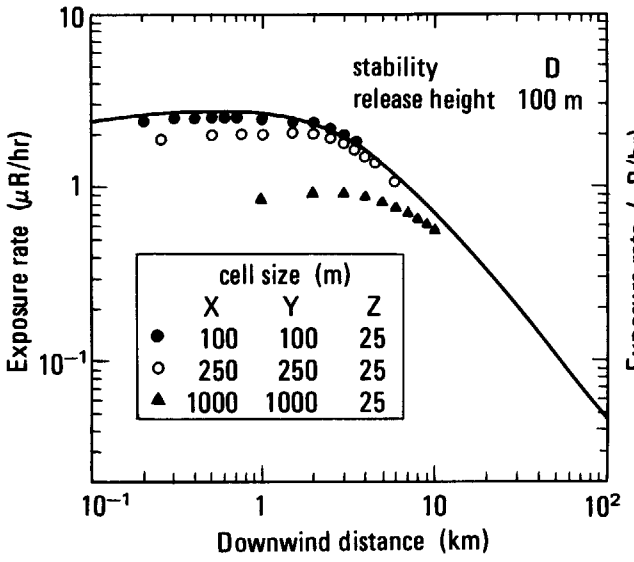

Fig. 3.5 Comparison of distribution on the downwind axis between the results of CIDE and GAMPUL in the case of Gaussian distribution. The release rate of radioactive materials is 1 Ci/hr.

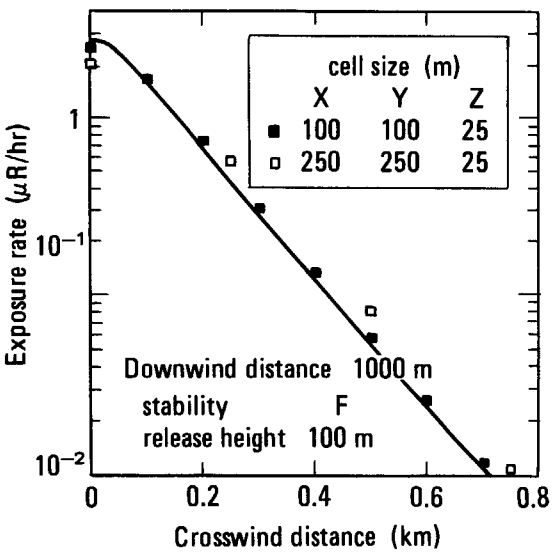

Fig. 3.6 Comparison of distribution on the crosswind axis between the results of CIDE and GAMPUL in the case of Gaussian distribution. The release rate of radioactive materials is 1 Ci/hr.

where

q = intake of radioiodine (Bq),
f_1 = thyroid uptake factor,
T_{eff} = effective half-life of iodine (day),
ϵ = effective absorbed energy of radioiodine (MeV),
m = thyroid mass (g).

Recent internal dosimetric models require the summation of attributable doses from source organs giving energy of penetrating radiation to an estimated target organ, that is,

$$H_T = 1.6\times10^{-10}\sum_s [U_s \cdot \sum_i SEE(T\leftarrow S)_i], \quad (3.1.4\text{-}4)$$

where

H_T = committed dose equivalent to a organ T (Sv),
U_s = number of nuclear transformations over 50 years in a source organ S,
$SEE(T\leftarrow S)_i$ = specific effective energy of radiation i given from a source organ S to a target organ T (MeV g^{-1}/dis).

Table 3.2 Values of parameters used for calculating thyroid doses

Age group (nuclide)	f_1	T_{eff} (day)	SEE (MeV/g·dis.)	Respiration (m^3/day)
Infant (aged 1)	0.2			6
I-129		40	3.4×10^{-2}	
I-131		6.7	1.0×10^{-1}	
I-132		0.095	2.8×10^{-1}	
I-133		0.83	2.2×10^{-1}	
I-134		0.37	3.5×10^{-1}	
I-135		0.28	2.1×10^{-1}	
I-136		9.6×10^{-4}	1.0×10^{0}	
Child (aged 4)	0.2			14
I-129		40	1.7×10^{-2}	
I-131		6.7	5.0×10^{-2}	
I-132		0.095	1.4×10^{-1}	
I-133		0.83	1.1×10^{-1}	
I-134		0.37	1.8×10^{-1}	
I-135		0.28	1.1×10^{-1}	
I-136		9.6×10^{-4}	5.0×10^{-1}	
Adult (aged 20)	0.2			29
I-129		40	3.4×10^{-3}	
I-131		6.7	1.0×10^{-2}	
I-132		0.095	2.8×10^{-2}	
I-133		0.83	2.2×10^{-2}	
I-134		0.37	3.5×10^{-2}	
I-135		0.28	2.1×10^{-2}	
I-136		9.6×10^{-4}	1.0×10^{-1}	

*) f_1 ; thyroid uptake factor
T_{eff} ; effective half-life from thyroid
SEE ; specific effective energy

According to ICRP publication 30[22], the metabolism of iodine is to recycle by making the thyroidal hormone inorganic, it represents three compartment model composed of an inorganic iodine compartment of total body, an organic one of total body and a thyroid one.

However, the dose to thyroid is almost composed of the contribution of radioiodine existing in itself, and the energy imparted from other organs is negligible. If the effective half-life of iodine in thyroids[23] is used as values considering iodine recycling, the simple Eq. 3.1.4-3 can be useful in estimating the thyroid dose instead of the new dosimetric model using three compartments. The values of parameters used in the Eq. 3.1.4-3 are shown in **Table 3.2**, including data of respiratory rate[24,25].

3.2 Experimental Validation of Main Models

3.2.1 Simulations of the Fumigation in Coastal Region

(1) Outline of experiments

All of Japanese nuclear power plants are located in the coastal regions that differ from the inland with regard to the effect on the atmospheric diffusion. This difference is caused by the occurrence of sea breezes and a coastal internal boundary layer (IBL). The IBL is caused by the difference in surface temperature and surface roughness between sea and land. In the case of onshore flow, the atmospheric stability is gradually modified from stable to unstable from the coastline. Consequently, the IBL increases in depth with downwind distance. The airborne effluent released in the stable onshore flow above IBL may result in the fumigation after entering into the IBL. Experimental studies[26] show the importance of fumigation and trapping in the coastal site and the necessity of the modeling of these phenomena.

Field experiments started in 1980 at Tokai, Japan have been carried out to provide the data of transport and diffusion in coastal region. The focus of measurements for the first four years was on the fumigation in coastal region and that of the last two years is on the effect of the terrain. In **Table 3.3**, it is listed the outlines of series of experiments in the coastal region during 1980, 1981, 1982 and 1983. In this section, simulated results of experiments in first three years are described.

The experimental site is a mainly plain area bordering on the Pacific in the 120 km northern part of Tokyo. The deployments of equipments are shown in **Fig. 3.7**.

Table 3.3 Outline of series of experiments in coastal region

	1980	1981	1982	1983
Release type	Continuous line source of SF_6 Release height : 150 m	Continuous line source of SF_6 Release height : 120 m	Continueous point source of SF_6 and $CBrF_3$ Release height : 120 m	Continuous point source of SF_6 and $CBrF_3$ Release height : 120 m and 60 m respectively
Objective of experiment	Vertical dispersion within 5 km downwind	The same as 1980 experiment	Horizontal distribution at the ground level within 15 km downwind	Horizontal and vertical distribution within 15 km downwind
The number of runs	Seven runs on August 15 through 19	Eleven runs on August 20 through 28	Eight runs on August 4 through 8	Eight runs on August 4 through 9

In the experiments in 1980 and 1981, the tracer gas, SF_6, was released by a helicopter for 1.5 hour along the seashore at 150 m and 120 m height above the ground level, respectively. The aim of the experiment with a line source was to research the vertical dispersion by the compensation of horizontal dispersion. The measurements of vertical profiles of wind speeds, wind directions and temperatures at the tethering points of balloons were performed during the experiment in addition to the routine measurements, at 20 points, of wind speeds, wind directions near the ground level. Sampling-units for measuring vertical distribution were attached to the tethered balloons up to a height of 300 m every 50 m interval. About 30 points of tracer sampling-units at the ground level were arrayed uniformly within 10 km downwinds from the source line. The measurements of concentrations were performed once

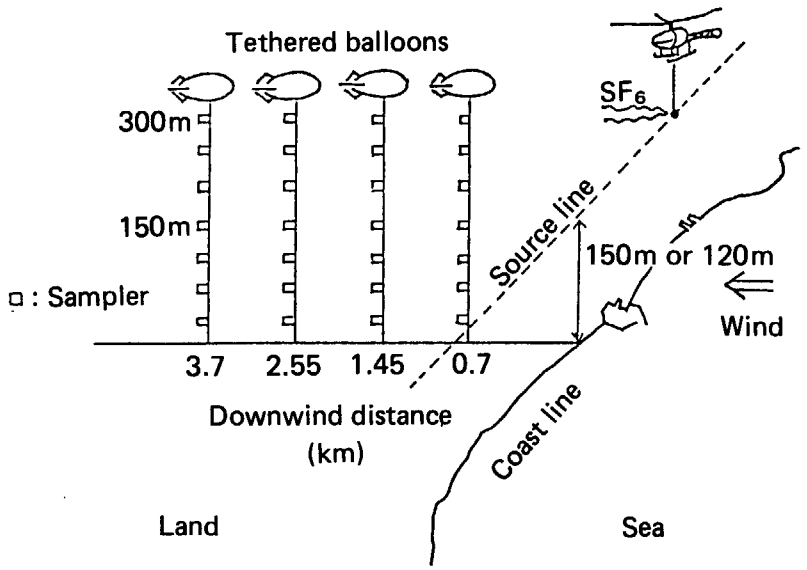

(a) Deployment in 1980 and 1981 experiments.

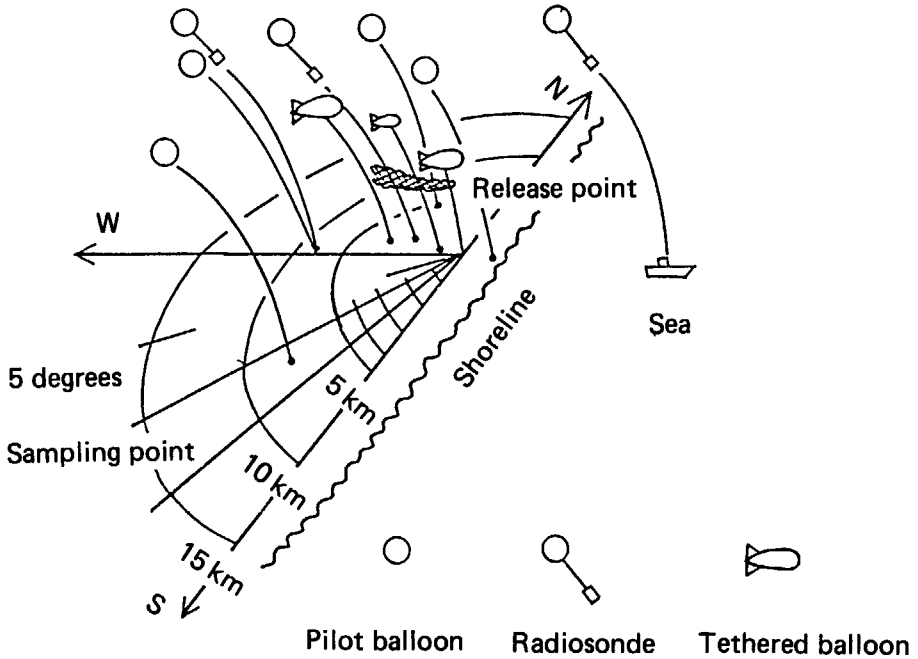

(b) Deployment in 1982 and 1983 experiments.

Fig. 3.7 Deployments of equipment in a series of experiments.

during 30 minutes after 1 hour since the start of release. Tracer samples were analyzed by the use of gas chromatography.

In the experiments in 1982, the tracer gas was released from the fixed point 120 m above the ground level using the tethered balloon at the seashore. The measurements of vertical wind speed, direction and temperature profiles at the five points, i.e., the sea, the release point and inland points, were performed during the experiment in addition to the routine measurement near the ground level at 30 points.

The ground level tracer sampling-units were arrayed on the arcs with radii of 0.6, 1.0, 2.0, 3.0, 4.0, 5.0, 10.0 and 15.0 km every angular interval of 5 degrees. In three experiments, the periods of release were 3 hours and samplings were performed twice during 30 minutes after 1 hour and 2.5 hours since the start of release. In the rest experiments, these were once after 1 hour since the start of release. The releases were continued for 1.5 hour.

(2) Simulations and comparisons

The calculations were made by using the WIND04 code and the PRWDA code for complex simulations. The effort for simulation of the IBL was performed using a multi-layer model to the IBL. Three different layers were specified by a layer completely adjusted to the ground roughness, a transition layer whose turbulence was intermediate and a stable layer above the IBL. The K_j was calculated by using Eq. 3.1.3-9 and the atmospheric stability category was classified by the reference of temperature lapse rate specified in U.S.NRC Regulatory Guide 1.23[27]. **Figure 3.8** shows the general concept of a simulation model for the IBL.

As is shown in the Figure, this model cannot take into account the increase of the IBL near the coastline, because the simulation taking into account the three-dimensional increase of the IBL near the coastline is impractical and difficult due to the complex shoreline and the scarcity of meteorological data. Many experiments at JAERI show that turbulent conditions were divided into three groups; the superadiabatic layer adjusted completely by the land, the neutral layer which is intermediate between unstable and stable layers and the stable layer of shoreflow. And the increases of adjusted layers were limited within 2 km downwind, though the transition layer increases extremely in about 5 km inland in some cases[28,29]. For these reasons, the multi-layer model may be reasonable for the simulation of the IBL in spite of a great simplification.

The comparisons of simulated results with observed ones were performed on the vertical

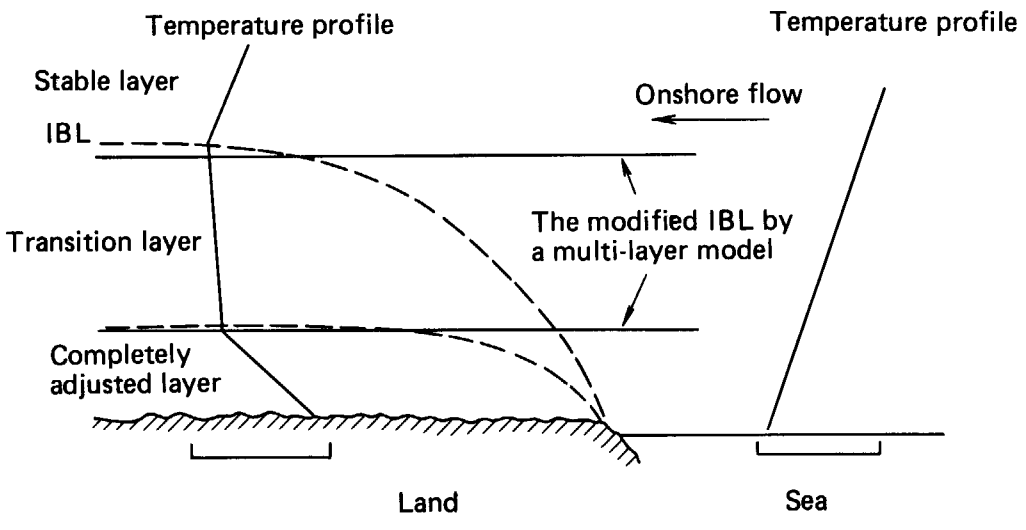

Fig. 3.8 Modeling for an internal boundary layer (IBL).

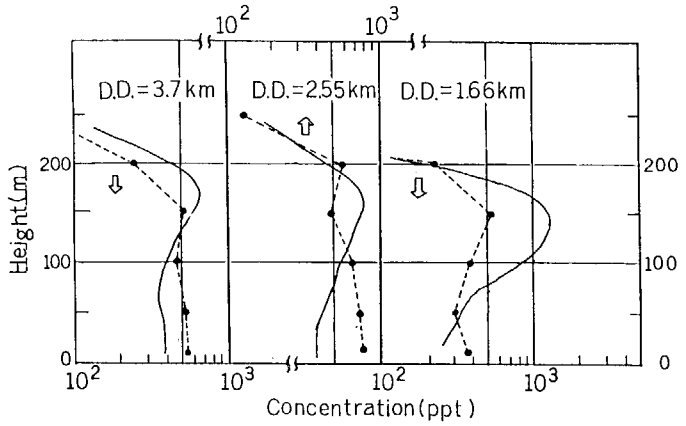

(a) Run 4 in 1980

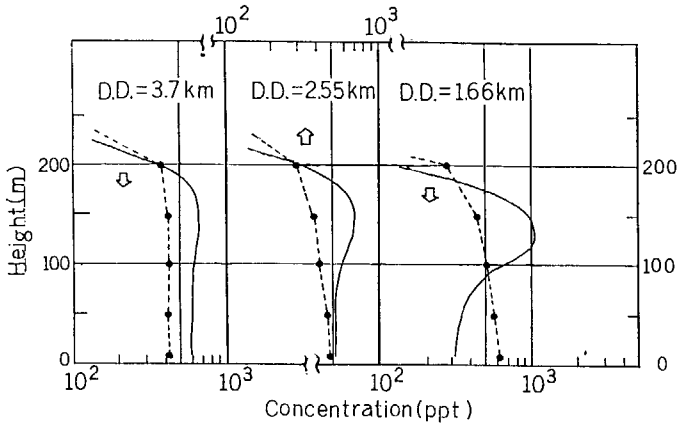

(b) Run 5 in 1980

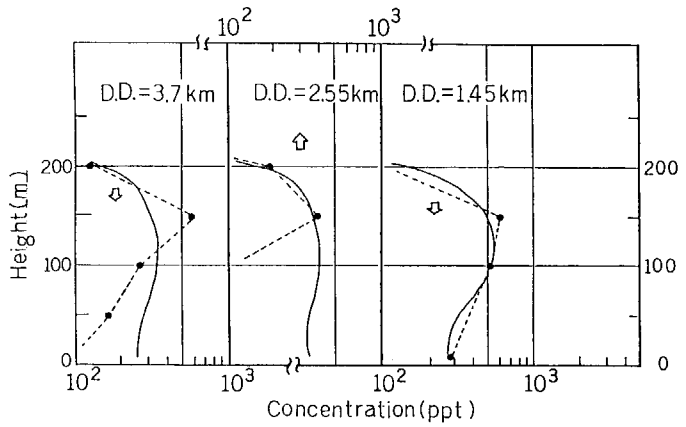

(c) Run 2 in 1981

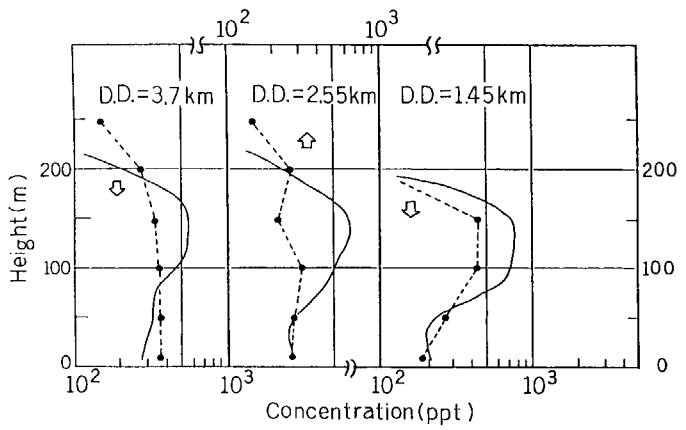

(d) Run 4 in 1981

Fig. 3.9 Comparison of vertical concentration distribution at the tethered points of balloons between observed data and calculated ones by PRWDA. D.D. shows downwind distance.

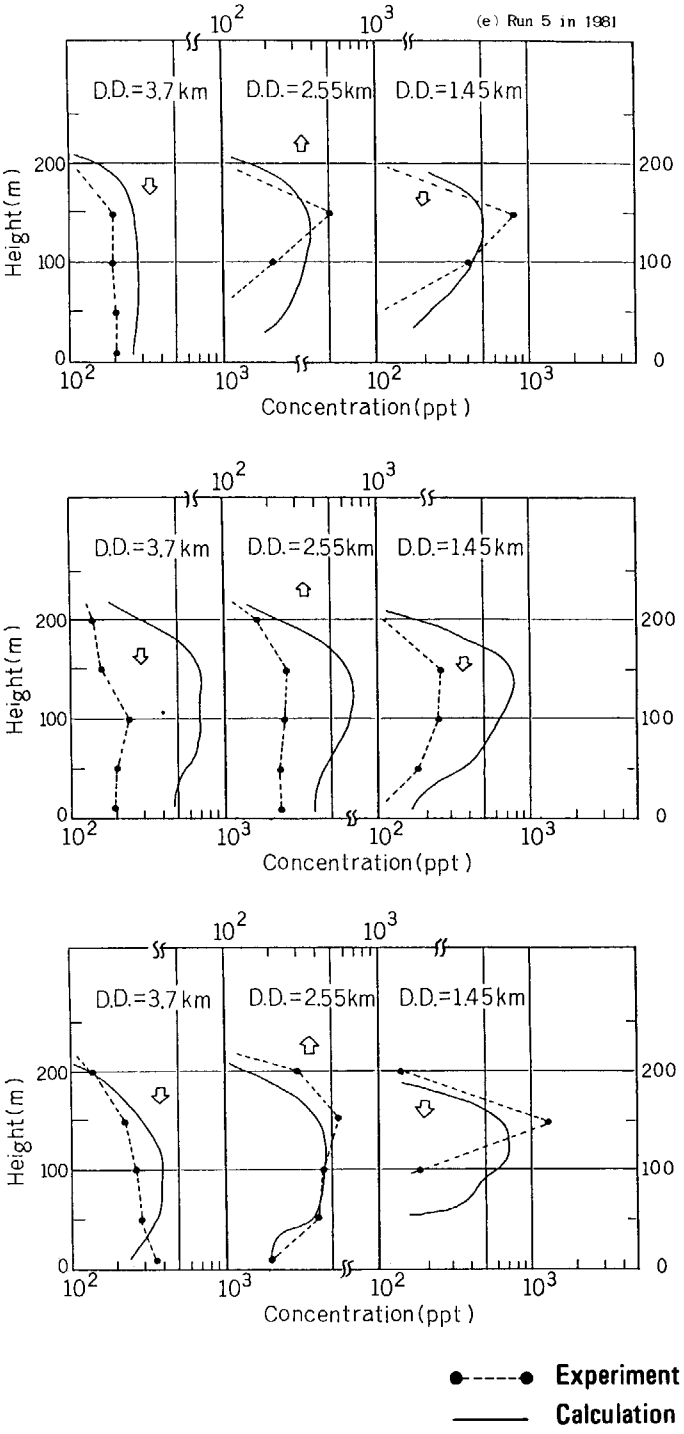

Fig. 3.9 Continued.

distribution in 1980 and 1981 and on the horizontal distribution at the ground level in 1982. The fumigation appeared in seven runs in 1980 and 1981. **Figure 3.9** shows the comparisons of vertical concentration distributions. In each figure, solid lines show calculated results and dotted lines show experimental ones. **Figure 3.10** shows the comparisons of the downwind concentration distributions at the ground level. The results of the Gaussian plume model in the Figures are calculated by using the atmospheric stability category determined from the surface wind speed and the insolation. As shown in these Figures, the multi-layer model can simulate the complex vertical dispersion by considering the flow in the stable layer at the upper region.

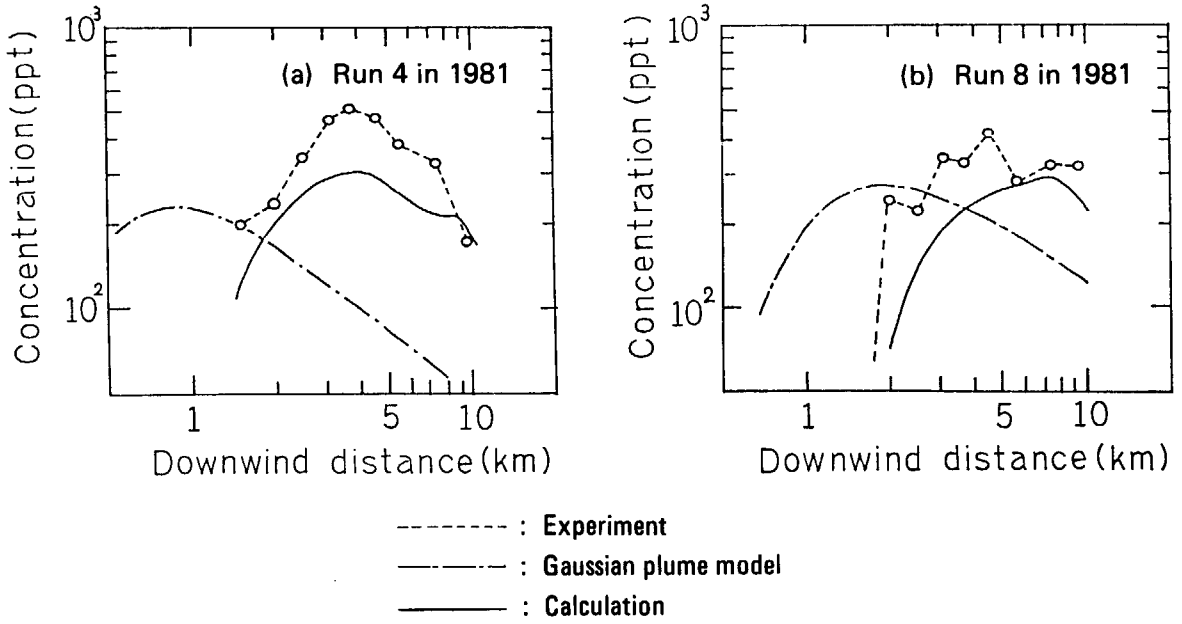

Fig. 3.10 Comparison of downwind concentration distribution at the ground level between observed data and calculated ones by PRWDA.

The comparisons of horizontal distributions in 1982 experiments are shown in **Fig. 3.11**. In each figure, solid lines are calculated results and dotted lines are the experimental ones. Values of isopleths are 3000 ppt(part per trillion ($\times 10^{-12}$)) at the inside and 300 ppt at the outside. On Run 1, the IBL and the wind direction changed with time. The mean airflow changed gradually from ESE to ENE with time, which results in the horizontal spread wider than other runs. In this simulation, meteorological data were inputted at the intervals of every one hour, so the plume center line by calculation was clearer to WSW than the observed one.

On Run 2, the samplings were carried out twice after 1 hour and 2.5 hours from the start of release. In the first sampled results, the two peaks of concentration appeared at 0.6 km and at 3.0 km(less than 3000 ppt). The turbulent condition estimated from the temperature lapse rate showed that the neutral condition was dominant near the height of release. The cause of peak at 0.6 km could not be made clear from the observed meteorological data and the calculated peak position agreed with the second peak. On Run 4, the samplings were also carried out twice. During the first sampling, a clear leakage from SF_6 cylinders appeared and the effect of leakage could not be ignored against the observed results within several kilometers. The wind direction changed between the first and the second sampling period. On Run 5 and Run 6, the sampling-units seemed to catch the plume center line. On Run 7, on the other hand, the plume center line seemed to flow between the sampling-units. In most experiments, the horizontal concentration distributions agreed well with the observed results except the neighborhood of the release point. The overestimation of calculated results in the region close to the release point is to be considered by the ignorance of the IBL slope in the model. In the case that the plume is released in the stable onshore flow, the spread of the plume in the crosswind direction tends to become narrower than the P-G σ_y determined from the surface wind speed and the insolation. The calculated results by the present model also showed these phenomena by considering the upper stable or neutral layer.

(3) Short discussion

According to the comparisons, it became clear that the multi-layer model would be effective for simulation of the fumigation in the existence of the IBL despite the great sim-

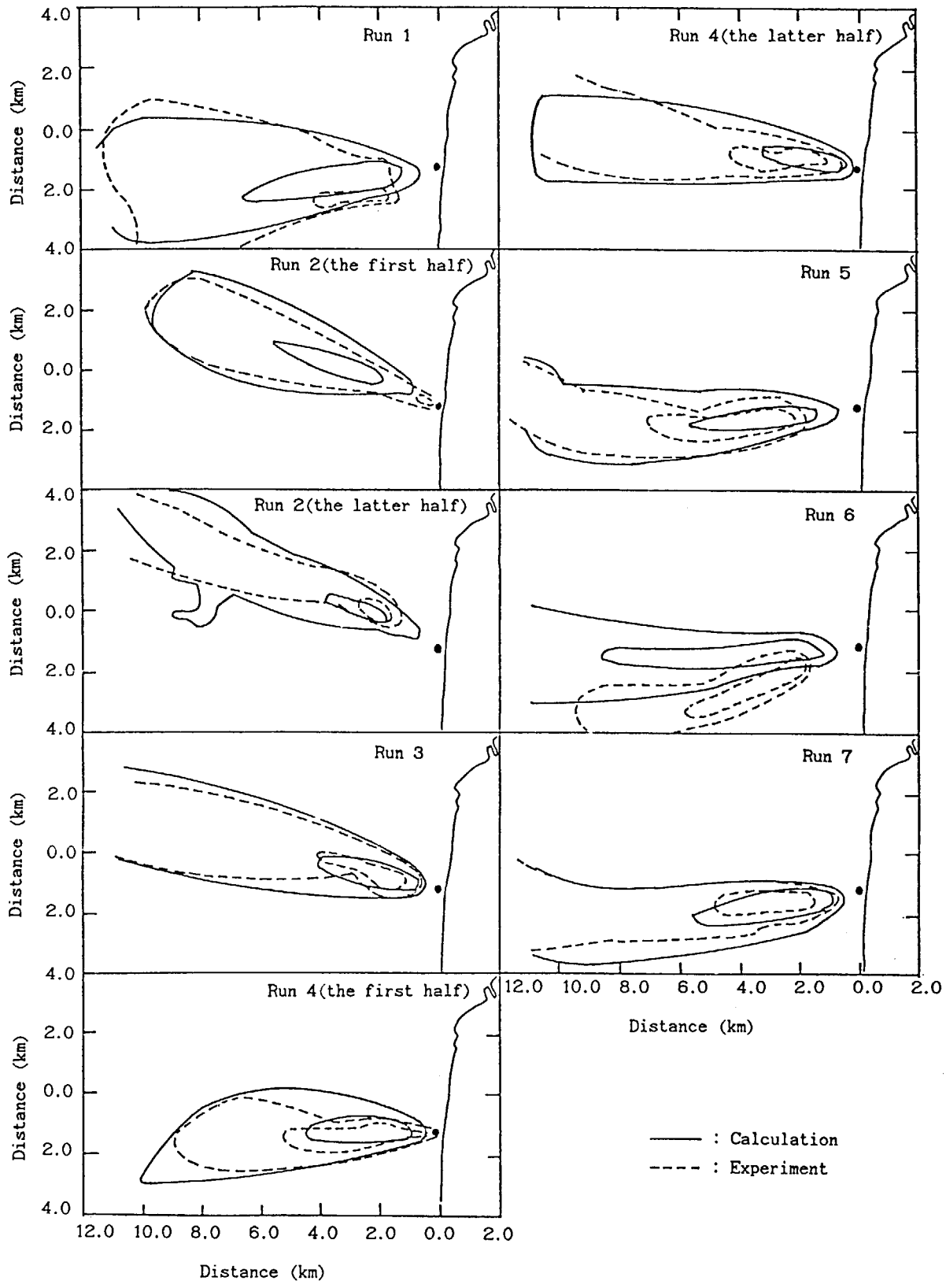

Fig. 3.11 Comparison of horizontal distribution pattern at the ground level in 1982 experiment between observed data and calculated ones by PRWDA.

plification. Although the ignorance of the increasing depth of the IBL close to the shoreline did not result in the big error against the experiments, the magnitude of error may be different depending on the relative position between the source height and modeled IBL. The error due to the assumption of the constant-height multi-layers could not be examined at the inland where the IBL became obscure. In the inland, the turbulence of airflow above IBL is expected to become the neutral condition from the stable one. This may cause the error in some degrees. Another problem is how to simulate the IBL made by the onshore flow in complex terrain, but the experimental studies about this problem are not enough.

The atmospheric stability categories of multi-layers are determined from the temperature lapse rate or the standard deviation of horizontal wind-direction fluctuation. But the routine measurement at the two level of tower in the site cannot supply enough data identify even the existence of the IBL. Therefore, the special measurement by a radiosonde or alternative instruments in an emergency or a routine observation of an acoustic sounder would be effective to resolve these difficulties.

3.2.2 Simulations in Complex Terrain

In this section two verification studies in complex terrain are introduced. As for the wind field and the dispersion over complex terrain, there are no field data which can be used as references for verification, because the field experiment in the complex terrain contains many difficulties. One of the verification studies is the simulation of the trajectories obtained by the flight of constant level balloons. The trajectory of the balloons are simulated by the use of the three dimensional wind field computed by WIND04. The horizontal scale of the simulation is within 100 km. The other study is a simulation of wind tunnel experiment by WIND04/PRWDA. A wind tunnel experiment itself is one of the simulation techniques, and the result should be verified by the comparison with the field experiments. However the wind tunnel experiments are carried out on the basis of similarity law of the fluid dynamics, so that we can expect considerable confidence of the results. Furthermore, the comparison between

Table 3.4 Summary of trajectory tracking in 1981

Run No.	Release time	Tracking duration	Recovery site
1	10/6 15:39	*****	Yamagata-cho, Ibaraki
2	10/7 12:18	*****	*****
3	10/7 15:02	*****	Nasu-cho, Tochigi
4	10/12 11:45	*****	Simotsuma city, Ibaraki
5	10/13 11:30	12:51 - 13:27	Katsura-mura, Ibaraki
6	10/13 13:08	14:28 - 15:38	Bato-cho, Tochigi
7	10/13 16:33	16:34 - 17:38	*****
8	10/14 12:50	13:10 - 14:25	Yachiyo city, Chiba
9	10/14 15:10	15:05 - 17:25	*****
10	10/15 10:45	10:45 - 12:01	Kuroiso city, Tochigi
11	10/15 13:20	13:20 - 15:49	*****
12	10/16 12:00	12:01 - 14:31	*****
13	10/16 14:56	14:57 - 26:41	*****
14	10/20 10:10	10:11 - 12:58	*****
15	10/20 13:25	13:25 - 14:25	Kanuma city, Tochigi
16	10/20 15:28	15:41 - 16:24	Tochigi city, Tochigi
17	10/21 10:25	10:25 - 11:51	Saigo-mura, Fukushima
18	10/21 12:25	12:25 - 13:21	Nasu-cho, Tochigi

different simulation techniques is important, because it clears the advantage and the defect of each technique.

(1) Simulation of trajectory

The balloon flights used in this study were conducted in October, 1981. Balloons equipped with rawin-sonde were released and tracked by two rawin-sonde tracking stations. The horizontal position of the balloon was calculated from the azimuthal angles observed by tracking stations. The altitude of the balloon was ballasted for 300 m, and the variation of the altitude was obtained from the pressure signals transmitted from the rawin sonde. Among 18 balloon flights, 14 flights were tracked by this method to the downwind distance of 20 km from the release point. The balloons were recovered in 11 flights at the distance ranging from several kilometers to a hundred kilometer. These balloon flights are summarized in **Table 3.4**.

The area of interest, which locates in the middle of Japan, and the distribution of meteorological stations are depicted in **Fig. 3.12**. The southern part of this area is a large plain, but the northern and the north-western areas are mountainous districts. The eastern edge is open to the Pacific Ocean. The location of Tokai, where the balloons were released, is shown in the Figure. All of meteorological stations are surface stations, and their heights above sea

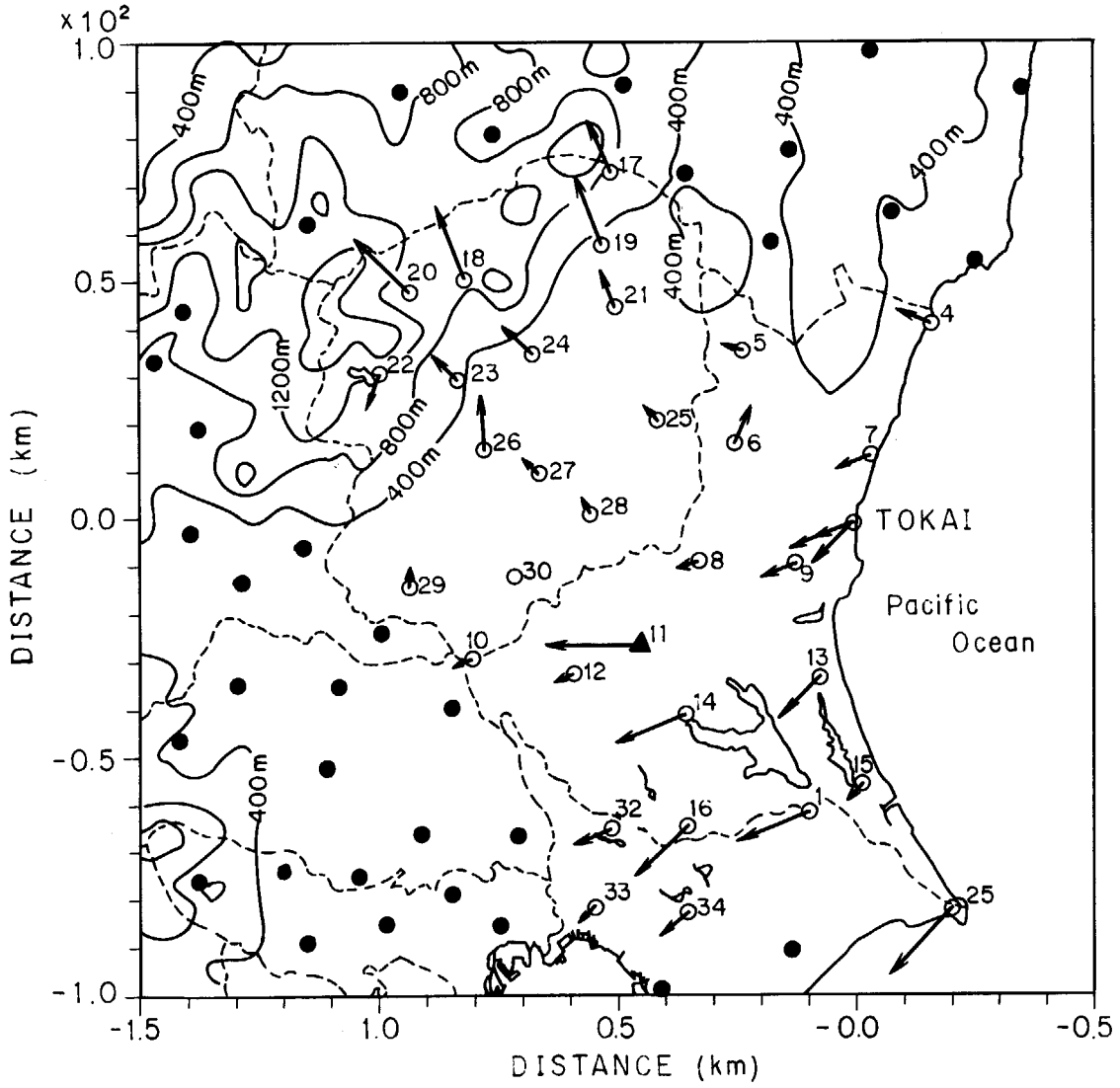

Fig. 3.12 Computational area and the wind observation included in it. The arrows show the examples of observed surface wind. Closed circles represent the meteorological stations whose data are available but are not included in this study.

level are ranging from zero meter to several hundreds of meters, among them the 11-th station locates on the top of a solitary mountain, Mt. Tsukuba, whose height is 876 m. In the numerical calculation, the whole area is divided into 50 X 50 X 20 cells. The size of a cell is 4000 m X 4000 m X 40 m. Then the whole of the computational volume is 200 km X 200 km X 800 m. The wind vector at each grid point is calculated by WIND04 using the surface wind data shown in **Fig. 3.12**. In order to judge the efficiency of mass-conservation technique, three kind of wind fields are calculated. In the first and the simplest case, WFD1, we only interpolate the data of surface wind over the three dimensional grid point by Eq. 3.1.2-1. The observed data at the 11-th station is not used in this interpolation, because of its singularity mentioned above. The vertical profile of the wind is roughly accounted for by the use of the power law. The terrain height is not included. The variational technique is not applied in this calculation. In the second case, WFD2, the interpolation is accomplished by the same method used in the first case, but the terrain height is included. Furthermore, the variational adjustment technique is applied so as to ensure the conservation of the mass. In the last case, WFD3, we use the wind observation as the 11-th station as the upper wind observation, Mt. Tsukuba. The topography is included and the variational adjustment is applied. The differences of three cases of wind field calculation are summarized in **Table 3.5**.

A trajectory of a balloon is computed by following a marker particle released into the wind field. The position of the marker particle at time t, X_t, is computed by

$$X_t = X_{t-\Delta t} + v_{t-\Delta t} \cdot \Delta t, \qquad (3.2.2\text{-}1)$$

where Δt is the time increment, which value is 1 min., and $v_{t-\Delta t}$ is the wind vector at the position of the marker particle.

A trajectory is calculated for each wind field, WFD1, WFD2 and WFD3, and is referred to as TRA1, TRA2 and TRA3, respectively.

The TRA3s of Run 15, 17, 18 are depicted in **Fig. 3.13**. Closed circles represent calculated trajectories. Open circles are the observed trajectories and the double circles are the points of balloon recovery. Closed circles and open circles are the positions of the balloon for every ten minutes after the release of the balloon.

The difference among the three methods is shown in **Fig. 3.14** as for the RUN10. Triangles, open circles and closed circles represent TRA1, TRA2 and TRA3, respectively. The altitude of the marker particle at every one hour after release is also shown in the figure. The altitude of TRA1 is held constant, 300 m, because no vertical wind component is specified in the WFD1.

TRA1 and TRA2 are not much different each other, whereas the TRA3 is different. The observed trajectory is between TRA2 and TRA3, but the point of recovery is only simu-

Table 3.5 List of the condition of wind field calculation

	Horizontal interpolation	Vertical interpolation	Variational adjustment (topography)
Case 1 (WFD 1)	Weighted by the reverse square of distance	Power law up to 800 m	NO
Case 2 (WFD 2)	same as Case 1	same as Case 1	YES
Case 3 (WFD 3)	same as Case 1	Power law (up to 200 m) Log linear interpolation	YES

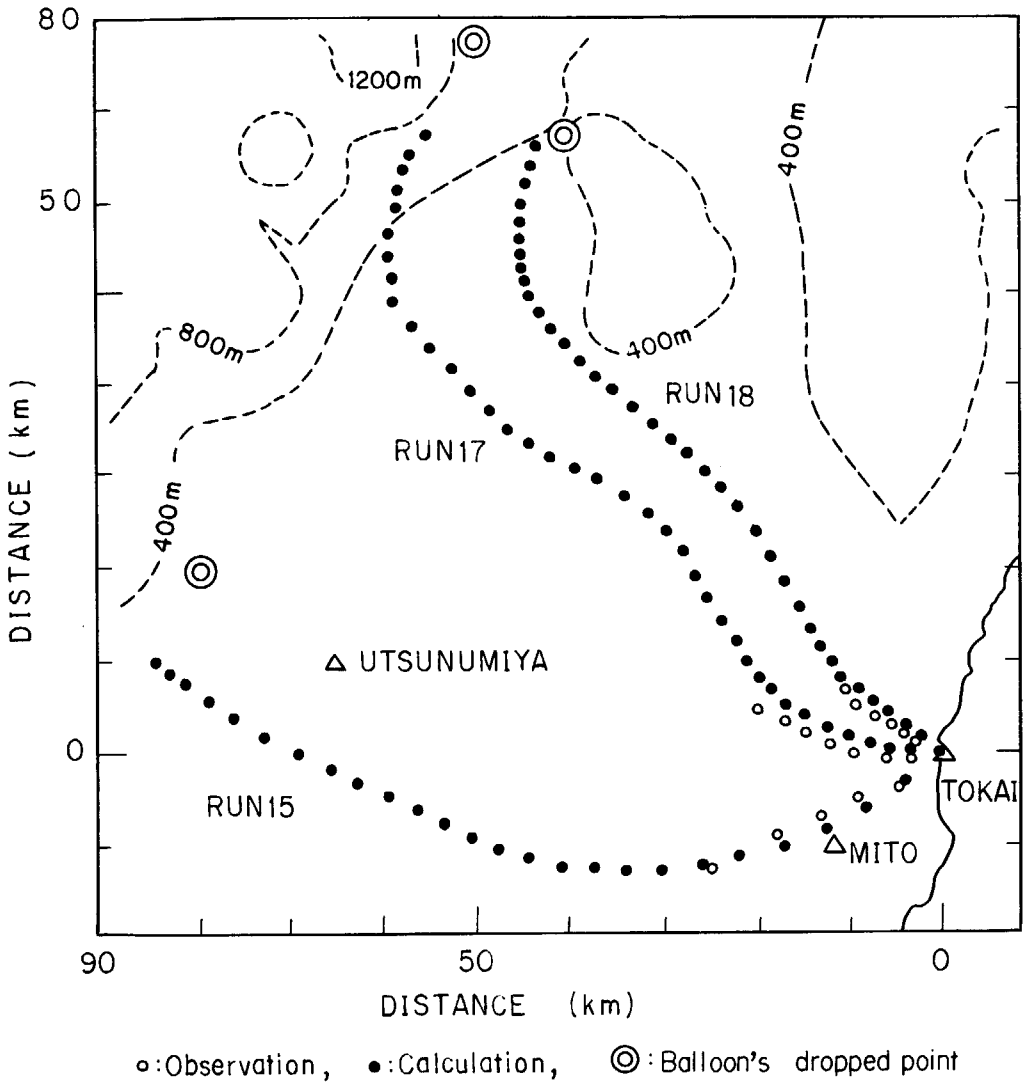

Fig. 3.13 Comparisons of the observed and computed trajectories. Closed circles represent the position of computed marker particles at every ten minutes. Open circles are the position of tetloons. Double circles represent the recovery points of the tetloons.

lated by TRA3. The difference of TRA3 from other trajectories are due to the use of the data of upper wind. This result implies the importance of the upper wind data. TRA1 and TRA2 differ slightly. This difference is due to the variational adjustment. It can be seen that the TRA2 goes around the hill as in the Figure, whereas the TRA1 go across it. It is because that the interpolated wind is adjusted so as to flow around the hill in the result of variational adjustment. In this case the trajectory is not much modified by the imposition of mass conservation. However in some other cases, TRA1 goes straight into the mountainous region, whereas the TRA2 is greatly modified so that it goes around the topographic obstacles.

(2) Simulation of wind tunnel experiment

Wind tunnel experiments are often used for the purpose of estimating the effect of complex topography and of the buildings on the dispersion of materials. As a part of research cooporation programs, a series of wind tunnel experiments has been performed by the Meteorological Research Institute of Japan. In these experiments the precise measurements of wind and concentration were carried out. In this subsection, the results of the calculations executed by WIND04 and PRWDA in the SPEEDI system are compared with the results of

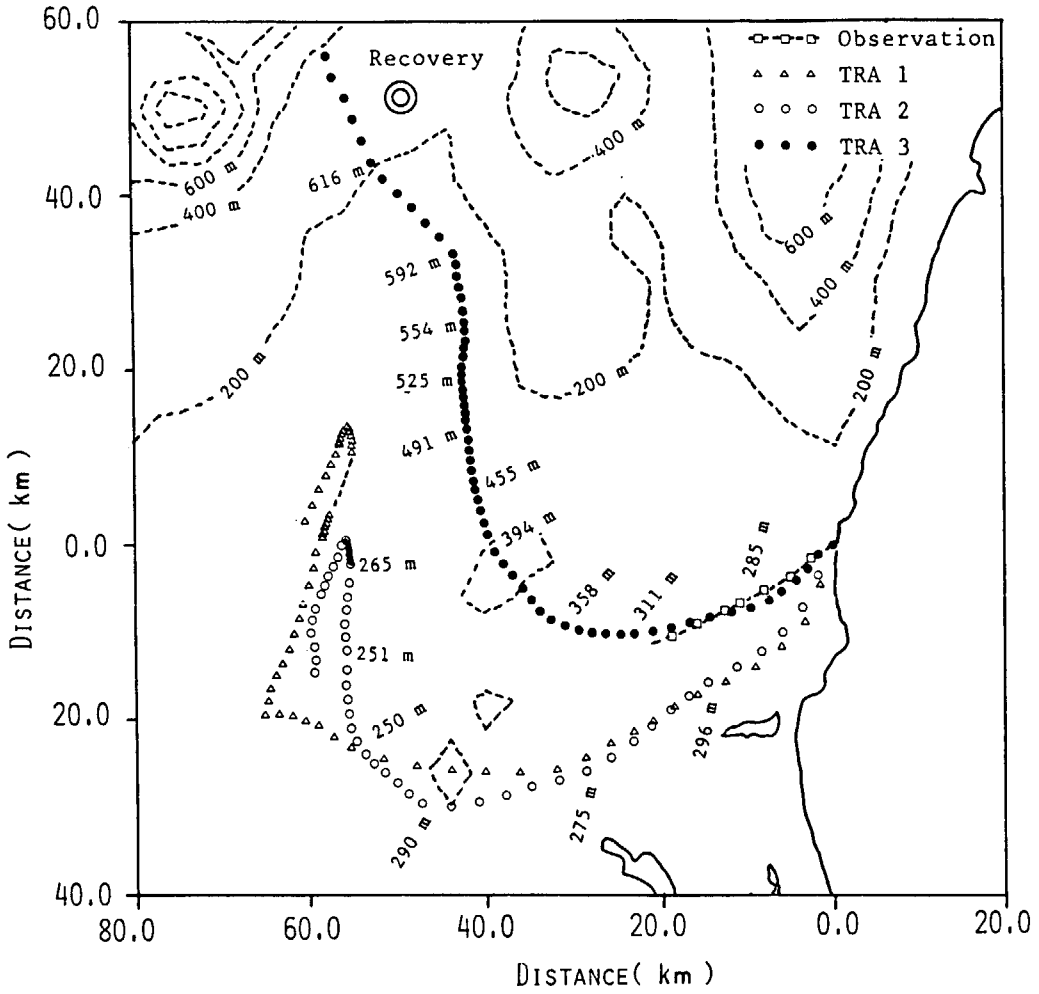

Fig. 3.14 Comparison of the three different computed and the observed trajectories. Triangles, open circles and closed circles show computed trajectories, ie. TRA1, TRA2 and TRA3, respectively. Broken line with rectangles is the observed trajectory, and the double circles are the balloon recovery points.

wind tunnel experiments.

Prior to the description of comparison, the equipments of the wind tunnel and the characteristic features of the wind tunnel experiments should be referred to. The wind tunnel experiments are performed in regard of neutrally stratified atmosphere. The wind speed is measured by a hot-wire anemometer. Propane gas is used as a tracer of the diffusion experiment. The gas is sampled by tubes, and the concentration is measured by a hydrocarbon-analyser. The reducing ratio of the topographic model is 1/2000.

The order of the Reynolds number of the flow of real atmosphere is about 10^8. If the wind speed in the wind tunnel is same to the real atmosphere, the order of the Reynolds number of the flow in the wind tunnel is still 10^4. There is no need to keep the Reynolds number of both flow exactly same, because both Reynolds numbers are sufficiently large. Fluid motion is not sensitive to the difference of Reynolds number in the high Reynolds number condition. The wind speed in the wind tunnel is set in 3 (m/s), and the vertical profile of the wind is created. The turbulent surface layer is exerted by the use of roughness panel and blocks, which are shown in the **Fig. 3.15**.

The results of experiments and those of calculation should be compared carefully considering the difference of the scale. In order to cancel the difference of the scale,

$$\chi = \frac{C \cdot U}{Q} = \frac{C_w \cdot U_w}{Q_w} \cdot S_l^2 \qquad (3.2.2\text{-}2)$$

is used, where C (Unit/m^3) is the concentration, U (m/s) is the wind speed at release point and Q is the release rate (Unit/s). Subscript w implies that the value is the result of the wind tunnel experiment. S_l is the reducing ratio of the model (= 1/2000).

The similarity of both values is judged by the following quantities,

Bias : $$\bar{D} = \bar{A} - \bar{B}, \qquad (3.2.2\text{-}3)$$

Variance : $$S_d^2 = \frac{1}{N-1} \sum_{n=1}^{N} (A_n - B_n - \bar{D})^2, \qquad (3.2.2\text{-}4)$$

Root Mean Square Error : $$RMSE = \left[\frac{N-1}{N} S_d^2 + \bar{D}^2 \right]^{1/2}, \qquad (3.2.2\text{-}5)$$

Correlation : $$R = \frac{\sum_{n=1}^{N} (A_n - \bar{A}) \cdot (B_n - \bar{B})}{\sum_{n=1}^{N} (A_n - \bar{A})^2 \cdot \sum_{n=1}^{N} (B_n - \bar{B})^2}, \qquad (3.2.2\text{-}6)$$

where A and B are experimental and computed values, respectively, and the bar implies the mean value over the set. The number of the evaluation points is 577 for all the region. The statistical quantities mentioned above are computed for all of the points and for some subset of the points (surface points, points at some fixed downwind distances).

The features of dispersion simulated in the wind tunnel are checked by the comparison of dispersion experiments over a flat plate with the Gaussian plume model (**Fig. 3.16**). The horizontal diffusion parameter σ_y and the vertical dispersion parameter σ_z are compared.

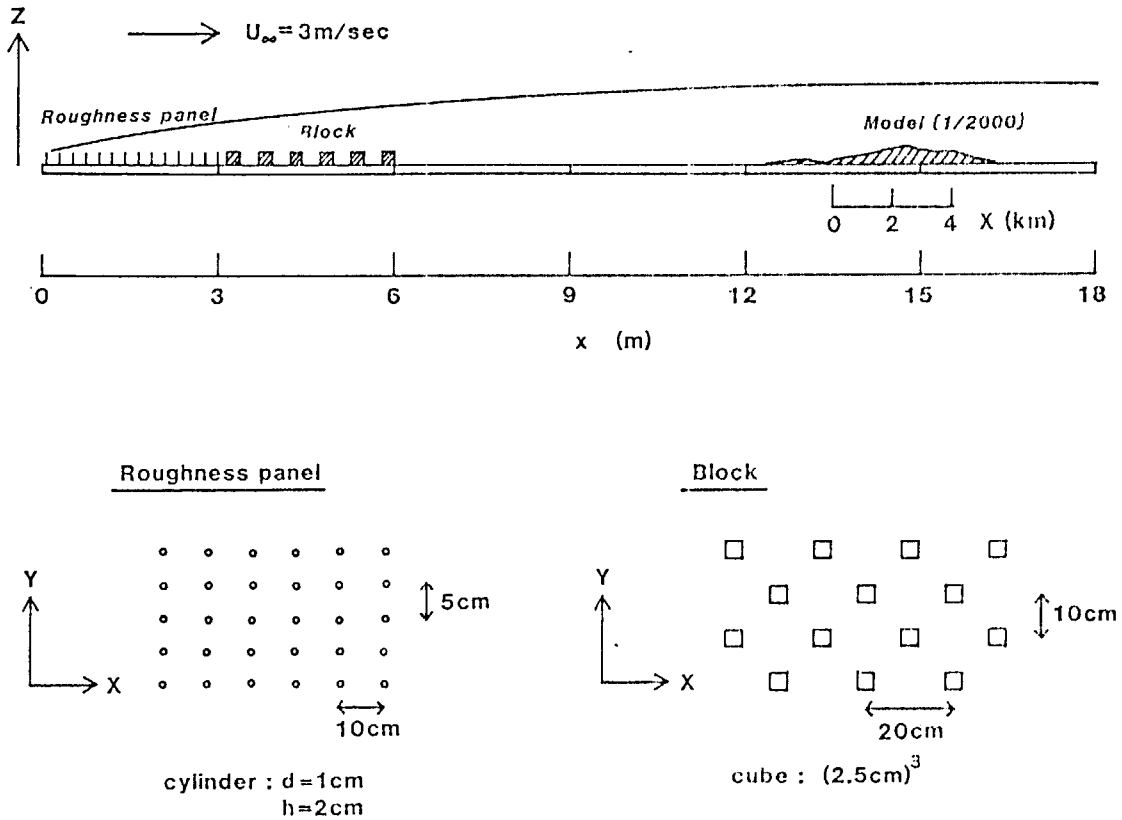

Fig. 3.15 Arrangement in the wind tunnel.

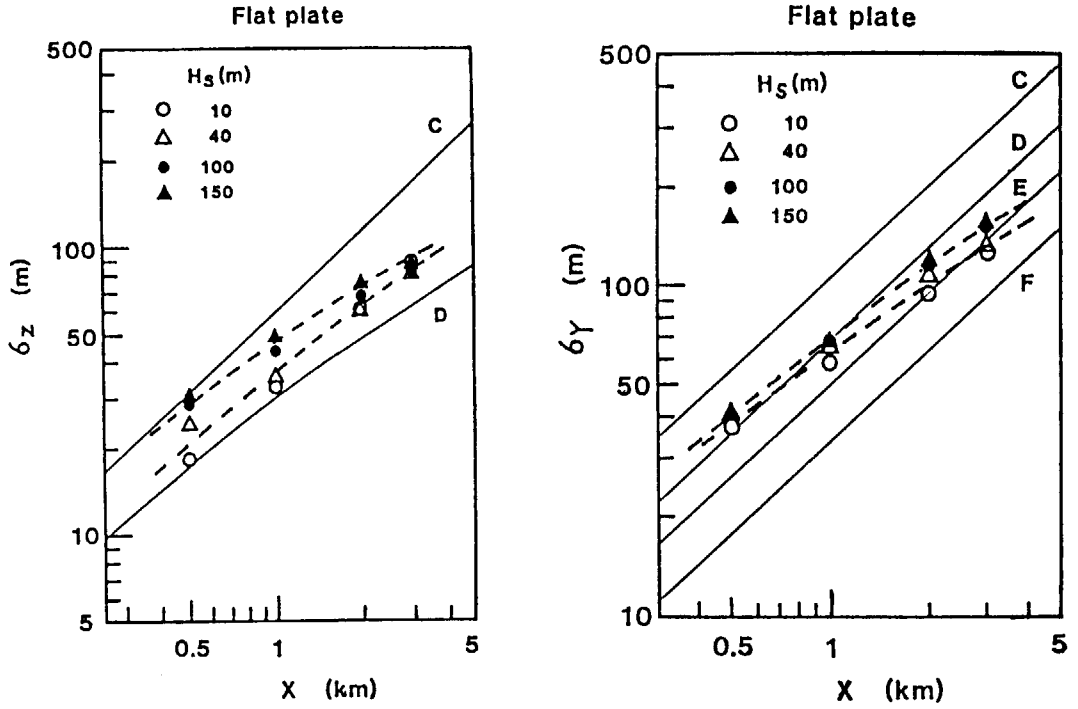

Fig. 3.16 Vertical diffusion parameter (σ_z) and horizontal diffusion parameter (σ_y) observed in the wind tunnel. Solid lines show the parameters corresponding to atmospheric stabilities of Pasquill.

It is noted that the σ_y in the experiments is close to that of Pasquill's stability class D (neutral) or E (slightly stable), and the σ_z is close to C (slightly unstable). The concentrations of the dispersion experiments over a flat plate are compared with the Gaussian plume model for various atmospheric stabilities in **Fig. 3.17**. In each sub-figure, the abscissa is the concentration of the wind tunnel experiment and the ordinate is the concentration computed by the Gaussian plume model. It can be seen that the results of the wind tunnel experiments are between stability class C and D, and the overall distribution is close to stability class C. Then, the following computation by SPEEDI is performed for stability C.

The region of concern is depicted in **Fig. 3.18**. It is the site of a nuclear power plant facing on the Sea of Japan. The area enclosed by dashed line is the scope of the experiment in the wind tunnel, and the solid lines show the boundary of the computational domain.

In the wind tunnel experiment, two opposing boundaries are walls of wind tunnel, so that the boundary condition of computation is slightly modified at the corresponding boundaries. An example of the comparisons is shown in **Figs. 3.19**, **3.20** and **3.21**. The pattern of the surface concentration is shown in **Fig. 3.19**. In **Fig. 3.20** is shown the distribution of materials in several vertical cross sections between 0.7 to 2.5 km down from the source. The center of the plume shifts eastward with the downwind distance, and the shift is large near the surface and is relatively small in the upper layer. The reason is that the wind near the ground is affected by the topography. In this present case, airflow, which goes around a big hill at the southwest part of the region, shifts the plume eastward. The result of computation retains this effects well. **Figure 3.21** shows the correlation of the values for total points. The experiment and computed values show good agreement. The correlation factor is 0.89. The statistical quantities are listed in **Table 3.6**. These statistical quantities are also computed for the surface concentration and for the concentration in the vertical cross section at some appointed downwind distances. Those values are also shown in **Table 3.6**.

It must be mentioned that the one of the governing parameters for the computation is the ratio of weighting coefficients of α_1/α_2 in the wind field calculation. In order to obtain the ratio which gives the best simulation of the wind tunnel experiments, the simulation is carried out for several values of α_1/α_2 = 0.02, 0.04, 0.08, 0.16 and 0.20. The correlation coefficients of the concentration for various values of α_1/α_2 are listed in **Table 3.7**. The ratio between 0.16 and 0.20 is suitable from the viewpoint of correlation.

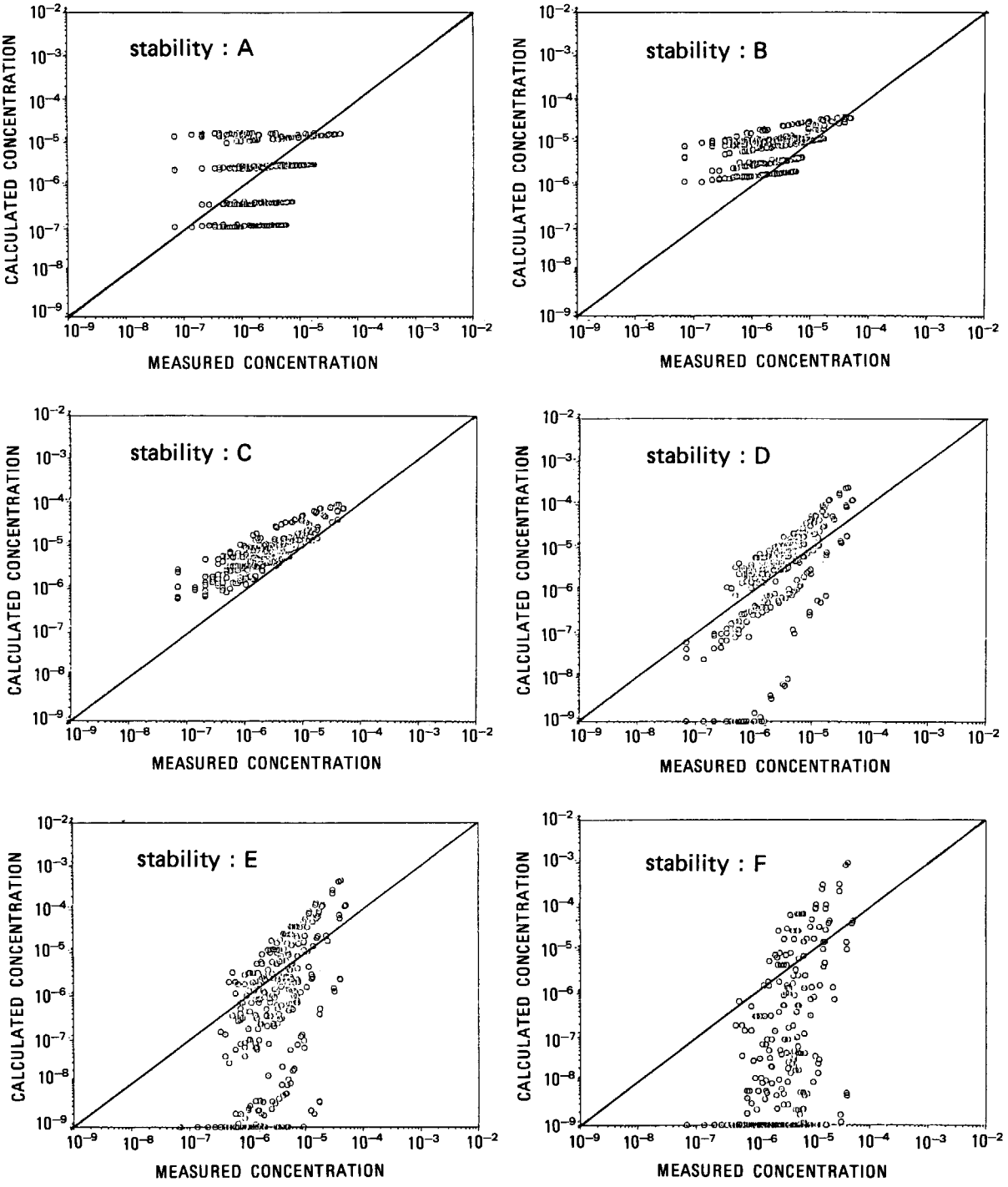

Fig. 3.17 Correlation between the diffusion experiment of neutral stability on the flat plate and the Gaussian plume model of various stability classes.

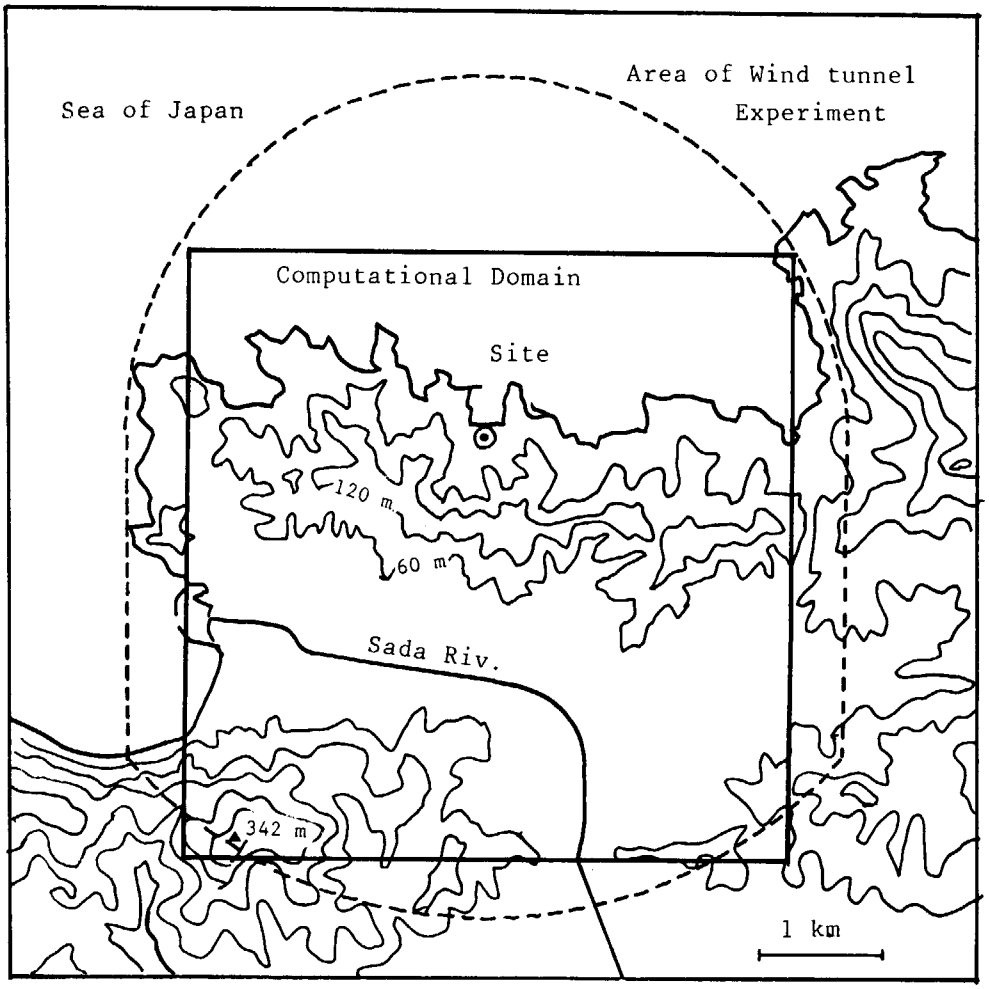

Fig. 3.18 Area of interest. The region of the wind tunnel experiment is enclosed by dashed lines. Solid lines show the boundaries of the computational domain. A circle with dot denotes the source point. The tracer gas is released 100 m, in real scale, above this point.

Table 3.6 Statistical comparison of computed concentration and wind tunnel experiment

Case	Mean	Bias	Variance	RMSE	Correlation
Total	3.56×10^{-6}	3.75×10^{-6}	4.53×10^{-11}	7.79×10^{-6}	0.892
Suface	7.58×10^{-6}	4.95×10^{-6}	1.29×10^{-10}	1.23×10^{-5}	0.663
700 m	7.81×10^{-6}	1.25×10^{-5}	3.66×10^{-10}	2.26×10^{-5}	0.841
1000 m	6.05×10^{-6}	7.62×10^{-6}	1.02×10^{-10}	1.26×10^{-5}	0.886
1500 m	4.29×10^{-6}	4.15×10^{-6}	1.83×10^{-11}	5.96×10^{-6}	0.936
2000 m	2.98×10^{-6}	2.93×10^{-6}	4.57×10^{-12}	3.62×10^{-6}	0.943
2500 m	2.35×10^{-6}	1.76×10^{-6}	2.47×10^{-12}	2.35×10^{-6}	0.941
3000 m	1.98×10^{-6}	1.32×10^{-6}	1.42×10^{-12}	1.78×10^{-6}	0.920

*) The figures of the first column show downwind distance.

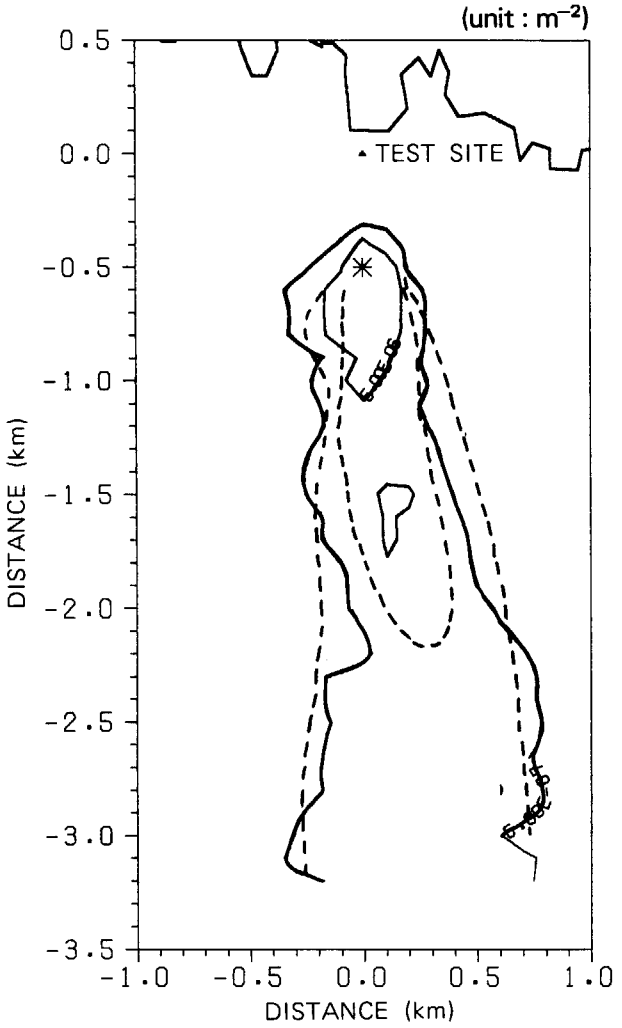

Fig. 3.19 Distribution of the surface concentration. The dashed lines show the result of experiment. Computational result is shown by solid lines.

Table 3.7 Correlation of the wind tunnel experiment and the computed concentration for various values of α_1/α_2

α_1/α_2	Total	Surface	700 m	1000 m	1500 m	2000 m	2500 m	3000 m
0.02	0.480	0.693	0.306	0.571	0.253	0.228	0.350	0.460
0.04	0.693	0.719	0.522	0.827	0.618	0.522	0.745	0.783
0.08	0.811	0.679	0.980	0.890	0.828	0.714	0.821	0.846
0.16	0.892	0.663	0.841	0.886	0.936	0.943	0.941	0.913
0.20	0.896	0.639	0.841	0.879	0.911	0.921	0.929	0.876

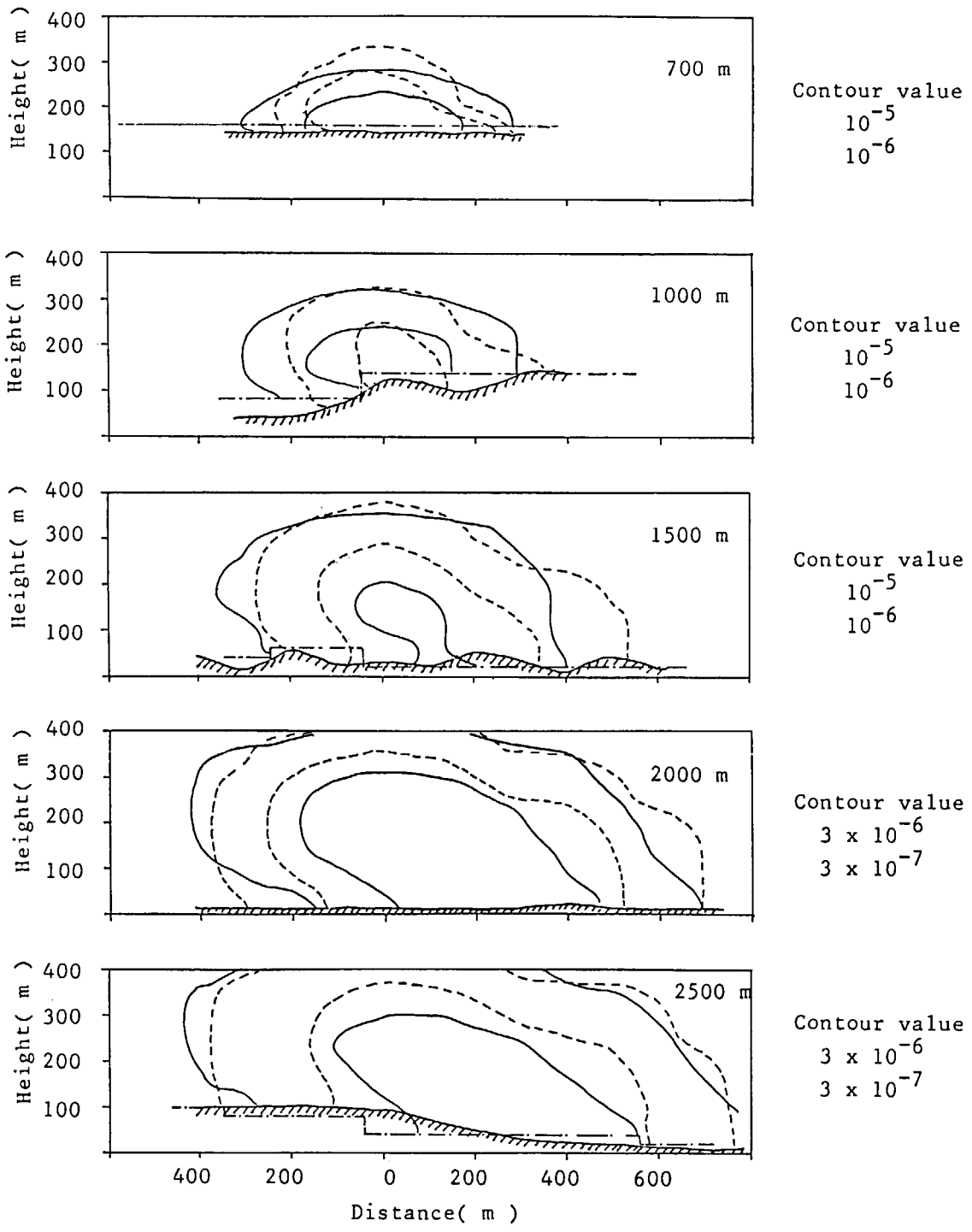

Fig. 3.20 Vertical cross section at various down wind distances. Lines are same as **Fig. 3.19**. The topography is described by solid curves with oblique lines, and the topographic model used in calculation is plotted by thick lines with dots.

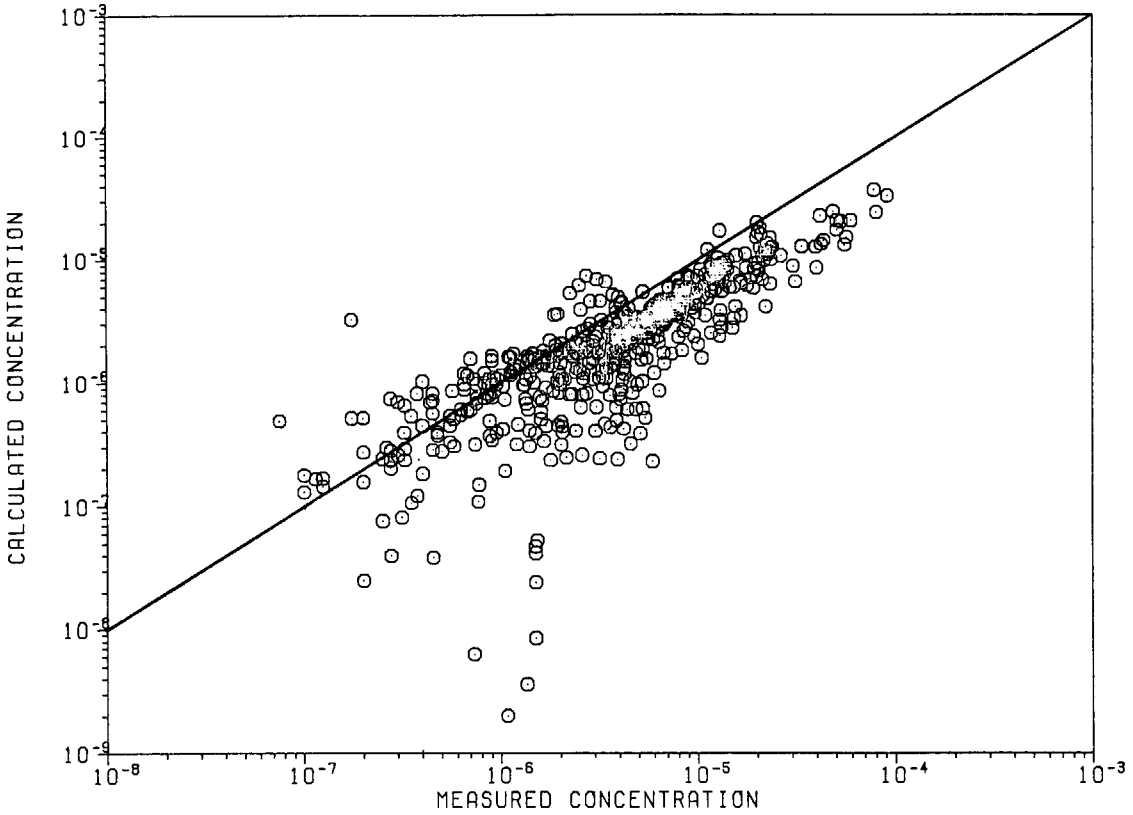

Fig. 3.21 Correlation of the computed concentration with the concentration obtained in wind tunnel.

3.3 Simple Models for Reference Calculation

3.3.1 Plume Model

In an emergency planning, it is necessary at the early stage of emergency to estimate roughly but quickly the external gamma-dose from radioactive noble gases, the thyroid dose following inhalation of radioactive iodine and the surface concentration of the depositing iodine for provision of countermeasures such as evacuation or of the environmental surveillance.

For this purpose, we have developed a computer code GSDOSE which calculates the external gamma-dose, the thyroid dose and the surface concentration quickly on the basis of the Gaussian plume model.

(1) Calculation of the external dose due to radioactive noble gases

The GSDOSE calculates the external gamma-dose from plumes by means of interpolation or extrapolation of the normalized doses which have been prepared in advance. The normalized dose is defined later in this section.

1) Calculation of release rates, effective energy and average energy

It is in general considered that the release information is limited at the early stage. Therefore the GSDOSE at first calculates the release rate $(\bar{q})$, the effective energy (E^*) and the average energy $(\overline{E})$ or mixed noble gases at time t_j during the release on the assumption that the release rate is constant between t_{j-1} and t_j.

The release rate of nuclide i is calculated as follows.

$$\bar{q}_i(t_j)=q_{0i}e^{-\lambda_i(t_{j-1}-t_0)}\frac{\{1-e^{-\lambda_i(t_j-t_{j-1})}\}}{(t_j-t_{j-1})\lambda_i}\ , \qquad (3.3.1\text{-}1)$$

where

q_{0i} : release rate of nuclide i at the shutdown time.
λ_i : decay constant of nuclide i,
t_j : a time during the release and
t_0 : shutdown time.

q_{0i} is initially calculated by the SPEEDI system.

The release rate and effective energy of mixed noble gases at t_j are then calculated from Eq. 3.3.1-2 and Eq. 3.3.1-3, respectively.

$$\bar{q}(t_j)=\sum_i \bar{q}_i(t_j)\ , \qquad (3.3.1\text{-}2)$$

$$E^*(t_j)=\frac{1}{\bar{q}(t_j)}\sum_i \bar{q}_i(t_j)E_i^* \quad (E_i^*=\sum_k^{N_i} f_{\gamma ik}E_{\gamma k})\ , \qquad (3.3.1\text{-}3)$$

where

E_i^* : effective energy of nuclide i,
$E_{\gamma k}$: energy of k-th gamma ray of a nuclide i (MeV/photon),
$f_{\gamma ik}$: intensity of k-th gamma ray per disintegration of a nuclide i (photon/dis) and
N_i : number of gamma rays per disintegration of a nuclide i,

which are provided from the nuclide data file in this sytem.

The average energy of mixed noble gases, which is used for interpolating or extrapolating the normalized doses with respect to the energy, is calculated as follows.

$$\bar{E}(t_j)=\bar{q}(t_j)E^*(t_j)/\sum_i\{\bar{q}_i(t_j)\sum_k^{N_i} f_{\gamma ik}\}\ , \qquad (3.3.1\text{-}4)$$

2) Calculation of external gamma-dose

The normalized dose is defined as the dose on the ground when a gamma-emitting nuclide is released at the rate of 1 Ci/h, the effective energy of the nuclide is 1 MeV and the wind speed is 1 m/s. Therefore the external dose due to the mixed noble gases from the beginning of release to the end is calculated as follows.

$$D(x,y,t_S,t_E)=\sum_j \bar{q}(t_j)E^*(t_j)\frac{D_0}{u(t_j)}\times(t_j-t_{j-1})\ , \qquad (3.3.1\text{-}5)$$

where

t_S : time when the release begins,
t_E : time when the release ends,
D_0 : normalized dose (rem·(m/s)·MeV^{-1}·Ci^{-1}) and
$u(t_j)$: wind speed at t_j (m/s).

3) Interpolation or extrapolation method of the normalized doses

The normalized dose is the function of five elements, that is, exposure points (x,y) which are prepared on the Cartesian coordinates, atmospheric stabilities, release heights (H) and average energies ($\bar{E}$). The normalized doses of 120960 kinds are prepared for all the combinations of these five elements which are given in **Table 3.8**.

The normalized doses are interpolated or extrapolated assuming a quadratic relationship between the dose and the elements, that is,

$$\log D_0=a\xi^2+b\xi+c\ . \qquad (3.3.1\text{-}6)$$

For the interpolation or extrapolation with respect to x or $\bar{E}$, logarithmic values of these elements are substituted in ξ, while for y or H are used the values themselves of

Table 3.8 Values of elements for which the normalized doses are provided

Gamma energy (MeV)	0.05, 0.08, 0.1, 0.15, 0.2, 0.5, 1.0			
Release height (m)	0, 10, 20, 40, 70, 100, 150, 200, 300, 500			
Stability	A, B, C, D, E, F			
Downwind distance (km)	−0.5 0.3 −0.2 0.4 −0.1 0.5 0.01 0.6 0.02 0.7 0.05 0.8 0.1 0.9 0.2 1.0	2.0 3.0 5.0 10.0	20.0 50.0	100.0 200.0
Crosswind distance (km)	0 0.01 0.02 0.04 0.07 0.1 0.15 0.2 0.3 0.45 0.7 1.0	0 0.02 0.05 0.1 0.2 0.3 0.45 0.7 1.0 1.5 2.0 4.0	0 0.2 0.5 1.0 1.5 2.0 2.5 3.5 5.0 7.0 10.0 20.0	0 1.0 2.0 4.0 7.0 10.0 15.0 20.0 25.0 35.0 50.0 100.0

these elements. The coefficients a, b and c are determined by the Gauss-Jordan method with a set of three equations for the nearest three points to a point for which the dose is to be calculated.

The interpolation of the normalized dose would not cause errors larger than 1% for most of the cases. The details of the interpolation or extrapolation method and precision are described in the reference (30).

(2) Calculation of thyroid dose due to inhalation of radioactive iodine

The ground level airborne concentration $\chi_i(x, y, t_j)$ of radioactive iodine i is calculated from the following equation:

$$\chi_i(x, y, t_j)=\frac{\bar{q}_i(t_j)Rd(x, t_j)}{3600\pi\sigma_y\sigma_z u(t_j)}\exp\left(\frac{-y^2}{2\sigma_y^2}\right)\exp\left(\frac{-H^2}{2\sigma_z^2}\right), \qquad (3.3.1\text{-}7)$$

where σ_y and σ_z are crosswind and vertical dispersion parameter (m), respectively.

$\bar{q}_i(t_j)$ is given by Eq. 3.3.1-1. The depletion factor $Rd(x, t_j)$ is given in GSDOSE as follows.

$$Rd(x, t_j)=\exp\left[-\frac{1}{u(t_j)}\left\{\Lambda x+\sqrt{2/\pi}\cdot V_g\int_0^x\frac{1}{\sigma_z}\exp\left(\frac{-H^2}{2\sigma_z^2}\right)dX\right\}\right], \qquad (3.3.1\text{-}8)$$

where

Λ : washout coefficient (1/s) and

V_g : deposition velocity (m/s).

The time integrated concentration of radioactive iodine i from the beginning of release

to the end is calculated from

$$\chi_i(x, y, t_S, t_E)=\sum_j \chi_i(x, y, t_j)\times(t_j-t_{j-1}) , \quad (3.3.1\text{-}9)$$

and then the thyroid dose is calculated as follows.

$$D_l(x, y, t_S, t_E)=Y_l B \sum_i \chi_i(x, y, t_S, t_E)(DF)_i , \quad (3.3.1\text{-}10)$$

where

D_l : thyroid dose equivalent of age group l (rem),
Y_l : coefficient which produces D_l from the thyroid dose for the adult group, (1 for adults, 2 for children and 1.5 for infants),
B : the breathing rate for adults (m^3/h),
$(DF)_i$: committed dose equivalent of the thyroid for adults who inhaled 1 Ci of the nuclide i .

(3) Calculation of surface concentration

The deposition rate due to dry deposition at t_j is calculated as follows.

$$S_{Di}(x, y, t_j)=V_g \chi_i(x, y, t_j)\times 3600 . \quad (3.3.1\text{-}11)$$

The deposition rate due to washout by rain at t_j is calculated as follows.

$$S_{Wi}(x, y, t_j)=\Lambda \chi_i^z(x, y, t_j)\times 3600 , \quad (3.3.1\text{-}12)$$

where $\chi_i^z(x, y, t_j)$, vertically integrated concentration, is calculated from

$$\chi_i^z(x, y, t_j)=\frac{\bar{q}_i(t_j)Rd(x, t_j)}{3600(2\pi)^{1/2}\sigma_y u(t_j)}\exp\left(\frac{-y^2}{2\sigma_y^2}\right) . \quad (3.3.1\text{-}13)$$

Therefore the surface concentration at t_J of each radioactive iodine is calculated as follows.

$$C_i(x, y, t_J)=\sum_j [\{S_{Di}(x, y, t_j)+S_{Wi}(x, y, t_j)\}\exp\{-\lambda_i(t_J-t_j)\}\times(t_j-t_{j-1})] . \quad (3.3.1\text{-}14)$$

3.3.2 Puff Model

To effectively give the real-time dose predictions within about 10-kilometer radius of a site, we use a puff dispersion model which can account for the spatial and temporal variations in meteorological conditions as well as time dependence of release rate of effluent. The development of this model is undertaken to integrate three capabilities for wind field, atmospheric dispersion, and dose calculations as shown in **Fig. 3.22** to minimize the amount and frequency of data transfer. Whenever meteorological data is acquired from the site and its surrounding stations, the wind fields for the area of interest are calculated to determine the advection of the puffs generated from the source location. Once the advection and size of all puffs have been calculated, updated ground level airborne concentrations, surface concentrations and external gamma-doses are simultaneously obtained at each grid point by summing up all the contributions from the puffs in the grid area. The ground level airborne concentrations are used to obtain the thyroid doses due to inhalation at each grid point with breathing rate and dose conversion factor.

(1) Wind field calculation

In determining the trajectories of each released puff, the wind fields must be specified as a function of location and time over the entire area. The wind field should be obtained by an objective analysis procedure based on a network of wind measurements at meteorological stations. Although thermal, topographic and frictional effects on atmospheric boundary layer flow may be significant for the microscale and mesoscale wind field, we only take

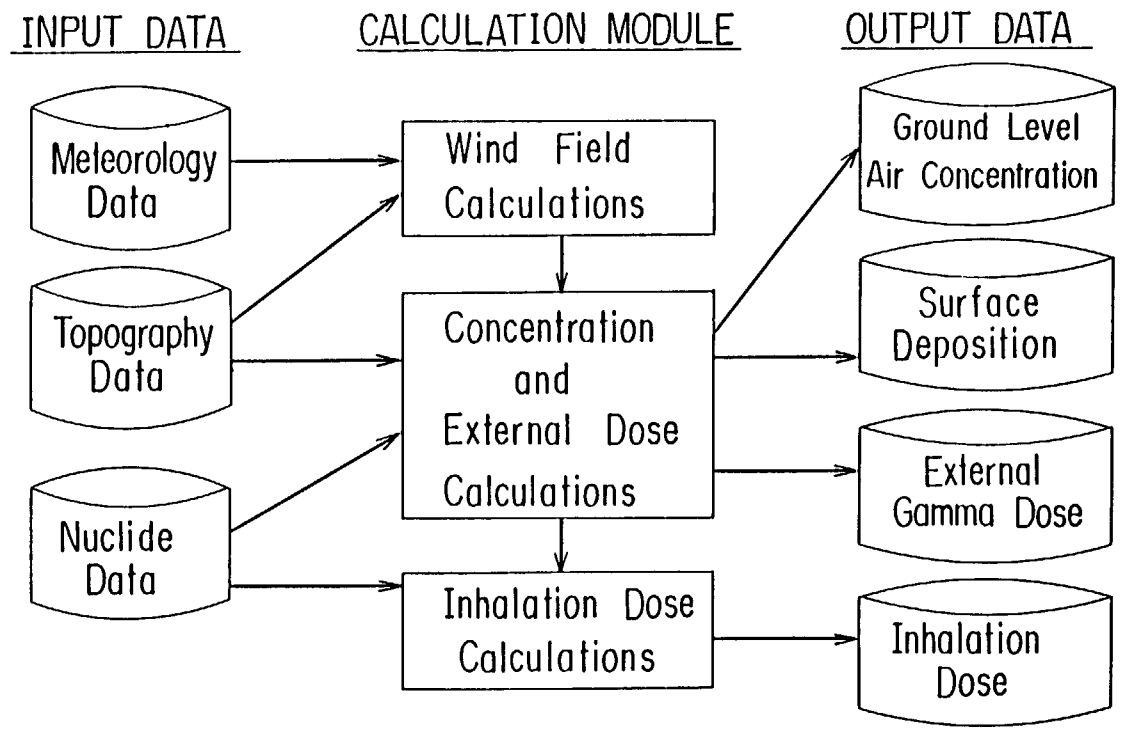

Fig. 3.22 Schematic of the LSPUFF model capabilities and their interrelationships.

topographic effects into account because the analysis should be simply and economically appropriate for real emergency applications. The analysis presented here was developed in original form by Endlich[31] and applied by Liu and Goodin[32] for use in mesoscale wind field. It is a point-iterative method to reduce the two-dimensional divergence in a wind field.

We consider the vertically integrated continuity equation and specified the divergence $D(i, j)$ at each grid point as

$$\frac{\partial(hu)}{\partial t}+\frac{\partial(hv)}{\partial t}=D(i, j) \qquad (3.3.2\text{-}1)$$

where the time variation of the inversion base above topography, $\partial h/\partial t$ is small in comparison with other spatial variations. Here u and v are the x and y mean wind velocity component within the mixed layer below the inversion base. As a starting point, a first guess of the surface wind field is interpolated from the measured data using inverse distance-squared weighting. The initial mean wind velocity within the mixed layer is computed from the interpolated surface wind field using the profile by the power law. The final step is to adjust the flux field of Eq. 3.3.2-1 with the objective of reducing $D(i, j)$. To remove the divergence at a grid point, alterations are made to the u components at the neighboring points of x direction and to the v components at the neighboring points of y direction. These alterations are made equal and of opposite sign. Thus, the entire grid must be scanned iteratively in order to uniformly reduce the divergence and this procedure proceeds until all values of $D(i, j)$ are less than some small value ε.

(2) Atmospheric dispersion and deposition

This model uses a puff dispersion model to predict the advection and diffusion of airborne releases. The puff model can simulate the instantaneous plume picture by a proper distribution of puffs of different sizes. Within an individual puff, the distribution of material is hypothesized to follow the Gaussian form:

$$\chi(x,y,z,t)=\frac{Q(t)}{(2\pi)^{3/2}\sigma_h^2(t)\sigma_z(t)}\exp\left\{-\frac{(x-x_0(t))^2}{2\sigma_h^2(t)}-\frac{(y-y_0(t))^2}{2\sigma_h^2(t)}\right\}$$

$$\times\left[\exp\left\{-\frac{(z-z_0(t))^2}{2\sigma_z^2(t)}\right\}+\exp\left\{-\frac{(z+z_0(t))^2}{2\sigma_z^2(t)}\right\}\right] \qquad (3.3.2\text{-}2)$$

in which $\chi(x,y,z,t)$ is the concentration at the point (x,y,z); $Q(t)$ is the total material in the puff; $\sigma_h(t)$, $\sigma_z(t)$ are standard deviations of the Gaussian distributions in the horizontal and vertical directions, respectively; $x_0(t)$, $y_0(t)$, $z_0(t)$ are coordinates of the center of the puff. Eq. 3.3.2-2 includes total reflection at the ground surface and assumes that alongwind and crosswind diffusion of the puff are equal. The horizontal locations $(x_0(t), y_0(t))$ of each puff center are determined by computing their advection for a finite time step using interpolated winds. These winds are computed by spatial interpolation between the puff center and the surrounding grid points and temporal interpolation between winds at the last and next observation times. The vertical location $z_0(t)$ is the release height above the ground. The presence of high terrain can result in a high dose due to the receptor on terrain being closer to the puff. To account for such situation the height correction for $z_0(t)$ is assumed by the method suggested by Egan.[33]

The terms, σ_h and σ_z which define the growth of the puff depend on the intensity and scale of the turbulence. In this model we apply the theory of relative diffusion given by Smith and Hay[34] to calculate the growth rate of the puff. They proposed

$$\left(\frac{d\sigma}{dx}\right)_{max}=\frac{2}{3}\beta i^2 \qquad (3.3.2\text{-}3)$$

which is representative of the maximum growth rate, where i is the intensity of turbulence; β is the ratio of Lagrangian to Eulerian scales of turbulence and x is the downwind distance. Eq. 3.3.2-3 becomes $\sigma = 0.22ix$ with the relation by Wandel and Kofoed-Hansen.[35] To a close approximation the values of the standard deviation of wind direction represent the intensity of turbulence i. These standard deviations can be obtained from the sensitive vane.

Concentration distributions from a given source can be evaluated in this model by the convolution of the piecewise constant emissions, Q_{m-n+1}, with integration of a Gaussian kernel Eq. (3.3.2-2) evaluated over periods of release duration Δt :

$$C(x,y,z,t)=\sum_{n=1}^{m}Q_{m-n+1}\int_{(n-1)\Delta t}^{n\Delta t}\chi(x,y,z,t-t')\,dt' \qquad (3.3.2\text{-}4)$$

The methods used in this model to predict dry deposition from the atmosphere are based on the concept of deposition velocity and the source depletion model.[36] The limitations of the source depletion model have been discussed by various authors,[37] but it normally remains valid for the spatial area of interest in this model. The removal of material by wet deposition is evaluated using the washout coefficient defined as a function of precipitation rate.

(3) Dose calculation

The estimates of external gamma-dose from a passing plume require the spatial integration over complex plume geometries when the plume dimensions are of the order of the mean free path of gamma radiation or smaller. Therefore the method of plume-shine calculation must coincide with the spatial model of atmospheric dispersion. It is recognized, however, that the numerical integration of radionuclide concentration requires extensive computation time. This model adopts the isotropic cloud approximation based on the unpublished work by Gamertsfelder[38] and provides simplified solutions of dose equations instead of integrals in graphical form in Meteorology and Atomic Energy[39] to reduce the running time.

The external gamma-dose rate to the receptor (x, y, z) from the cloud is given by

$$D_\gamma(x, y, z, t) = K\mu_{en}E_\gamma \int_0^\infty \int_{-\infty}^{\infty}\int_{-\infty}^{\infty} \frac{B(\mu r)e^{-\mu r}}{4\pi r^2} \chi(x', y', z', t)\,dx'\,dy'\,dz' \quad (3.3.2\text{-}5)$$

in which K is the dose conversion factor; E_γ is the photon energy; $B(\mu r)$ is the dose buildup factor; μ_{en} is the energy absorption coefficient in air; μ is the linear attenuation coefficient in air; χ is the concentration at the source (x', y', z'); r is the distance from the source to the receptor, $r^2=(x-x')^2+(y-y')^2+z-z')^2$. A single puff formula, Eq. 3.3.2-2 is used as χ to integrate Eq. 3.3.2-5. With the assumption of a power function representation of the dose buildup factor, $B(\mu r)=1+\sum_{n-1}k_n(\mu r)^n$, Eq. 3.3.2-5 for an isotropic cloud $(\sigma_h=\sigma_z=\sigma)$ can be written as :

$$D_\gamma = \frac{K\mu_{en}\mu E_\gamma Q}{2(2\pi)^{3/2}}(I_0 + \sum_{n=1} k_n I_n) \quad (3.3.2\text{-}6)$$

where

$$I_n = \frac{\mu^{n-1}}{\sigma}\int_0^\infty \frac{r^{n-1}e^{-\mu r}}{m}\left[\exp\left\{-\frac{(m-r)^2}{2\sigma^2}\right\} - \exp\left\{-\frac{(m+r)^2}{2\sigma^2}\right\}\right] dr \quad (3.3.2\text{-}7)$$

and m is the distance from the center of the puff to the receptor. While value of I_0 can be

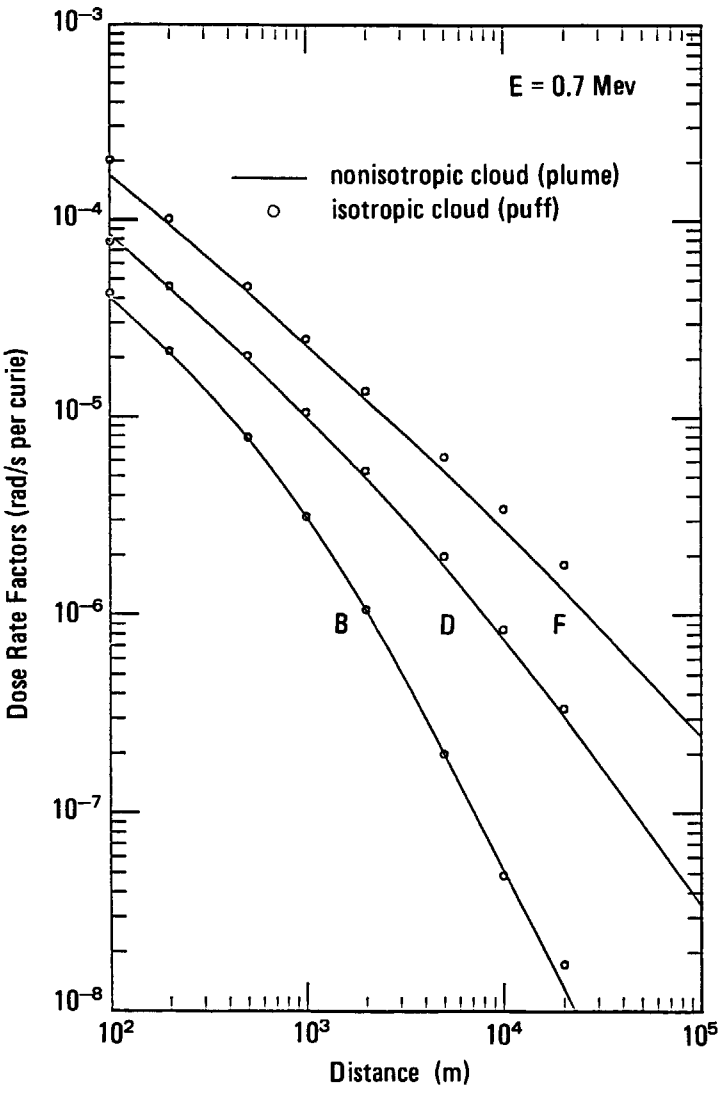

Fig. 3.23 Comparison of the LSPUFF model solutions with the Strenge's numerical solutions.

determined by numerical integration technique such as the fomula by Takahashi and Mori[40], the solution of $I_n(n>0)$ is straightforward in terms of the error function. Since the error function is available in computer software, the solution of these integrals allow rapid estimation of external gamma-dose rate.

The preceding equations are applied to an isotropic cloud ($\sigma_h=\sigma_z=\sigma$). Since the real diffusion of material results in a nonisotropic formulation, we adopt the method of correction for a nonisotropic cloud which is to use an average value of σ given by $\sigma=(\sigma_h\sigma_z)^{1/2}$. This puff model which incorporates the isotropic cloud approximation has been successfully tested against the finite cloud dose rate factors for the Gaussian plume model given by Strenge et al.[41] **Figure 3.23** shows a comparison of Strenge's numerical solutions for centerline plume dose rate factors with those from the puff model for three Pasquill stability classes, B, D and F. The agreement is good for each stability class.

(4) Limitations and extensions

The method presented here has some limitations. The important problem is how the wind vectors used to determine the advection of the center of a puff should be estimated in complex conditions, including nonuniform topographical features and sea breeze circulation. Although this model adopts the mean wind vector within the mixing layer, the advection of the center of a puff should be calculated by the mass-weighted mean wind vector. As suggested by Sheih[42], the wind shear is an important factor in determining concentration distributions and should not be neglected. However, we need some more information on vertical meteorological conditions to simulate the above effect.

Finally, for the unlikely and rapid release of all or a large fraction of volatile fission products, the plume rise can result in significantly lower predicted values of downwind radiation exposures. The estimates of plume rise will be incorporated in the present puff model.

4. System Capability of Emergent Response

4.1 Availability of Input Data

4.1.1 Meteorological Data

The reliability of the results of SPEEDI depends greatly on the quality and the quantity of the meteorological data used in the calculation. The requirement for the quantity of meteorological data are different among the physical models. The simplest model requires only the single wind data and the atmospheric stability at the site. The three dimensional models or the long range transport models require greater amount of meteorological data in order to make use of their full capability, though they are programmed so that they can fulfill their calculation with only a set of site data.

The sources of meteorological data available to SPEEDI are as follows,

1) site observation,

2) AMeDAS (Automated Meteorological Data Acquisition System),

3) local meteorological network operated by local governments,

and

4) other data sources.

Every nuclear plant observes various meteorological elements such as the wind speed and direction at the top of the stack, temperature and its lapse rate, insolation and net radiation. The meteorological data at the site are especially important, because they determine the distribution of radioactive materials in the vicinity of the site, where the maxima of concentration and surface dose take place. The meteorological data of site are usually collected by a minicomputer in the plant, together with the monitoring data for environmental radiation. They could be used in SPEEDI, if a link is established between the minicomputer and the SPEEDI host-computer with an agreement of the nuclear power plant.

AMeDAS has a dense network of the automated meteorological stations all over Japan. The average spacing between the stations is about 20 km. Wind speed and direction, temperature, insolation and precipitation are measured hourly, and the data are assembled to the AMeDAS center in Tokyo through telephone lines. These data are open to the public, and they can be obtained within the thirty minutes after each observation, if a link is established between the user's computer and the minicomputer of Japan Weather Association, which is in charge of distribution of the data. Several tens of the AMeDAS stations exist in the regional scale (200 km X 200 km) computation of SPEEDI, and they supply a sufficient amount of surface wind data to the regional transport model. As for the local scale (50 km X 50 km) computation, five or six AMeDAS stations are usually available.

Many local governments maintain their automated local meteorological and air quality monitoring stations. Some of the meteorological stations are set up as a part of monitoring for environmental radiation and the others are set up for air quality monitoring. Surface wind is observed at the most of the stations, and the data are assembled to the monitoring center hourly. Insolation and precipitation are also observed at some of the stations. The spatial density of the stations has variety among the networks of different local governments, and the distribution of the stations are not uniform. However they are valuable for the calculation over the local scale, because they fill up the sparse area between the AMeDAS stations. These data can also be used in SPEEDI, if a link is established between the monitoring center of each

local government and the SPEEDI host-computer. In the last group are included the observations conducted by the Ministry of Construction, fire office and/or other organization. Some of them are located in the sparse area of the present meteorological network. At these stations, data are not monitored either continuously or periodically. For this reason, it is not easy to use these data. However, if we construct a certain special network, these data will be available within a short time.

Most of the present meteorological data mentioned above are those of surface observation. In order to use the three-dimensional models in SPEEDI effectively, observations in upper layers (up to several hundreds of meters) are desirable. The upper wind data and the data of the atmospheric stability in upper layers are especially important, which largely affect the surface concentration and the dose. Additional surface stations are also required in some regions where the topography is complex, where an observed wind is only the representative of small area. Furthermore, intensity of the atmospheric turbulence, which directly affects the atmospheric diffusivity, is not monitored in the present status. The verification study of three-dimensional models (Section 3.2.2) implies that the inclusion of these data improves the precision of the results quite well. In order to obtain these data, special meteorological stations should be built around the nuclear sites. An example of the distribution of the meteorological stations around TOKAI site in Ibaraki-ken, where JAERI and other nuclear facilities locate, is shown in **Fig. 4.1**. Distribution of the AMeDAS stations are also shown in **Fig. 3.12**.

4.1.2 Source Term

(1) Outline of methods for release estimation

Data as source terms are critical in estimating the concentration and the dose from its radioactive cloud, and linearly affect the results of these in general. In the SPEEDI code system, every radioactive nuclide name and its release rate as source terms are expected to be received from a nuclear accident site. Such a detailed information as source terms, however, could not be obtained during early periods after the accident should occur. In such case, if a total amount of release rate of noble gas is only known as source terms, it is impossible to determine photon energy and decay constant for dose calculation. For this reason, the SPEEDI system has a program to estimate the isotopic composition of noble gas and iodine as a function of reactor type, i.e., BWR or PWR, and burnup data depending on the operational history of a reactor.

The following input types of release data as source terms are considered by SPEEDI.

Mode 1 : Either the total amount of release rates in noble gas or iodine (unit ; Ci/hour) is inputted, or release rate of a dominant nuclide. This mode is utilized in the case where each isotopic fraction of noble gas or iodine is unavailable.

Mode 2 : As to noble gas, the readings of an ionizing chamber as a stack monitor that is modified by geometrical efficiency is inputted, and about iodine the total release rate of ^{131}I that may be dominant among its isotopes is put in.

Mode 3 : Each release rate of all the isotopes in noble gas or iodine is inputted in order of mass number.

Mode 4 : The release rate of a nuclide is inputted, which can be selected among 56 nuclides including such fission products as ^{137}Cs and ^{90}Sr, etc. This mode is also utilized for calculating a single nuclide of noble gas or iodine.

In mode 1 and 2, the estimating routine of isotopic composition of noble gas or iodine is used. In SPEEDI, the isotopic composition of release rate of noble gas or iodine is estimated based on the following assumptions.

i) The same isotopic composition as a reactor inventory at shutdown time might be released

into the atmosphere. Separation of a particular isotope from other ones could not be performed by the isotope effect such as physisorption or chemisorption, which is caused by the difference among energy states of nuclei.

ii) The values of isotopic composition at shutdown time are based on burnup calculation considering reactor type of BWR and LWR.

(2) Estimation methods of release rates

The release rate of each nuclide in noble gas or iodine adjusted to reactor shutdown time, considering isotopic composition and radioactive decay, is estimated by the following equations.

Mode 1 : In case of total amount of release rates,

$$Q_i = \{Q/(\sum_i f_i \cdot \exp(-\lambda_i \tau)\} \cdot f_i \qquad (4.1.2\text{-}1)$$

where

Q = total amount of release rate,
f_i = isotopic fraction at reactor shutdown,
λ_i = decay constant of a nuclide i,
τ = duration between shutdown and measurement of a crude release rate,
Q_i = adjusted release rate of a nuclide i.

In case of a dominant nuclide k,

$$Q_i = (Q_k/\exp(-\lambda_k \tau)) \cdot (f_i/f_k) \qquad (4.1.2\text{-}2)$$

where

Q_k = release rate of a dominant nuclide k.

Mode 2 : The exposure rate (mR/hr) measured with an ionizing chamber as a stack monitor is proportional to absorbed energy in air. Let K_0 ((mR/hr)/(Ci/m^3)) denote the measured value of a specified noble gas having unit concentration. K_0 usually shows the characteristics of an ionizing chamber. The following relation is derived from the proportionality of absorbed energy in air measured with the same monitor.

$$R/K_0 = \Big[\sum_i \{p_i \cdot q_T \cdot \exp(-\lambda_i(t-t_0)) \cdot E_{fi} \cdot \mu_{en}(E_{ai})/\rho\}\Big] / (E_{f0} \cdot \mu_{en}(E_{a0})/\rho) \qquad (4.1.2\text{-}3)$$

$$q_i = p_i \cdot q_T \qquad (4.1.2\text{-}4)$$

where

R = exposure rate,
p_i = isotopic fraction of a nuclide i at shutdown,
q_i = concentration of a nuclide i at shutdown,
q_T = total concentration of noble nuclides at shutdown,
t = time when exposure rate is measured,
t_0 = shutdown time,
E_{fi} = effective photon energy (MeV/dis),
E_{ai} = average photon energy (MeV/photon),
E_{f0} = effective photon energy of a specified nuclide,
E_{a0} = average photon energy of a specified nuclide,
μ_{en}/ρ = mass energy absorption coefficient.

The effective photon energy and average photon energy of a nuclide i are expressed, respectively, as

$$E_{fi} = \sum_j (f_{ij} \cdot E_{ij}) \qquad (4.1.2\text{-}5)$$

$$E_{ai}=\left\{\sum_j (f_{ij}\cdot E_{ij})\right\}/(\sum_j f_{ij}) \qquad (4.1.2\text{-}6)$$

where

E_{ij} = j photon energy emitted by a nuclide i,

f_{ij} = intensity of a photon j per disintegration of a nuclide i.

By combination of the equations from Eq. 4.1.2-3 to Eq. 4.1.2-6, Q_i is obtained, by which the release rate needed in dose calculation of SPEEDI is given as

$$Q_i=(p_i\cdot q_i)\cdot w \qquad (4.1.2\text{-}7)$$

$$=(R/K_0)\times(p_i\cdot E_{f0}\cdot \mu_{en}(E_{a0})/\rho)/(\sum_i p_i\cdot \exp(-\lambda_i(t-t_0))\cdot E_{fi}\cdot \mu_{en}(E_{ai})/\rho)\times w\,, \qquad (4.1.2\text{-}8)$$

where

w = exhaust volume in hour of stack (m^3/hr).

(3) Isotopic composition

1) Effects of variation in reactor output

In the SPEEDI system, the isotopic composition of noble gas or iodine is employed to evaluate the release rate of each nuclide as source terms using a total amount of these nuclides or measured valued with stack monitors etc. The isotopic composition is obtained based on the assumption that a reactor shutdown should occur immediately after the rated output had gone on with average burnup of the reactor core. It is, however, likely that the output of a reactor may change to some extent by the event that might be related with the accident. The inventory of noble gas or iodine markedly depends on the operational history of a reactor shortly before its shutdown, since the half-lives of many nuclides among noble gases or iodines are less than a few days. The effects of variation in reactor output shortly before shutdown on the evolution of isotopic composition following it had been analyzed by the NICCA code for calculating the activity of fission nuclides normally accumulated in fuel rods.[43] When the calculation is carried out based on the assumption that the shutdown should occur immediately after the continuation of rated output, the isotopic fraction of nuclides with longer half-lives was largely underestimated and that with shorter ones was overestimated in comparison with the results obtained considering the variation in reactor output shortly before the shutdown. From the standpoints of dose evaluation, it was found that the external exposure to total noble isotopes was estimated to be at most approximately 20% higher 10 hour immediately after the shutdown, but the thyroid dose to total iodine isotopes was underestimated to be 30% at maximum.

Generally speaking, it became obvious that the external dose from total nuclides was overestimated with no consideration for the variation of reactor output shortly before the shutdown, and that the error of the dose evaluation increased with reduction of reactor output and decreased with both its duration and time after the shutdown. On the other hand, the thyroid dose from total isotopes of iodine was more largely underestimated by increasing reduction rate of reactor output and its duration, and in the same way as noble nuclides decreased with time after the shutdown, since the fraction of ^{131}I among iodine exerted a large influence on the dose evaluation.

2) Effects of buildup of nuclides after shutdown

In the methods described in the subsection (2), we do not consider the buildup of the isotopes that are produced by the decay chains of other fission products. Particularly, concerning the isotope of iodine, ^{132}I, produced by the β decay of a fission nuclide ^{132}Te, its isotopic fraction among iodine is much different from that in the case of no consideration for the buildup from its parent nuclide. The contribution of ^{131}I among iodine for thyroid doses

due to the inhalation of unit activity, however, occupies 83% but that of ^{132}I dose only 0.49%. For this reason, the effect of the buildup of ^{132}I from its parent nuclide may be small from the viewpoint of dose evaluation. However, whether to consider the buildup of the isotopes that are produced by decay chains may be attributed to the behavior of fission products in a reactor until atmospheric release.

4.2 Operational Tests

4.2.1 Expected Response

The primary data essential to the calculation of SPEEDI are the meteorological, release and geographical data. In general, the efforts will be made for the acquisitions of these data in the first stage. The geographical data of all sites in Japan are already stored in the system, and even when an unexpected area experiences an accident, a new topographical datapool can be built in about thirty minutes by the extraction from the master data base which has been developed by the Land Agency of Japan. Meteorological data are obtained through the AMeDAS system and the observation systems of local governments. Because these data are observed in routine work, the locations of measuring points can be stored in the SPEEDI system beforehand. In the case that several observed data, upper air observation data, etc., are supplied in the emergency, the addition of locations will be performed within five minutes. The temporal data are the observed meteorological data and the source information. The SPEEDI system has no data transmission media in the present stage and the data must be manually entered into computer files. The time lag concerning this work will become an obstacle against the quick response. In the practical stage, the data transmission media connected with the meteorological data observation systems such as the AMeDAS and the observation systems of local governments will be established by telephone lines, radio and microwave and so on. Even when the transmission system are settled, the time lag from the observation at each point to the acquisition will remain in about twenty minutes for AMeDAS and ten minutes for each local government. About the source information, the possibility to obtain the data in real-time depends on the nature of an accident. Almost all stack monitors currently used are only effective to the noble gas, so the release rate of iodine may not be immediately available.

For these circumstances, if the data can be obtained through the computer link and SPEEDI can monopolize a processor of the host computer system, the effort to make the geographical and meteorological data available to SPEEDI will become very small. Even when the accident occurs at an unexpected area, the preparation of SPEEDI's response will be established within one hour. It may take much time to get the effective meteorological data obtained from extra observations.

After the preparation, the types of the operation will be categorized into two. The first case is that the emission of radioactive materials into the environment is anticipated, where the SPEEDI's staffs have a plenty of time to prepare for the response before the accidental release. From the initial stage, the SPEEDI system will be able to perform the real-time and forecasting simulations according to normal procedure. The exercise of operation with the field experiment, which will be mentioned in the next sub-section, is one of the examples in this case.

The second case is that several hours elapsed between the beginning of release and the activation of SPEEDI. The SPEEDI system will respond with the calculation of the dose distribution since the start of the release, and after that it comes up to real-time and forecast simulations as soon as possible. And it will take one or two hours for the calculations to

overtake real time. The estimation of the time does not, of course, involve the delay time caused by human failures which may occur in the chaotic condition in emergency facilities. After these works, calculations will be made for the simulation including the forecast of dose distribution two or three hours hence. In any way, it is desirable for the staffs to experience many types of exercises.

4.2.2 Exercise with the Field Experiment

The exercises of real-time response were carried out in the series of field experiments in 1983. The method of experiment was almost the same as that of experiment in 1982 mentioned in subsection 3.2.1.

Geographical data of Tokai site are already stored in the system as one of the service sites. The meteorological data were obtained by telephone from the air-pollution-control center of Ibaraki-ken and by the acoustic sounder deployed in JAERI site. **Figure 4.2** shows the locations of meteorological measuring system. The system of local government measured the wind direction and speed at the height 10 m and the acoustic sounder measured the vertical profile of wind speed, wind direction and the standard deviation of wind direction. These data were acquired at intervals of one hour to the SPEEDI system. The time lag of data acquisition to the SPEEDI system was about fifteen minutes after the real-time observation. After the acquisition, meteorological data, including the location of meteorological measuring system, were stored in the data file within three minutes. Data concerning the nature of release were obtained by telephone from an experiment control center. Therefore the total time lag between the start of real-time prediction and the meteorological observation was about twenty minutes.

In this section, the exercise on Run 5 is described as an example. The progress with time of real-time response on Run 5 is shown in **Table 4.1**. The release started at 1000 JST (Japanese Standard Time) on 4th August and continued three hours. The operation of the SPEEDI system started at 0950 JST. In the first ten minutes till the release started, the initial conditions were set by the SITE, TIME and REL commands. After making the meteorological datapool of 1000 JST, the prediction of the average concentration for one hour from 1000 to 1100 JST was performed by the WIND04 code and the PRWDA code. Till the next meteorological data were inputted, the rest time was utilized to the graphic output. These procedures were repeated three times till 1300 JST. Temporal data essential to the calculation were inputted as the operands of the SITE, TIME, REL, WIND and CONC commands. The input variables supplied to the SET command were only the cell size, in this case 500 m X 500 m X 25 m was applied, and the IBL data to the PRWDA code was obtained from the standard deviation of wind direction.

These exercises were performed in the time sharing system of JAERI computing center, so the SPEEDI system did not monopolize the processor. For this reason, the computation time to obtain the results depended on the congestion of jobs in the computer system and the average for one response-operation was about forty-five minutes. If the SPEEDI system has the highest priority for use of the vector processor in JAERI, the output can be obtained within three minutes.

The graphic outputs of the SPEEDI system were handed to the researcher who was engaged in experiments and were utilized for the planning of next sampling. The typical outputs of wind field and concentration distribution are shown in **Figs. 4.3** and **4.4**. The overlay map of **Fig. 4.4** shows the shoreline and roads. Although the outlook of Figures are the same as the examples of the system output in sub-section 2.2.3, the unit of concentration contours is not (Ci/m^3) but (ppt).

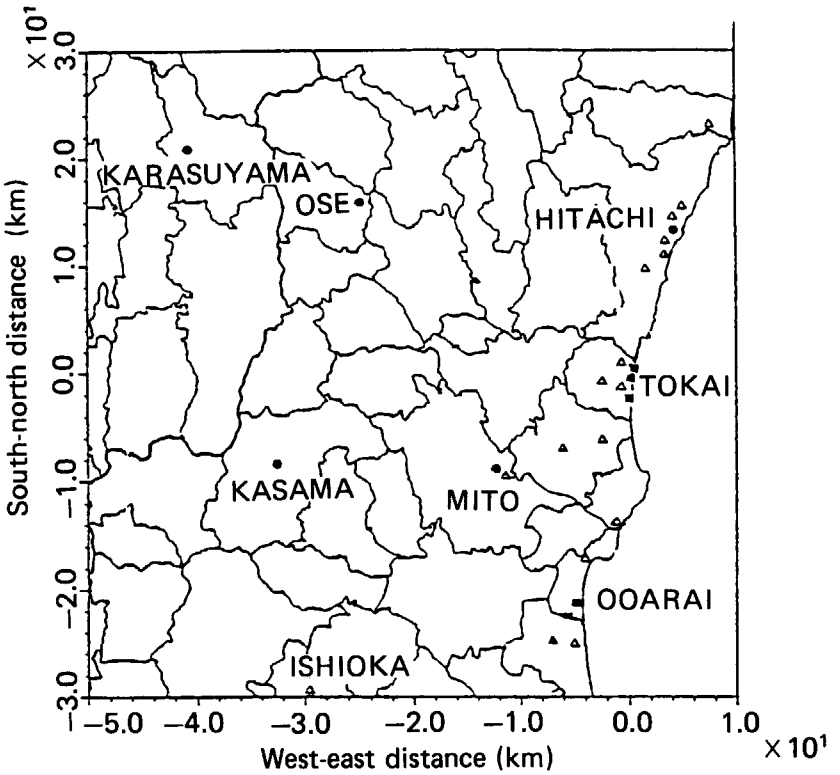

Fig. 4.1 Distribution of the various kind of meteorological stations around Tokai nuclear site. Solid squares are site observations, dots are AMeDAS stations and the triangles are local network operated by the local government.

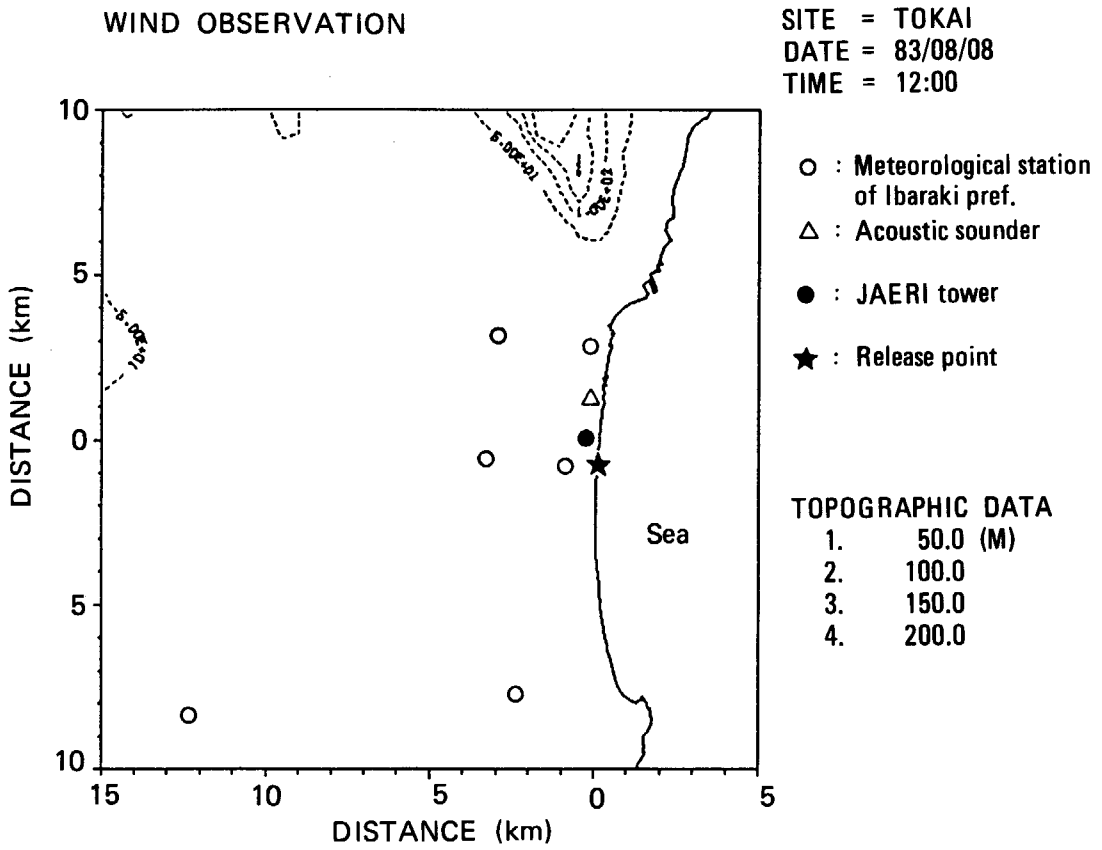

Fig. 4.2 Location of meteorological measuring system which supplied data to SPEEDI in real time.

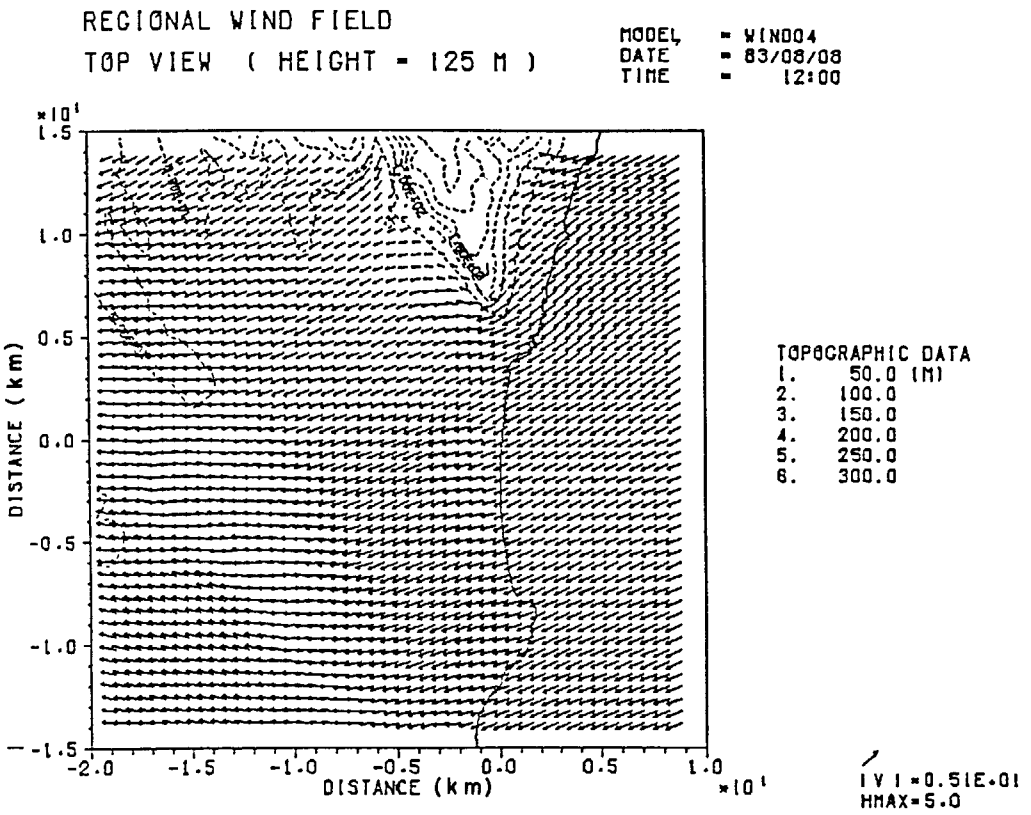

Fig. 4.3 Typical output of wind field at 125 m from the sea level in real-time response tests.

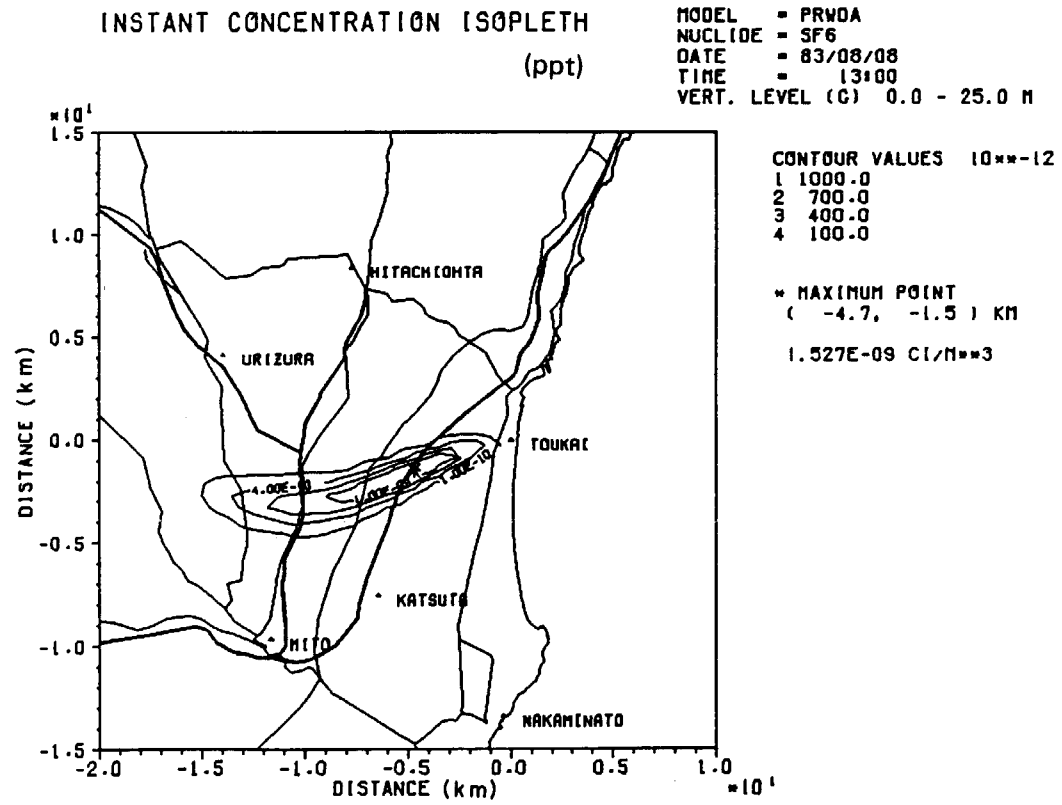

Fig. 4.4 Typical output of concentration distribution on the ground level in real-time response tests.

Table 4.1 Progress with time of real-time response

Time	Experiment	Acquisition of meteorological data	Output of SPEEDI
			Start (9:50)
10:00	The start of release	(10:19)	Initial data set Observed wind data (10:30) 3–D wind field (10:45) Concentration (10:59)
11:00	Sampling (11:30)	(11:17)	3–D wind field (11:35) Concentration (11:52)
12:00	(12:30) Sampling	(12:15)	Observed wind data (12:20) Concentration (12:41)
	The end of release		

5. Conclusion

The ultimate goal of the development of SPEEDI is to complete a practical computer code system for rapid calculation of the various information on radiation levels and radioactive concentration under the situation of accidental release from nuclear facilities. From this point of view, the design and development of SPEEDI have been carried out, and the final version has completed, which satisfies the practical needs for the application to the national service network system for real-time estimation and prediction in an emergency situation.

At a starting point of the design of this code system the next three basic requirements were taken into accounts. These are: (1) to have modular code structure, (2) to have versatile datapool system and (3) to have functions for colour graphics and hard copy for easy understanding of output. In the present version of SPEEDI these all requirements have been realized successfully.

The first aim of development of SPEEDI is at the preparation for the countermeasures against accidental release especially in the early phase of release. Therefore, SPEEDI should perform the real-time analysis and prediction calculation in a reasonably short time and has to provide information with adequate reliability.

In the case of our large-scale computer FACOM M-380 the results of doses can be obtained within less than 10 minutes in sequential calculations, and by the use of a new vector processor VP-100, which has been recently introduced to JAERI, the computation time has been further reduced within a few minutes. Furthermore, SPEEDI has two calculational modes of local scale of within 25 km and regional scale of up to 100 km from a facility, and the evaluated domain can be selected depending on the magnitude of the consequences of the accident.

The necessity of capability of the long term evaluation is often discussed to obtain the information for making a decision of evacuation from and re-entry to the contaminated area after an accidental release and also, the propriety of the range of evaluation area is frequently discussed relating to the emergency planning zone (EPZ) which may be set in a range of 8-10 km from a nuclear plant in Japan. But in case of SPEEDI we have basically designed the system to cover the time range till an accidental release of radioactive materials become substantially controlled, and to select the evaluation area flexibly taking into account the scale of accident and meteorological condition regardless EPZ.

The verification of various physical models used in SPEEDI has been continued by comparison studies using actual concentration and meteorological observation data obtained from SF_6 gas tracer field experiments. The comparisons showed that the coastal typical diffusion phenomena under the presence of an internal boundary layer could be well simulated by using calculation models provided in SPEEDI. On the other hand, in order to clarify the feasibility of the wind field model to the site in the complex terrain the field experiments have been carried out around the isolated mountain mass since 1983 and the comparison of experiment and calculation has been continued using actual data on wind flow, concentration distribution and trajectory of non-lift balloon. On the basis of these comparisons we can conclude that SPEEDI gives an effective information on environmental radiation in the vicinity of the plant, though these models are being verified for application to the diffusion in regional scale with complex terrain beyond the range of 10-15 km from a release point.

There are many problems to be solved and clarified hereafter; they are, for example,

(1) verification of the wind field model on the site of wide and complex terrain mentioned above, (2) the sensitivity study using field experimental data for optimum deployment of meteorological observatory network and (3) survey of site specific conditions of each nuclear plant and evaluation of feasibility of models to their sites.

SPEEDI should essentially be given the effluent rate and amount of radioactive materials from the plant. However, considering the case that the source information cannot be offered rapidly both from monitoring and accidental analysis especially in early stage of accident, SPEEDI has a simple program for estimation of the relative nuclear fraction of effluent radioactive materials.

One of the most important problems for the practical use of SPEEDI is how to obtain and evaluate the input source data for quantifying the calculated results. Hereafter, we consider that we should develop a method for estimation of source terms as input data to SPEEDI by calculation and by emergency survey for measurement of environmental distribution of gamma exposure and radioactive concentration. Furthermore, we think that it is also very important to develop a practical method for comparison and adjustment of calculated results with measurements. By the establishment of cooperation between environmental monitoring and predicted calculation, SPEEDI will function as a versatile system for emergency environmental countermeasures.

Now the development of SPEEDI has arrived at the final stage and a new plan is arranged for practical application to the emergency preparedness, that is establishment of central computing facilities and automated data acquisition network system which collects radiological monitoring and meteorological observation data around 14 nuclear plant sites in Japan. For the establishment of emergency advisory system in Japan this new program starts from FY 1985 and is expected to be completed in a few years.

Acknowledgements

The authors wish to express their sincere thanks to following committee members, research groups, engineers and institutes, whose advices and assistances made the construction of the SPEEDI code system very easy.

JAERI Committee on Environmental Radiation Research (Dr. Jiro Kondo, Chairman, National Institute for Environmental Studies) for control and guidance of the research project including the construction of the SPEEDI.

Subcommittee of the Committee (Dr. Tatsuji Hamada, Chairman, Japan Radioisotope Accosiation) for control and guidance of the research project on environmental monitoring and prediction of dose, in which the construction of the SPEEDI has been included.

Members of National Meteorological Research Institute which participate in the SPEEDI working group for helpful discussions.

Research groups of the Lawrence Livermore National Laboratory and Savannah River Laboratory of E.I. du Pont de Memours & Co. for suggestions in construction of physical models in the SPEEDI.

Land Agency of Japan whose numerical mesh data made SPEEDI a practical system.

Dr. Makiko Kato of National Meteorological Research Institute for experimental data and **Figures 3.15, 3.16** of wind tunnel and Messrs. Michio Kakuta and Takashi Hayashi of JAERI for experimental data of atmospheric diffusion.

Drs. Tatsuoki Takeda and Toshihide Tsunematsu of Dept. of Thermonuclear Fusion Research, JAERI for use of the graphic package ARGUS, and Mr. Mineyoshi Tomiyama of Computing Center, JAERI for use of the file handling utility DATAPOOL.

Dr. Yoshitaka Naito of Dept. of Fuel Safety Research, JAERI for provision of isotopic composition data.

Nuclear Code Committee of JAERI (Dr. Satoru Katsuragi, Chairman, JAERI) for assistance in design concept of the SPEEDI.

Messrs. Kunihiko Horikami of Nuclear Energy Data Center, Motoi Okuda of Fujitsu, Ltd. and Kazuaki Yamamoto of FACOM Information Processing, Ltd. for programming a part of the SPEEDI system.

Systems engineers, Messrs. Tsuneyoshi Nishi and Hiroshi Aizawa of Fujitsu, Ltd. who converted and tested the SPEEDI on a minicomputer.

Members of JAERI Computing Center who programmed some software utilities of SPEEDI.

Publication List on SPEEDI

(1) Tabei, M. and Nakamura, Y. : A Software for Transformation and Map Drawing of Numerical Information for Land, JAERI-M 82-041 (1982) [in Japanese].

(2) Imai, K. edit. : Environmental Safety Research for Emergency in JAERI, Hoken Butsuri, **18**, 259 (1983) [in Japanese].

(3) Ishikawa, H. : A Computer Code which Calculates Three Dimensional Mass Consistent Wind Field, JAERI-M 83-133 (1983) [in Japanese].

(4) Chino, M., et al. : The Numerical Simulation (I) of Field Tracer Experiment by a System for Prediction of Environmental Emergency Dose Information (SPEEDI), JAERI-M 83-233 (1983) [in Japanese].

(5) Chino, M. and Ishikawa, H. : Dose Evaluation Model in Complex Terrain by Using Particle Diffusion Method Combined with Three-Dimensional Wind Field, J. At. Energy Soc. Japan, **26**, 526 (1984) [in Japanese].

(6) Chino, M. and Ishikawa, H. : Dose Evaluation Method in Emergency by Using Puff Model Combined with Three-Dimensional Wind Field, J. At. Energy Soc., Japan, **26**, 897 (1984) [in Japanese].

(7) Kai, M. : A Computer Code for Calculating a γ-External Dose from a Randomly Distributed Radioactive Cloud, JAERI-M 84-006 (1984) [in Japanese].

(8) Chino, M., et al. : SPEEDI: System for Prediction of Environmental Emergency Dose Information, JAERI-M 84-050 (1984) [in Japanese].

(9) Hidaka, A. and Iijima, T. : AIRGAMMA: A Computer Code for Quick Assessment of the Cloudshine Dose due to Accidental Releases of Radioactive Materials, Hoken Butsuri, **20**, 33 (1985) [in Japanese].

(10) Chino, M., et al. : Simulation of Atmospheric Dispersion in the Existence of Internal Boundary Layer by a Three-Layer Model, J. Japan Soc. Air Pollution, **20**, 158 (1985) [in Japanese].

(11) Kai, M., Moriuchi, S. and Ohkubo, S. : Variation in Isotopic Composition of a Reactor at Its Shutdown – from the Viewpoint of Source Terms Used by the SPEEDI, JAERI-M 85-012 (1985) [in Japanese].

(12) Asai, K., et al. : Design, Construction and Experiences with System for Prediction of Environmental Emergency Dose Information (SPEEDI), J. At. Energy Soc. Japan, **27**, 839 (1985) [in Japanese].

(13) Hidaka, A. and Kai, M. : Treatment of Photon Energy Released from a Nuclide for Estimation of the Dose due to Radioactive Plumes. (to be published)

References

1) Dickerson, M.H. and Orphan, R.C. : Atmospheric Release Advisory Capability. Nucl. Safety, **17**, 281 (1976).
2) Asai, K. and Katsuragi, S. : Modular Programming Method at JAERI. JAERI-1274 (1982).
3) Tomiyama, M., et al. : Datapool: Its Concept and Facilities. JAERI-M 8715 (1980) [in Japanese].
4) Takeda, T., et al. : Integrative Graphic Subroutine Package ARGUS-V4. Computer Physics Communications, **34**, 15 (1985).
5) Land Agency of Japan : Method of Use and Case Studies of Mesh Data. (1978) [in Japanese].
6) Sherman, C.A. : A Mass-Consistent Model for Wind Field over Complex Terrain. J. Appl. Meteor., **17**, 312 (1978).
7) Lange, R. : ADPIC– A Three-Dimensional Particle-In-Cell model for the Disposal of Atmospheric Pollutants and Its Comparison to Regional Tracer Studies. J. Appl. Meteor., **17**, 320 (1978).
8) Japan Meteorological Agency : AMeDAS: Automated Meteorological Data Acquisition System. (1984) [in Japanese].
9) Sakagami, J., Hirose, M., Hino, M. and Yokoyama, O. : The Air Pollution Forecast and Control System (APMS), Modeling of Environmental Systems. IFIP meeting, Tokyo, April (1976).
10) Ishikawa, H. : A Computer Code which Calculates Three Dimensional Mass Consistent Wind Field. JAERI-M 83-133 (1983) [in Japanese].
11) Sklarew, R.C., Fabrik, A.J. and Prager, J.E. : Particle-In-Cell Method for Numerical Solution of the Atmospheric Diffusion Equation and Applications to Air Pollution Problems. System, Science and Software, La Jolla, Calif., Rep. 3SR-844 (1971).
12) Chino, M. and Ishikawa, H. : Dose Evaluation Model in Complex Terrain by Using Particle Diffusion Method Combined with Three-Dimensional Wind Field. J. At. Energy Soc. Japan, **26**, 526 (1984) [in Japanese].
13) Diehl, S.R., et al. : Random-Walk Simulation of Gradient-Transfer Processes Applied to Dispersion of Stack Emission from Coal-Fired Power Plants. J. Appl. Meteor., **21**, 69 (1982).
14) Ley, A.J. and Thomson, D.J. : A Random Walk Model of Dispersion in the Diabatic Surface Layer. Quart. J. R. Met. Soc., **109**, 847 (1983).
15) Hall, C.D. : The Simulation of Particle Motion in the Atmosphere by a Numerical Random-Walk Model. Quart. J. R. Met. Soc., **101**, 235 (1975).
16) Dickerson, M.H. and Gudiksen, P.H., Editors : Atmospheric Studies in Complex Terrain Technical Progress Report FY-1979 through FY-1983, UCID-19851, 287-290 (1983).
17) Gifford, F.A. : The Use of Routine Meteorological Observation for Estimating Atmospheric Dispersion. Nuclear Safety, **2**, 47 (1973).
18) Kai, M. : A Computer Code for Calculating a γ-External Dose from a Randomly Distributed Radioactive Cloud. JAERI-M 84-006 (1984) [in Japanese].
19) Clarke, R.H. : The WEERIE Program for Assessing the Radiological Consequences of Airborne Effluents from Nuclear Installations. Health Phys., **25**, 267 (1973).
20) Imai, K. and Iijima, T. : Assessment of Gamma-Exposure due to a Radioactive Cloud Released from a Point Source. Health Phys., **18**, 207 (1970).
21) Hayashi, T. and Shiraishi, T. : Assessment of Gamma Exposure Rate due to a Radioactive Cloud from a Stack. JAERI-M 8793 (1980) [in Japanese].
22) ICRP Publication 30 : Limits for Intakes of Radionuclides by Workers. Parts 1-3 with Supplements and Index. Pergamon Press, Oxford (1979-1982).
23) Kai, M. : Biological Half-Life of Radioiodine in Normal Japanese Thyroid. Hoken Butsuri 18, 3 (1983) [in Japanese].
24) ICRP Publication 23 : Reference Man: Anatomical, Physiological and Metabolic Characteristic. Pergamon Press, Oxford (1975).
25) Hofmann, W., Steinhausler, F. and Pohl, E. : Dose Calculations for the Respiratory Track from Inhaled Natural Radioactive Nuclides as a Function of Age – I. Compartmental Deposition, Retention and Resulting Dose. Health Phys., **37**, 517 (1979).
26) Lyons, W.A. and Cole, H.S. : Fumigation and Plume Trapping on the Shores of Lake Michigan during Stable Onshore Flow. J. Appl. Meteor., **12**, 494 (1973).
27) U.S. NRC : Onsite Meteorological Programs, Regulatory Guide 1.23 (1972).

28) Chino, M., et al. : The Numerical Simulation (I) of Field Tracer Experiment by a System for Prediction of Environmental Emergency Information (SPEEDI). JAERI-M 83-233 (1983) [in Japanese].
29) Chino, M., et al. : Simulations of Atmospheric Dispersion in the Existence of Internal Boundary Layer by a Three-Layer Model. J. Japan Soc. Air Pollution, **20**, 158 (1985) [in Japanese].
30) Hidaka, A. and Iijima, T. : AIRGAMMA: A Computer Code for Quick Assessment of the Cloudshine Dose due to Accidental Releases of Radioactive Materials. Hoken Butsuri, **20**, 33 (1985) [in Japanese].
31) Endlich, R.M. : An Iterative Method for Altering the Kinematic Properties of Wind Fields. J. Appl. Meteor., **6**, 837 (1967).
32) Liu, C.Y. and Goodin, W.R. : An Iterative Algorithm for Objective Wind Field Analysis. Mont Wea. Rev., **104**, 784 (1976).
33) Egan, B.A. : Turbulent Diffusion in Complex Terrain in Lectures on Air Pollution and Environmental Impact Analysis., American Meteorological Society (1975).
34) Smith, F.B. and Hay, J.S. : The Expansion of Clusters of Particles in the Atmosphere. Quart. J. R. Met. Soc., **87**, 82 (1961).
35) Wandel, C.F. and Kofoed-Hansen : On the Eulerian-Lagrangian Transform in the Statistical Theory of Turbulence. J. Geo. Res., **67**, 3089 (1962).
36) Van der Hoven, I. : Deposition of Particles and Gases in Meteorology and Atomic Energy-1968. TID-25190, U.S. Atomic Energy Commission, 202-208 (1968).
37) Horst, T.W. : A Surface Depletion Model for Deposition from a Gaussian Plume. Atoms. Environ., **11**, 41 (1977).
38) Gamertsfelder C.G. : Hazards Calculation Notebook. Aircraft Nuclear Propulsion Department, General Electric Co., unpublished.
39) Healy, J.W. and Baker, W.R.E. : Radioactive Cloud-Dose Calculations in Meteorology and Atomic Energy-1968. TID-25190, U.S. Atomic Energy Commission, 301-377 (1968).
40) Takahashi, H. and Mori, M. : Double Exponential Formulas for Numerical Integration. Publications of R.I.M.S., Kyoto Univ. **9**, 721 (1974).
41) Strenge, D.L., et al. : SUBDOSE – A Computer Program for Calculating External Doses from Accidental Atmospheric Releases of Radionuclides. BNWL-B-351 (1975).
42) Sheih, C.M. : A Puff Pollutant Dispersion Model with Wind Shear and Dynamic Plume Rise. Atoms. Environ., **12**, 1933 (1978).
43) Kai, M., Moriuchi, S. and Ohkubo, S. : Variation in Isotopic Composition of a Reactor at Its Shutdown – from the viewpoint of Source Terms Used by the SPEEDI. JAERI-M 85-012 (1985) [in Japanese].
44) Tabei, M. and Nakamura, Y. : A Software for Transformation and Map Drawing of Numerical Information for Land. JAERI-M 82-041 (1982) [in Japanese].

Appendix

Appendix 1 : WEADUS, WEADUS2

a. WEADUS

In the present status, SPEEDI has no software such as an automated data acquisition and update of weather datapool. WEADUS, i.e. Weather Data Update System., is a computer program which creates and updates the weather datapool by manual input of meteorological data from a character display terminal. WEADUS has following functions,

1) creation of weather datapool,
2) registration of additional stations,
3) input and rearrangement of the meteorological data,
4) supplement of the meteorological data,
5) display of site data,
6) display of data of each station, and
7) display of meteorological data at each time.

When meteorological data is given in form of a sheet, they can be inputted by the function 3. If the meteorological data are not obtained at some stations, we may input -999 instead of the observed data and may make input the appropriate values lately by the function 4. When some stations are additionally set up during an accident, those stations are registered in the weather datapool by the function 2. The stored data can be checked by the function 5 to 7.

b. WEADUS2

In addition to the functions of WEADUS, WEADUS2 has a function of forecasting the wind vector up to six hours ahead at each meteorological station. When a set of wind data is made input, WEADUS2 checks these data in the statistical way at first. If the abnormal data are found, they are replaced by -999, which implies no data. Then WEADUS2 predicts the hourly wind vector at each station up to six hours ahead by a statistical prediction method.

Appendix 2 : RGONDP

RGONDP is a software that creates the regional datapool at any site in Japan. The SPEEDI system already has complete regional datapool for every nuclear site in Japan. However a nuclear accident may take place at an unexpected site. A typical accident of this class is the one during the transportation of radioactive material. In such a case, regional datapool around the place of accident must be created immediately.

(1) Master data

The master data have been offered by the Land Agency of Japan. These data contain the data of the terrain height, coastlines, lakes, administrative boundaries, roads, railroads and the land uses. The terrain height data are obtained at every 250 m X 250 m grid point. The whole data are arranged according to the three different scales of mesh. The first mesh covers the area, which longitudinal width is one degree and the latitudinal width is forty minutes. The second mesh divides the first mesh into 8 X 8 area. The third mesh divides the second mesh into 10 X 10 area.

(2) Site specification

The range of the region that the regional datapool covers is specified by the following parameters,

a) latitude and longitude of virtual origin of the map,
b) the position of southwest corner of the region,
c) south-north and west-east lengths of the region and
d) mesh number of the south-north and west-east direction.

The relation of these data are illustrated in the **Fig. A.1**.

(3) Data conversion

The master data are arranged in the latitude and longitude, whereas the regional datapool is referred to the local cartesian coordinates. The master data should be converted into the local cartesian coordinates. Among many conversion methods, RGONDP prepares the rectangular projection method, the conical projection method and the stereographic projection method. The line data such as the coastlines and the administative boundaries are simply computed by the conversion of the coordinates of the points. However the spatially averaged data such as the mean height of a unit mesh of terrain should be converted with the consideration of the difference of the mesh size. In general, the mesh of regional datapool does not coincide with the mesh of master data. The basic concept of the data transformation is described by Tabei et al. (1981)[44]. A typical example is illustrated in **Fig. A.2**. Not only the mesh size but also the direction of coordinates differ, because of the effect of spherical surface of the earth. The mean height of unit mesh of regional datapool is computed with the weight of the area of the associated master mesh.

(4) Data processing

The general flow of the data processing is shown in **Fig. A.3**. At first, the first mesh numbers of the master data which contains the data of the interested area are selected, and

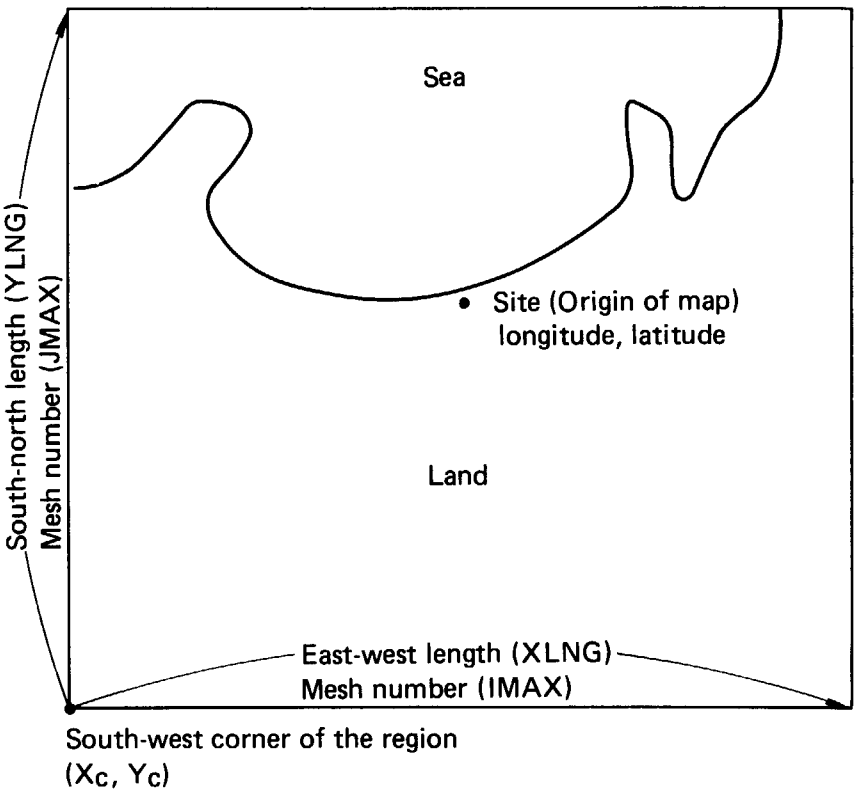

Fig. A.1 Specification of the domain of regional datapool.

the necessary data are copied on the magnetic disk from master magnetic tapes. Then, the data are rearranged into the local cartesian coordinates and are stored in the regional datapool.

A new datapool is created within thirty minutes in the normal operation of JAERI computing center.

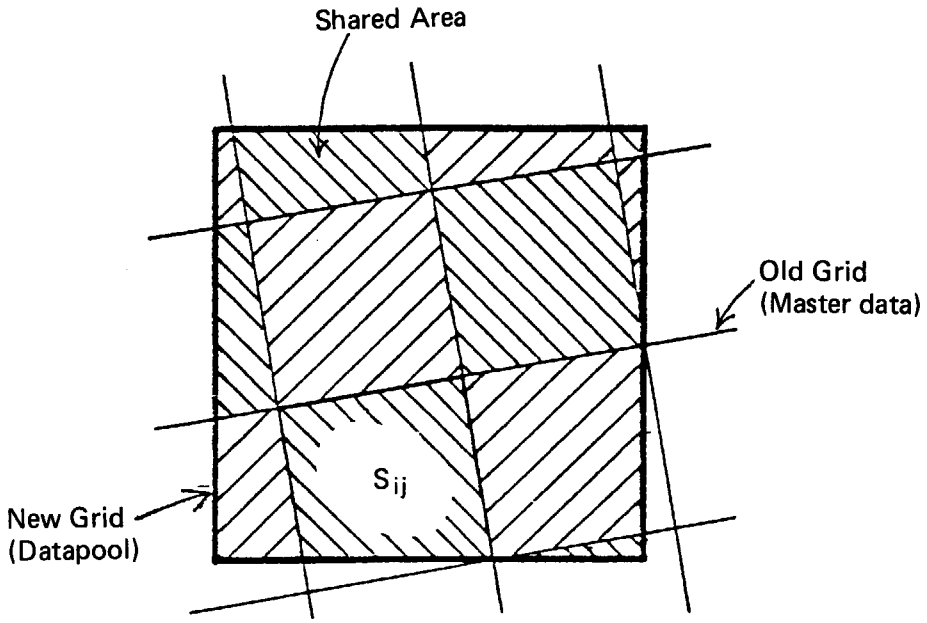

Fig. A.2 Mesh data transformation using the concept 'Shared Area' (after Tabei et al.).

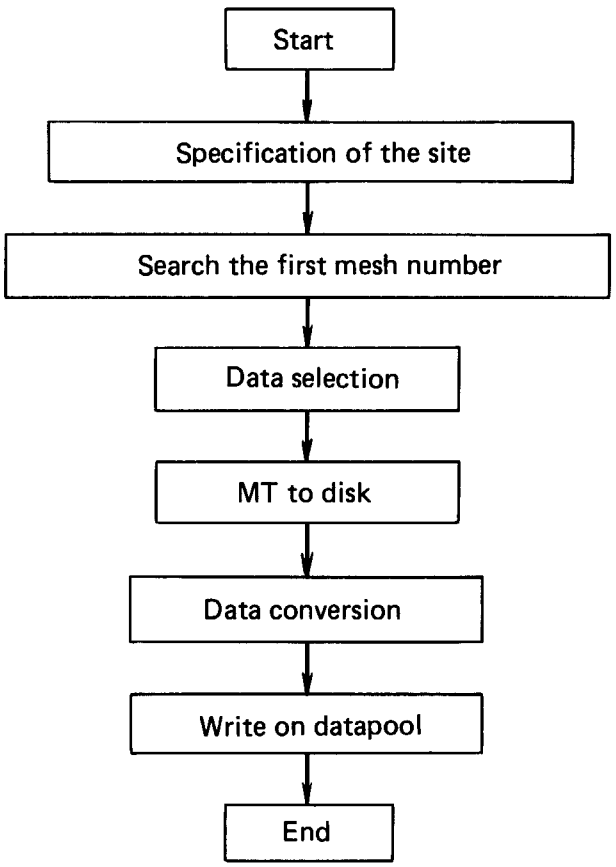

Fig. A.3 Data processing flow.

Appendix 3

The contents of the ICT1 of SPEEDI is listed in **Table A.1**.

Table A.1 List of ICT1

```
 10000  V03L04841130
 20000  J0418.SYSMAP4.DATA                          F111100
 30000  0                                  TOPOGRAFHICAL  D.P.
 40000  J7070.WEATHER.V4.DATA                      F121110
 50000  0                                  WEATHER        D.P.
 60000  J7070.WIND.V4.DATA                        F132100
 70000  0                                  WIND           D.P.
 80000  J7070.INCONC.V4.DATA                      F210210
 90000  0                                  INSTANT CONC.  D.P.
100000  J7070.SFCONC.V4.DATA                     F220210
110000  0                                  SURFACE CONC.  D.P.
120000  J0418.PART.V3.DATA                       F200210
130000  0                                  PARTICLE TYPEFILE
140000  DUMMY                                    F310020
150000  0                                  DOSE(GM)       D.P.
160000  J7070.DOSECUM.V4.DATA                    F320020
170000  0                                  DOSE(CUM)      D.P.
180000  J7070.DOSETHY.V4.DATA                    F330020
190000  0                                  DOSE(THY)      D.P.
200000  DUMMY                                    F340020
210000  0                                  DOSE(INH)      D.P.
220000  J0418.NCCREAT.DATA                       F160000
230000  0                                  NUCLIDE CREATE FILE
240000  J0418.NUCLIDE.DATA                       F170010
250000  0                                  NUCLIDE INF. FILE
260000  J0418.SYSCOREZ.DATA            SITE      F020001
270000  0                                  SITE FILE
280000  J0418.SYSSUB.V3L4.CNTL                   F540002
290000  0                                  SUBMIT FILE
300000  /END
310000  S01C  SITE NAME
320000  S01C  SITE NAME
330000  S02C  FACILITY NAME
340000  S02C  FACILITY NAME
350000  S03I  SITE ID. NUMBER
360000  S04I  LATITUDE
370000  S05I  LONGITUDE
380000  S06R  SITE TERRAIN HEIGHT
390000  S07R  RELEASE HEIGHT
400000  S08C  REACTOR TYPE(BWA/PWR)
410000  S08C  REACTOR TYPE(BWR/PWR)
420000  S09R  BURN-UP (MWD/MTU)
430000  S10R  SITE.XO
440000  S11R  SITE.YO
450000  S12R  STACK GAS(M**3/HR)
460000  T01I  REL DATE(YYMMDD)
470000  T02I  REL START(HHMMSS)
480000  T03I  SHUTDOWN DATE(YYMMDD)
490000  T04I  SHUTDOWN TIME(HHMMSS)
500000  T05I  EST. DATE(YYMMDD)
510000  T06I  EST. START(HHMMSS)
520000  T07I  EST. PERIOD(HHMMSS)
530000  T08I  DUMP INT. (HHMMSS)
540000  W01C  WIND MODEL NAME
550000  W01C  WIND MODEL NAME
560000  W02C  REGIONAL/LOCAL
570000  W02C  REGIONAL/LOCAL
580000  W03I  EST. DATE (YYMMDD)
590000  W04I  EST. START(HHMMSS)
600000  W05I  EST. PERIOD(HHMMSS)
610000  W06I  DUMP. INT. (HHMMSS)
620000  W07C  STABILITY(A-G)
630000  W07C  STABILITY(A-G)
640000  W08R  INVERSE LAYER HEIGHT
650000  W09R  MIXED LAYER HEIGHT
```

Table A.1 (Continued)

660000	W10R	SURFACE LAYER HEIGHT
670000	W11R	SRH (MEDIC)
680000	W12I	NO. OF X MESHES
690000	W13I	NO. OF Y MESHES
700000	W14I	NO. OF Z MESHES
710000	W15R	X MESH SIZE
720000	W16R	Y MESH SIZE
730000	W17R	Z MESH SIZE
740000	W18I	WIND. DP. OPEN FLAS
750000	W91I	DISPLAY DATE(YYMMDD)
760000	W92I	DISPLAY TIME(HHMMSS)
770000	W93C	DISPLAY SITE NAME
780000	W93C	DISPLAY SITE NAME
790000	C01C	CONC. MODEL NAME
800000	C01C	CONC. MODEL NAME
810000	C02C	REGIDNAL/LOCAL
820000	C02C	REGIONAL/LOCAL
830000	C03I	EST. DATE (YYMMDD)
840000	C04I	EST. START(HHMMSS)
850000	C05I	EST. PERIOD(HHMMSS)
860000	C06I	DUMP. INT. (HHMMSS)
870000	C071	REL. PERIOD (HHMMSS)
880000	C08I	NUMBER OF NUCLIDE
890000	C09C	NUCLIDE NAME 1
900000	C09C	NUCLIDE NAME 1
910000	C10C	NUCLIDE NAME 2
920000	C10C	NUCLIDE NAME 2
930000	C11C	NUCLIDE NAME 3
940000	C11C	NUCLIDE NAME 3
950000	C12R	REL. FRACTION 1(CI/H)
960000	C13R	REL. FRACTION 2(CI/H)
970000	C14R	REL. FRACTION 3(CI/H)
980000	C15R	DEPOSITION RATE 1
990000	C16R	DEPOSITION RATE 2
1000000	C17R	DEPOSITION RATE 3
1010000	C18R	H=DEVIATION
1020000	C19R	V=DEVIATION
1030000	C20R	MIN. X OF METEOR. MESH
1040000	C21R	MIN. Y OF METEOR. MESH
1050000	C22R	X MESH SIZE
1060000	C23R	Y MESH SIZE
1070000	C24I	METEOR. DATA FLAG
1080000	C251	DEPOSITION FLAG
1090000	C26I	DAY=NIGHT FLAG
1100000	C27R	LOWEST LAYER HEIGHT
1110000	C28R	2ND. LAYER HEIGHT
1120000	C29C	STAB. OF 2ND. LAYER
1130000	C29C	STAB. OF 2ND. LAYER
1140000	C30C	STAB. OF TOP LAYER
1150000	C30C	STAB. OF TOP LAYER
1160000	C31R	RELEASE CALIBER
1170000	C32R	TEMP. OF ATMOSPHERE
1180000	C33R	TEMP. OF PLUME
1190000	C34R	EXHAUST VELOCITY
1200000	C37I	CONC. DP. TYPE (0/1)
1210000	C38I	CONC. DP. OPEN FLAG
1220000	C40C	PARAMETER RESET MODE
1230000	C40C	PARAMETER RESET MODE
1240000	C51R	R1 AT SD. (CI/H)
1250000	C52R	R2 AT SD. (CI/H)
1260000	C53R	R3 AT SD. (CI/H)
1270000	R01I	REL.EST. DATE(YYMMDD)
1280000	R02I	REL.EST. TIME(HHMMSS)
1290000	R03I	INPUT TYPE (1/2/3/4)
1300000	R04C	NUCLIDE NAME 1
1310000	R04C	NUCLIDE NAME 1
1320000	R05C	NUCLIDE NAME 2
1330000	R05C	NUCLIDE NAME 2
1340000	R06C	NUCLIDE NAME 3
1350000	R06C	NUCLIDE NAME 3
1360000	R07R	RELEASE RATE 1 (CI/H)
1370000	R08R	RELEASE RATE 2 (CI/H)
1380000	R09R	RELEASE RATE 3 (CI/H)
1390000	R10R	KR83M RELEASE RATE
1400000	R11R	KR85 RELEASE RATE
1410000	R12R	KR85M RELEASE RATE
1420000	R13R	KR87 RELEASE RATE
1430000	R14R	KR88 RELEASE RATE
1440000	R15R	KR89 RELEASE RATE
1450000	R16R	KR90 RELEASE RATE
1460000	R17R	XE131M RELEASE RATE
1470000	R18R	XE133 RELEASE RATE
1480000	R19R	XE133M RELEASE RATE
1490000	R20R	XE135 RELEASE RATE
1500000	R21R	XE135M RELEASE RATE
1510000	R22R	XE137 RELEASE RATE
1520000	R23R	XE138 RELEASE RATE
1530000	R24R	XE139 RELEASE RATE
1540000	R25R	I129 RELEASE RATE
1550000	R26R	I131 RELEASE RATE
1560000	R27R	I132 RELEASE RATE
1570000	R28R	I133 RELEASE RATE
1580000	R29R	I134 RELEASE RATE
1590000	R30R	I135 RELEASE RATE
1600000	R31R	I136 RELEASE RATE
1610000	R32C	FP1 NUCLIDE NAME
1520000	R32C	FP1 NUCLIDE NAME
1630000	R33C	FP2 NUCLIDE NAME
1640000	R33C	FP2 NUCLIDE NAME
1650000	R34C	FP3 NUCLIDE NAME
1660000	R34C	FP3 NUCLIDE NAME
1670000	R35R	FP1 RELEASE RATE
1680000	R36R	FP2 RELEASE RATE
1690000	R37R	FP3 RELEASE RATE
1700000	R40C	PARAMETER RESET MODE
1710000	R40C	PARAMETER RESET MODE
1720000	R41C	STACK MONITOR GAS
1730000	R41C	STACK MONITOR GAS
1740000	D01C	DOSE MODEL NAME
1750000	D01C	DOSE MODEL NAME
1760000	D02C	REGIONAL/LOCAL
1770000	D02C	REGIONAL/LOCAL
1780000	D03C	CONC MODEL NAME
1790000	D03C	CONC MODEL NAME
1800000	D04I	EST. DATE (YYMMDD)
1810000	D05I	EST. START (HHMMSS)
1820000	D061	EST. PERIOD (HHMMSS)
1830000	D07I	DUMP INT. (HHMMSS)
1840000	D08I	DOSE. DP. OPEN FLAG
1850000	D11I	DOSGM DP. VIRGIN FLG
1860000	D12I	DOSCM DP. VIRGIN FLG
1870000	D13I	DOSTH DP. VIRGIN FLG
1880000	D14I	DOSIN DP. VIRGIN FLG
1881000	D20I	CALC. OPT (0/1)
1882000	D21R	ORIGIN X
1883000	D22R	ORIGIN Y
1884000	D23R	AXIS LENG
1885000	D24I	PRE. DETE (YYMMDD)
1886000	D25I	PRE. TIME (HHMMSS)
1887000	D26I	STATION ID.
1890000	G01C	FIG. NAME
1900000	G01C	FIG. NAME
1910000	G02C	MODEL NAME
1920000	G02C	MODEL NAME
1930000	G03I	SITE ID. NO.
1940000	G04I	START DATE(YYMMDD)
1950000	G05I	START TIME(HHMMSS)
1960000	G06I	END DATE(YYMMDD)
1970000	G07I	END TIME(HHMMSS)
1980000	G08R	X (MINIMUM) (KM)
1990000	F09R	X MAXIMUM (KM)
2000000	G10R	Y (MINIMUM) (KM)
2010000	G11R	Y MAXIMUM (KM)
2020000	G12R	Z=HEIGHT (M)

Table A.1 (Continued)

2030000	G13I	Z=TYPE (0/1)
2040000	G14C	NUC. NAME
2050000	G14C	NUC. NAME
2060000	G15C	BACK FIG. 1
2070000	G15C	BACK FIG. 1
2080000	G16C	BACK FIG. 2
2090000	G16C	BACK FIG. 2
2100000	G17C	BACK FIG. 3
2110000	G17C	BACK FIG. 3
2120000	G18C	BACK FIG. 4
2130000	G18C	BACK FIG. 4
2140000	G19C	BACK FIG. 5
2150000	G19C	BACK FIG. 5
2160000	G20C	BACK FIG. 6
2170000	G20C	BACK FIG. 6
2180000	G21C	SORT OF SECTION
2190000	G21C	SORT OF SECTION
2090000	G16C	BACK FIG. 2
2200000	G22R	DIST FROM SITE (KM)
2210000	G23R	RIGHT=ANGLE LENG. (KM)
2220000	G28R	Z MAXINUM (M)
2230000	G29C	AGE.
2240000	G29C	AGE
2250000	G30C	DTYPE
2260000	G30C	DTYPE
2270000	G31C	DEBUG FLUG
2280000	G32C	REGION
2290000	G32C	REGION
2300000	G33I	ERROR STOP FLAG
2310000	G34C	BIRD TYPE
2320000	G23C	BIRD TYPE
2330000	G35R	BIRD PARTICLE H(M)
2340000	G36C	BIRD PART PLACE1
2350000	G36C	BIRD PART PLACE1
2360000	G37C	BIRD PART PLACE2
2370000	G37C	BIRD PART PLACE2
2380000	G38R	BIRD SITE XO
2390000	G39R	BIRD SITE YO
2400000	G40R	LENGTH OF ARROW(MM)
2410000	G41I	Z=MAGNIFICATION
2420000	G42I	DIRECT. OF WIND
2430000	G43R	VELOCITY OF WIND
2440000	G44I	APPROXIMATE
2450000	G45I	CONTOUR NO.
2460000	G46R	MAX CONC. VALUE
2470000	G47R	2ND CONC. VALUE
2380000	G48R	3RD CONC. VALUE
2490000	G49R	4TH CONC. VALUE
2500000	G50R	5TH CONC. VALUE
2510000	G51I	REGIONAL FLAG(1/2)
2520000	G52I	PARTICLE NO.
2530000	G53I	GRID WRITE(0/1)
2540000	G54I	LOG DISPLAY WIDTH
2550000	G55R	ORIGIN Y(MM) DEF=52.
2560000	G60I	DEVICE TYPE(0/1)
2570000	G61I	ARGUS TITLE(0/2)
2580000	G62I	ARGUS FRAME(1/3)
2590000	G63I	BASE COLOR
2600000	G64I	FRAME COLOR
2610000	G65I	PLACE NAME COLOR
2620000	G66I	COAST LINE COLOR
2630000	G67I	TOPOGR. COLOR
2640000	G68I	ROAD COLOR
2650000	G69I	WEATHER COLOR
2660000	G70I	WIND COLOR
2670000	G71I	MAX CONC. COLOR
2680000	G72I	2, 3 CONC. COLOR
2690000	G73I	4, 5 CONC. COLOR
2700000	G74I	6 CONC. COLOR
2710000	G81I	PARTICLE COLOR
2720000	G82I	ACCUM. COLOR
2730000	G83R	BIRD ALPHA
2740000	G84R	BIRD BETA
2750000	G85R	BIRD GAMMA
2760000	G86R	BIRD XL
2770000	G87R	BIRD DD
2780000	G88I	BIRD COLOR TOPO
2790000	G89I	BIRD COLOR PART
2800000	G90I	BIRD COLOR PART BACK
2810000	G91I	BIRD COLOR PARAM COMMENT
2820000	G92I	BIRD COLOR STACK
2830000	G93I	BIRD COLOR COMENT
2840000	G94I	BIRD COLOR FLACE NAME
2850000	G95I	BIRD FIGURE TYPE
2860000	G96I	BIRD FLACE PLOT FLAG
2870000	G97I	BIRD PARTICLE POINT
2880000	P01C	GROUP NAME
2890000	P01C	GROUP NAME
2900000	P02C	REGION
2910000	P02C	REGION
2920000	P03I	DISPLAY DATE(YYMMDD)
2930000	P04I	DISPLAY TIME(HHMMSS)
2940000	P05C	DOSE MODEL NAME 1
2950000	P05C	DOSE MODEL NAME 1
2960000	P06R	SHELTERING LEV. (CUM)
2970000	P07R	SHELTERING LEV. (CUM)
2980000	P08R	SHELTERING LEV. (CUM)
2990000	P09R	MEDICAL LEVEL (CUM)
3000000	P10R	MEDICAL LEVEL (CUM)
3010000	P11R	SHELTERING LEV. (INH)
3020000	P12R	SHELTERING LEV. (INH)
3030000	P13R	SHELTERING LEV. (INH)
3040000	P14R	MEDICAL LEVEL (INH)
3050000	P15R	MEDICAL LEVEL (INH)
3060000	P16R	LIMITATION LEV. (1)
3070000	P17R	LIMITATION LEV. (2)
3080000	P18R	LIMITATION LEV. (3)
3090000	P19R	LIMITATION LEV. (4)
3100000	P20R	LIMITATION FACTOR 1
3110000	P21R	LIMITATION FACTOR 2
3120000	P22R	LIMITATION FACTOR 3
3130000	P23C	CONC MODEL NAME
3140000	P23C	CONC MODEL NAME
3150000	M01C	DATA POOL ID.
3160000	M01C	DATA POOL ID.
3170000	M02C	SITE NAME/MODEL NAME
3180000	M02C	SITE NAME/MODEL NAME
3190000	M03C	LOCAL/REGIONAL
3200000	M03C	LOCAL/REGIONAL
3210000	N01I	DISPLAY DATE(YYMMDD)
3220000	N02I	DISPLAY TIME(HHMMSS)
3230000	N03I	ESTIMATE DATE(YYMMDD)
3240000	N04I	ESTIMATE DATE(YYMMDD)
3250000	N05I	INPUT TYPE(1/2/3)
3260000	N06C	NUCLIDE NAME 1
3270000	N06C	NUCLIDE NAME 1
3280000	N07C	NUCLIDE NAME 2
3290000	N07C	NUCLIDE NAME 2
3300000	N08R	RELEASE RATE 1(CI/H)
3290000	N07C	NUCLIDE NAME 2
3300000	N08R	RELEASE RATE 1(CI/H)
3310000	N09R	RELEASE RATE 2(CI/H)